Renewable energies driven electrochemical wastewater/soil decontamination technologies: A critical review of fundamental concepts and applications

Soliu O. Ganiyu[1], Carlos A. Martínez-Huitle[1*], Manuel A. Rodrigo[2**]

[1]Universidade Federal do Rio Grande do Norte, Laboratório de Eletroquímica Ambiental e Aplicada, Instituto de Química, 59078-970, Natal RN, Brazil.

[2]Chemical Engineering Department, University of Castilla-La Mancha, Edificio Enrinque Costa Novella, Campus Universitario s/n, 13005 Ciudad Real, Spain.

Paper submitted to ***Energy and Environmental Science***

Corresponding Author Carlos A. Martinez Huitle; Manuel A. Rodrigo

E-mail: carlosmh@quimica.ufrn.br; manuel.rodrigo@uclm.es

Note:

1. We request that Prof. Rodrigo should assist in providing the soft copy of Fig. 9 and 11, which are some of the paper from his lab. Hopefully he has access to the softcopy.

Abstract

Electrochemical wastewater and soil treatments are exciting set of technologies that has been well-studied over the recent years as one of the most-effective remediation techniques for the removal of hazardous pollutants from liquids effluents and soil. The main requirement of these technologies is electricity and their sustainability can be largely improved if they are powered by renewable energy sources. Likewise, this green energy powering can help to apply these technologies in remote areas, such as rural communities in developing countries, where no electricity grid is available. This review presents a comprehensive discussion on fundamental concepts and applications of renewable energy driven electrochemical technologies for treating hazardous pollutants in wastewater and contaminated soils. In the first section, the fundamentals of different electrochemical remediation technologies are presented, whereas the next two sections focused on the most applied technologies for powering these electrochemical devices: the solar Photovoltaic (PV) (Section 3) and the wind turbines (Section 4). After that, the non-near future is faced with the study of the principles of biomass energy production and how bioelectrochemical systems are starting to be evaluated for powering electrochemical technologies (Section 5). Then, new approaches in the renewable energy driven electrochemical technologies such as triboelectric nanogenerators and photocatalytic fuel cells are described in Section 6. The last section focused on the challenges expected for the near future, describing the most promising storage system and evaluating the scale-up, environmental and economic concerns of the technologies studied in this work.

Keyword: Renewable energy; electrochemical technologies; wastewater and contaminated soils; solar energy; wind energy; biomass energy

1 Introduction

Electrochemical Advanced Oxidation Processes (EAOPs) has been extensively developed as alternative treatments for the removal of hazardous species, such as persistent organic pollutants (POPs), chlorinated hydrocarbons or polycyclic aromatic hydrocarbons, from water, wastewater, soil-washing wastes, landfill leachate and effluents of several industrial plants, including the treatment of reverse osmosis concentrates.[1–8] These techniques, based on the electrochemical production of the hydroxyl radical, are unique, because they possesses many advantages over other Advanced Oxidation Processes (AOPs) and even, in certain cases, over some commercial wastewater treatment technologies, like the biological treatments or the membrane filtration processes.[9–13] Thus, they exhibit a very high energy efficiency, a great versatility, high amenability, excellent environmental compatibility and are highly effective for removing all kind of organic pollutants.[1,6,11,14–16] Due to their high versatility, a large variety of EAOPs has been studied in the last decades by different research groups all around the World for the electrochemical degradation of several classes of refractory organic pollutants and their fundamental principles and applications are detailed in some substantial reviews and chapters of comprehensive books.[2–7,9,16–22] .

EAOPs are defined as hydroxyl radical ($^{\bullet}OH$)-mediated electrochemical treatments, where pollutants are destroyed by electrogenerated reactive oxygen species (ROS) mainly $^{\bullet}OH$ and oxidants formed from this powerful radical.[1,3,5,7,8,21,23] The $^{\bullet}OH$ radical is a very powerful oxidizing agent that reacts non-selectively with organic molecules, resulting in their oxidation until attaining a very high mineralization degree or, in most cases, their complete combustion to CO_2, water and inorganic ions.[4,6,11,13,15] In a broad sense, EAOPs can be grouped into two categories: (i) electrooxidation/anodic oxidation and (ii) Fenton's reaction based electrochemical processes (electro-Fenton, solar and UV photoelectro-Fenton and heterogeneous electro/photoelectro-Fenton processes).

In electrooxidation (EO), organic molecules are oxidized in the anode region by electrogenerated ROS (Eq. (4,5)), either physisorbed or chemisorbed $^{\bullet}OH$ depending on the electrode material/electrocatalyst used.[9,13,14,17,24] Thus, some anode materials interact strongly with the generated radical and promote its oxidation to chemisorbed oxygen or superoxide.[25,26] These materials, known as "active anodes", possess low oxygen evolution overpotential (e.g.

platinum, Ru and Ir based mixed metal oxides and graphite-carbon electrodes) and can only achieve a soft degradation of organic pollutants (electrochemical conversion) with very limited mineralization degree.[1,27] Other anodes (so-called "non-active") have higher oxygen evolution overpotential and interact weakly with the produced radicals (e.g. doped PbO_2, SnO_2, boron-doped diamond), thus allowing them to freely react with organic molecules until their ultimate mineralization (electrochemical combustion).[1,24,28–34] In anodic oxidation processes, many other oxidants are produced on the anode surface, such as ozone, hydrogen peroxide and peroxosalts. They interact with organics in the bulk and they are also responsible for the high efficiency of these processes.

$$M_{(s)} + H_2O \rightarrow M(^{\bullet}OH) + OH^{-} + e^{-} \quad (4)$$

$$M(^{\bullet}OH) \rightarrow MO + H^{+} \quad (5)$$

In this context, it is important to state that, when treating solutions containing high concentration of Cl^{-} ions (i.e. reverse osmosis concentrates), reactive chlorine species (RCS) (Cl_2, HClO, and/or ClO^{-} which are predominant at pH < 3.0, 3.0 – 8.0 and > 8.0 respectively) (Fig. 1) are produced in bulk solution via reactions (Eq. (6–8)) along with ROS.[9,35–39] The RCSs are very strong oxidants that can effectively degrade any class of organic pollutants. However, this process always lead to the formation of toxic byproducts, especially haloacetic acids and trihalomethanes and other refractory organochlorinated intermediates which are difficult to mineralize.[35,40–42]

$$2\,Cl^{-} \rightarrow Cl_{2(aq)} + 2\,e^{-} \quad (6)$$

$$Cl_{2(aq)} + H_2O \rightarrow HClO + Cl^{-} + H^{+} \quad (7)$$

$$HClO \leftrightarrow ClO^{-} + H^{+} \quad (8)$$

Fenton's based electrochemical technologies generate homogeneous $^{\bullet}OH$ indirectly from the reaction between H_2O_2 and catalytic Fe^{2+} (Fenton's reagents), totally or partially electrogenerated *in-situ* during the electrolysis at acidic pH values (pH 2.8 – 3.5).[4–6,9,16,22,43] This process is more efficient than EO at analogous experimental conditions because of: (i) large quantities of radicals produced in the solution via Fenton's reaction, in addition to those generated at the surface of anode and (ii) the proximity of the Fenton's generated radicals to the pollutants molecules, since they are generated in the bulk and not in the nearness of the electrode surface.[5,38,44]

$$H_2O_2 + Fe^{2+} + H^+ \rightarrow {}^{\bullet}OH + Fe^{3+} + H_2O \quad (9)$$

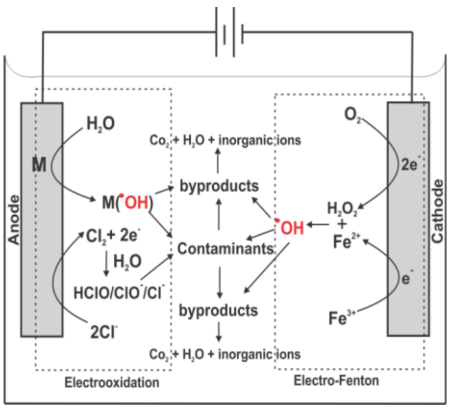

Figure 1: Schematic representation of mechanism of oxidations production in electrooxidation and electro-Fenton processes.

Photoelectro-Fenton's process is an upgraded variety of electro-Fenton process, in which the solution treated under EF conditions is simultaneously irradiated with UV light or solar irradiation (solar photoelectro-Fenton) to accelerate the mineralization rate of organics via the photolysis of $[Fe(OH)]^{2+}$ (Eq. (10)), thus regenerating the Fe^{2+}, that can catalyze the Fenton's reaction (Eq. (9)) and produce additional $^{\bullet}OH$.[5,45–48] Besides, the irradiation of the treated solution induced the photolysis of the complexes of Fe(III) with generated carboxylic acids according to reaction in Eq. (11), thus enhancing the efficiency of the process.[3,5,49,50]

$$[Fe(OH)]^{2+} + h\nu \rightarrow Fe^{2+} + {}^{\bullet}OH \quad (10)$$

$$[Fe(OOCR)]^{2+} + h\nu \rightarrow Fe^{2+} + CO_2 + R^{\bullet} \quad (11)$$

These EAOPs are not the unique contribution of electrochemical technology to the preservation of the environment. Thus, there are many other technologies ready to face different environmental challenges and which have been extensively studied in the recent years.

Regarding the treatment of liquid wastes, it is worth to mention three of them: electrocoagulation, electrodialysis and capacitive deionization.

Electrocoagulation (EC) is an alternative to coagulation that uses electric current to produce coagulant species from the dissolution of sacrificial anodes (typically Fe or Al and less frequently other metals, like magnesium). Following complex speciation processes, which depend on the pH and composition of the waste, many coagulant species are formed in the reaction media, including not only the amorphous metal hydroxides but also many charged species.[51] These species may neutralize the charges of micellar pollutants (or those of micro-drops in case of emulsions), favoring the formation of flocs from the colloids contained in wastes with turbidity or the phase coalescence in emulsions, thus, allowing to separate pollutants from the wastewater.[2,9,21,52,53] The coalescence of coagulated particles is favored by the soft mixing generated by the bubbles of hydrogen produced on the cathode. This process is known as electro-flocculation, being one of the key advantages of the whole electrocoagulation process, because it helps to save mixing energy with respect to conventional coagulation. Then, these tiny bubbles can also adhere to the surface of the flocs, diminishing their relative density, and allowing their transport to the surface of the treated waste, where they can be easily removed. This process is known as electro-flotation and it is the main, but not the unique separation technology involved in the electrocoagulation, because heavier coagulated particles are separated by sedimentation (Fig. 2a).[21,52] The easier regulation of pH, the lower production of sludge and the lower impact on the conductivity are the main advantages of the electrocoagulation, which is also becoming a process with a great applicability in the treatment of drinking water.[54,55]

Electrodialysis is an electrochemical process that removes ionized salts from seawater, brackish water or even from wastewater, by ion migration, through anion and cation exchange permeable-selective membranes under the influence of an applied DC electric potential.[56–58] As a consequence, two or more streams are produced with different composition. Sometimes, the technology is used only to split the treated stream into a concentrate and a dilute stream. In this case, several anion and cation membranes are stacked alternately between two electrodes, generating channels where ions are exhausted and others where the brine is concentrated (Fig. 2b).[56,59] In other cases, the electrodialytic technology is used to produce pure acids or alkalis and, in this case, the use of bipolar membrane is very important in order to achieve efficient processes. Anyhow, the membranes are the key elements of this technology, which is now very mature and plenty of full scale applications. An alternative to electrodialysis is the capacitive deionization, which has the great advantage of operating without membranes and that it is based on the transient concentration of ions in the nearness of electrodes under the application of an electric field. This technology is promising but not yet as mature as the electrodialysis and much work has to be done in the next years in order to reach a similar level of development.

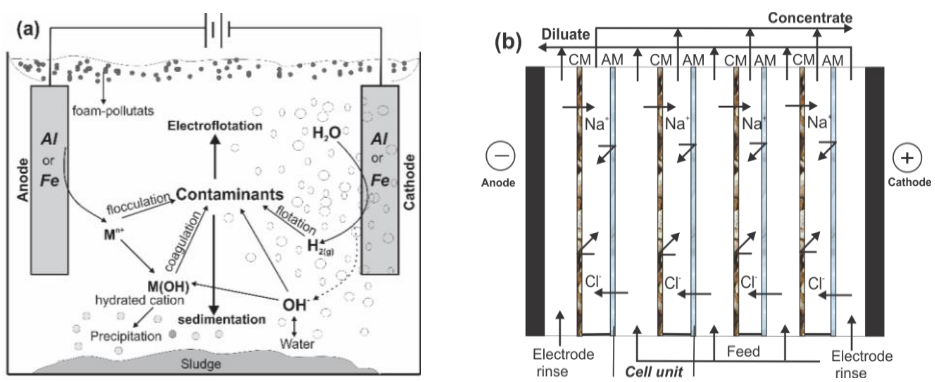

Figure 2: Schematic representation of mechanisms of (a) electrocoagulation and (b) electrodialysis. Fig 1a and 1b adapted from ref.[21] and[57] respectively.

In addition to the treatment of liquid wastes, soil remediation can also be faced with electrochemical technology, not only by treating the liquid wastes generated from the soil washing process, but also by promoting the in-situ treatment with the direct application of electric field to soil. Thus, electrochemically-assisted soil remediation involves all the phenomena that develop with the application of direct-current electric-field among electrodes placed into a contaminated soil,[7,58,59] and includes physical processes (like heating, adsorption and volatilization), chemical processes (like dissolution /precipitation, ionic exchange and complexation), electrochemical (like water oxidation & reduction and chlorine formation) and electrokinetic processes (like electro-osmosis, electromigration and electrophoresis).[7,60,61] As a consequence, soil remediation induced by application of electric fields is very complex because the interaction among all the processes activated is not easily predictable. Anyway, it allows a very efficient removal not only of metal ionic pollutants (for which it is a reference technology) but also of many other pollutants such as pesticides,[7,62] fuels[63] and chlorinated organics.[64]

The major challenge of all electrochemical technologies is the need for an electricity source to power the processes. This may become a drawback especially in developing countries and rural areas with limited access to the electricity grid.[8,42,65] However, this problem may be easily overcome by using renewable energy. Thus, recent researches have been tailored towards the development of self-powered electrochemical system, designed by exploring the possibility of applying renewable energy source for powering the electrochemical environmental applications either directly or regulated by energy storage systems.[42,62–64] Solar photovoltaic, wind and biomass are some of the renewable energy sources that have been utilized to power different electrochemical technologies. Among them, solar photovoltaic seems to be more interesting and appealing for commercial application, because it is a mature technology that depends only on sunlight irradiation and can generate large amount of electricity at a reasonable cost.[65–68] However, the energy produced is not constant due to the time changes in solar irradiation intensity. Because of that, the use of intermediate energy storage facilities such as conventional batteries and redox flow batteries[69,70] have been investigated to achieve stable and efficient integrated systems.[71–73] The same situation occurs with wind turbines, which has fluctuating power output that makes very important its connection to energy storage devices in order to efficiently power electrochemical devices. Biomass energy based on energy recovery from waste has been developed and studied as self-sustained electrochemical systems. In particular, microbial fuel cell (MFC) devices capable of simultaneously generating electric power from microbial wastewater degradation.[74–78] These systems are still under the first steps of development, although in case of a successful development it may become the most sustainable electrochemical treatment technology, since the electricity comes directly from the treatment of wastes.

Recently, new approaches based on triboelectric nanogenerators (TENG)[79–82] and photocatalytic fuel cells[83–85] have been investigated as low electrical energy renewable sources for driven electrochemical wastewater and soil treatment technologies. Triboelectric generators are electrostatic power generator that converts mechanic energy to electrical energy by utilizing the mechanism of variable capacitance.[79,81,86] In TENG, electrostatic charges are created on the surfaces of two dissimilar materials which are in physical contact. The contact induces triboelectric charges and create a potential drops when the two surfaces are separated by mechanical force. The force can drive electrons to flow between the two electrodes built on the top and bottom surface of the material. Although TENG has low energy generation capacity, it is inexpensive and can be easily transported from one place to another. Photocatalytic fuels cells have also been investigated for in-situ driving of electrochemical technologies. They use faster and direct transportation of photogenerated electrons in photocatalysis (i.e. replacing the bioactive anode of MFC with photoanode) via external circuit to produce electricity.[85,87]

Although, a substantial reviews papers and some relevant book chapters are available on electrochemical wastewater and soil treatment technologies,[1,2,4,5,7–11,13,14,16,19,21–23,42,52,53] to our knowledge only few papers[62] have summarized some data on the renewable energy driven electrochemical technologies for the remediation of contaminated water/wastewater and soils. In this review paper, we present a comprehensive and rigorous review on this topic with consideration given to all varieties of sustainable energy sources that have been utilized to power electrochemical wastewater treatment, starting from the first solar photovoltaic powered electrochemical system to the present new devices developed until now. Firstly, the basic concept of solar photovoltaic energy production and its application in electrochemical separation and degradation of pollutants as well as wind energy counterpart were discussed. Detailed explanation on the principle of energy production, configurations and utilization of the energy produced in MFCs for BESs – electro-Fenton's system as well as the mechanisms of reactive oxygen species (oxidants) generation and organic pollutants degradation were vividly considered. Recently developed renewable energy sources vis-á-vis TENGs, PFCs and batteries were extensively discussed with focus on their basic principles of energy production, rectification and amplification, mechanism of oxidants formation as well as organic pollutants degradation. The possible scale-up and applicability on industrial scale, taken into consideration the design, parameter optimization as well as implementation were also discussed. Critical challenges and future prospects concerning the economic and environmental analysis required for the industrial and commercial success of renewable energy driven electrochemical technologies were extensively examined and brief conclusion remarks were provided.

2 Sources of green/renewable energy

Renewable energy sources (RESs) have been projected to play an important and strategic role in the future global energy portfolio.[67,71,88] Originally, RESs were proposed as an alternative to the depletion of the fossil fuels, and it presently represents an optimal solution for achieving sustainable energy system. However, the current situation of global warming, as a result of continuous emission of greenhouse gases, has forced the regulatory agencies and policy makers to identify RESs as one of the urgent and immediate measures to address the climate change.[89–93] The global energy demand is anticipated to grow by 37% by 2040, with most consumption concentrated in Asia,[71,94] but the greatest worries is the recent modification in energy mix owing to: (i) unresolved conflict in the Middle East and escalated tension between Russia and Ukraine, which is threating the region with cheap oil price and gas security respectively, (ii) nuclear energy which still remain major source of power for many countries, even with the controversies and strict regulation on security and environmental issues concerning it and (iii) promotion of regulations that discourage the development of energy sources with low carbon content, which may affect the actualization of the targeted energy demand.[71] Unfortunately, fossil fuels still remain the main source of energy in most countries and continuous emission of greenhouse gas, which threating the climate change as well as damaging the various ecosystems, still persist in those region.[90,95,96] Some authors has projected that, to achieve the targeted maximum global temperature increase of 2ºC, the fossil fuels reverses must remain unused within the period of 2010 to 2050.[97] The global aim is to make all energy sources in this 21st century clean, renewable, reliable and affordable in all sectors including transport, electricity, heating etc.[93,98,99] However, the main challenges mitigating the development of RESs are excessive subsides given to fossil fuels, which make it seem cheaper source of energy as well as inappropriate and ineffective policies that make adoption of some RESs on commercial scale appear difficult.[71,94]

Solar PV and wind energy are the major contributors to the growth of global renewable energy with approximately 74 GW and 52 GW installations respectively at the end of 2017.[100–102] There was also increasing expansion in bioenergy with total new addition of 9 GW, majorly from China, India and Thailand.[101] The most critical engineering parameter in solar and wind energy is solar irradiation and wind speed, which determines the energy yield of the solar PV and wind turbine, respectively. Unfortunately, these parameters are controlled by nature. As such, they vary from season to season and from one location to other.[67,103,104] The variation and fluctuation of these parameters is a big challenge in selection of sites for solar PV installations and wind farms. Therefore, all optimization and strategies to achieve maximum power from installations are channeled toward design of higher energy conversion PV cells and wind turbines, strategic installation and use of accessories to track solar radiation and wind speed.[105–107] These topics are extensively discussed in section 3 – 5 of this manuscript.

Nevertheless, over the last decade, excellent progress has been achieved in utilizing RESs is several key sectors of the World economy, especially the solar PVs and wind turbines, which are capable of generating large amount of electricity when several units are combined. For instance, RESs accounted for almost two-third of net new power capacity addition around the globe in 2016 (Fig.3a), with approximately 164 GW electricity capacity additions.[100,101]

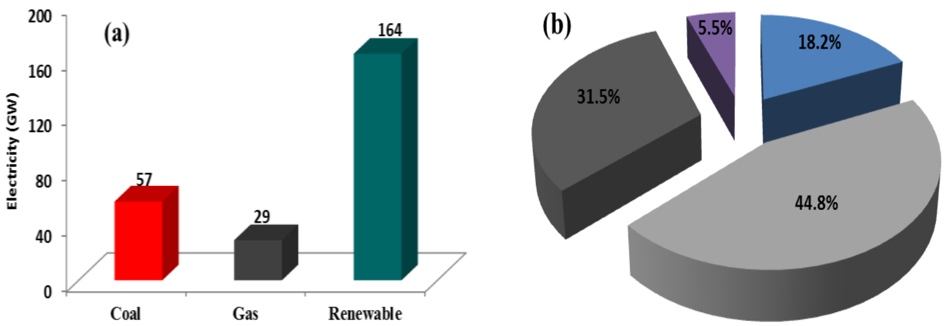

Figure 3: (a) Electricity capacity additions by fuels in 2016 and (b) renewable electricity generation by source in 2016: (■) hydro, (■) solar, (■) wind and (■) bioenergy. (Data obtained from IEA and IRENA renewable statistic 2017).

Interestingly, new solar PV and wind turbines contributed over 40% (i.e. 74 GW) and 30% (i.e. 52 GW) respectively (Fig. 3b), of the RESs new power capacity, with almost half of the solar PV expansion emanated from China. China remains the undisputed renewable energy growth leader, with about 40% of global renewable capacity growth, which is mostly accelerated by their concerns about air pollution.[95,107–109] It has been projected that by 2022 three countries namely, China, US and Indian will account for two-third of global renewable expansion (Fig.4).[100] The key factor responsible for the astronomic growth in renewable energy, especially solar PV and wind, is the gradual change in renewable energy policies in many countries, from government-set tariffs to competitive auctions, which has allowed 30–40% reduction in remuneration level for solar PV and wind in two years (2010─2012) in some key countries such as India, Turkey and Germany.[96,100,110] The auction prices for solar PV and wind continue to fall even though the average generation cost of new-built projects remain higher.[96,100]

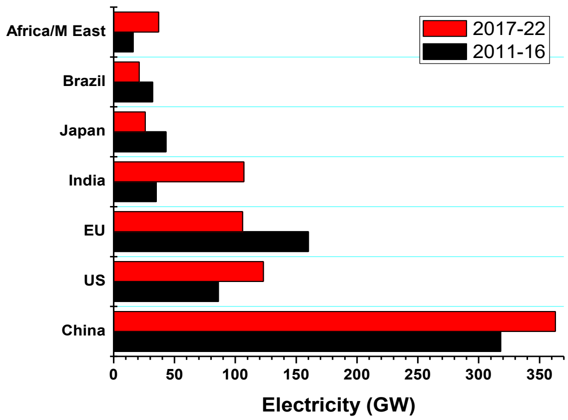

Figure 4: Renewable electricity capacity growth by continent/country (■) 2011–2016 and (■) 2017–2022. Data obtained from IEA statistic and data 2017.

The RESs have been incorporated into several key sectors, not only for the purpose of overcoming the economic challenge of fossil fuels and conventional energy, but also to eradicate incessant pollution caused by fossil fuels. For instance, because of the extremely abundant of wind, wave and solar energy resources on ocean, RESs have been utilized to power large ships to reduce the energy consumption and eliminates extremely large pollutants' emission, especially in the large ocean-going ships.[105] Similarly, RESs with energy storage systems especially solar PV have substituted several fossil fuels electric generating sets and conventional electricity in residential areas,[71,98,111,112] water pumping systems,[113–116] irrigation for farm lands,[117–119] heat and cooling system,[120,121] and mining industries[122,123].

Recently, RESs have been investigated as a clean, avoidable and more accessible energy source for powering electrochemical treatments.[62,63,124,125] This become necessary not only because of low cost of renewable energy compared to huge investment in electricity required for electrochemical technologies, but also because of its portability and accessibility, even in the most remote areas or isolated communities, where electricity grids are not easily accessible or available. In most cases, the electrochemical wastewater treatment system is connected either directly to the output of the renewable energy source or via intermediate energy storage system. The use of energy storage system such as batteries may constitute additional problem in term of cost, loss of energy in charge-discharge cycles as well as environmental impact of batteries disposal after usage,[63,71] but it has advantage of maintaining steady energy supplies to the electrochemical reactors rather than the fluctuating output usually encounter in most RESs.

Two major challenges are mitigating the coupling of RESs with electrochemical reactors: (i) how to manage the fluctuation of the energy source and (ii) how to fit the energy demand and production. Although up till date, the success of renewable energy driven electrochemical technologies in wastewater and soils remediation have most been demonstrated in laboratory or pilot scales (with few commercial installations for PV powered electrodialysis), the potentiality of the systems for commercial and industrial applications is extremely high because it helps to solve the World's two most pertinent challenges: energy and pollution. Pioneering studies on renewable energy driven electrochemical wastewater/soil treatment technologies were focused on the use of solar PV cell and MFCs – bioelectrochemical technologies, possibly due to the industrial revolution in PV cell production and economic benefit of MFCs. Some studies have also considered wind energy to power electrochemical technologies due to its availability and possibility of generating higher quantity of electricity.[124,126] Of recent, new generation of portable low energy RESs such as TENGs, PFCs and durable energy storage devices mostly batteries have been investigated as RESs for driven electrochemical technologies on laboratory scale. The next four sections describe in detail the fundamental principles of electricity production in these aforementioned renewable energy sources, different configurations in used, mechanisms of pollutants degradation and summary of relevant studies that have utilized them to power different kind of electrochemical devices.

3 Solar (photovoltaic cell) energy driven electrochemical technologies

Photovoltaic energy (PV) is one of the most promising technologies. It has been projected as being a strategic electricity source which has becoming one of the major supplier of electricity both for industrial and household use. PV cells converts sunlight into electric energy directly, via photovoltaic effect and has emerged as a valuable and sustainable approach to overcome global energy and environmental crisis.[93,113,123,127] According to IRENA, the generated cumulative power capacity by PV systems as at end of 2016 was 397 GW, representing 18% of the global renewable energy generation capacity and 34% growth with respect to the previous year.[101] Studies have shown that the payable cost of electricity of decentralized solar PV systems is falling below the variable portion of retail electricity prices that system owner pays in some markets, across residential and commercial segments.[94,128] Indeed, more PV capacities have been added since 2010 than in the four previous decades.[129] The renewable energy market was previously dominated by European countries (Italy and Germany in particular) up to 2013, but China, Japan and USA have recently recorded significant growth, with China to remain the leader in PV global market and account for the 37% of global capacity by 2050.[100,129]

The PV power generation systems have invariable nature and do not produce any harmful byproducts.[67,127,129] The solar intensity may vary with season and region, but it is an inexhaustible and freely available energy resource across the globe. The PV energy source can be used as stand-alone or grid-connected systems and the source has been used in water pumping, battery charging, home power supplies, street lighting, refrigeration, mining, swimming pools heating system, hybrid vehicles, telecommunications, military space and satellite power systems and hydrogen production.[122,123] Solar PV cells have also been investigated as clean and alternative electricity sources for driven electrochemical wastewater and contaminated soil treatments.[55,62] This is an important development because energy cost has been the main challenge of electrochemical environmental technologies as mention earlier, even though it remains the most effective treatment technique for removing recalcitrant organic pollutants. The use of renewable energy sources such as PV, which is inexpensive and portable will enable easy adaptation of electrochemical technologies for industrial application as well as in rural and remote area where access to electricity grid is very limited.

3.1 Solar photovoltaic cells: Principle, design, operation and energy optimization

3.1.1 Principle of solar photovoltaic and types of PV cell technologies

Solar cells consist of semiconductors (mostly silicon) with positive–negative (P-N) junction which form a potential barrier.[67,130] When semiconductor materials are exposed to solar light, some portions of the photons of the light radiation are absorbed by semiconductor crystal (P-N junction), which creates the excitation of a significant numbers of electrons and a potential difference across the junction. The electric field at the P-N junction drives the electrons into the N-region, while the positive charge holes are driven to P-region in a process called photovoltaic effect.[131] An in-built potential barrier in the cell acts on the free electrons to generate a voltage, which can drive a current through a circuit.[65,131] The semiconductor materials that convert solar light to electrical energy are termed photovoltaic cells.[65] Solar PV array electricity production fluctuates, depending on the operation and field conditions such as sun's geometry locations, solar irradiation intensity and local temperature.[65,132] The equivalent circuit of a PV cell is shown in Fig 5. The absorbed photons create a potential difference across the P-N junction with the flow of charge-carriers (electrons and holes) resulting in photo-current (I_{PV}), which is paralleled by a P-N junction diode (D).[65,133]

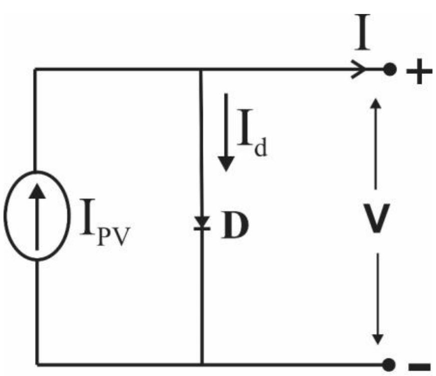

Figure 5: Simplified equivalent circuit of a photovoltaic cell[133]

Previous studies have shown that the preferred operating temperature for PV ranges between 0ºC to 75 ºC.[131] PV installations operating at high ambient temperatures and high PV modules surface temperature are usually associated with PV panel overheating, which reduces the efficiency drastically.[134] The effect of temperature on the electrical efficiency of solar PV modules is analyzed according to Eq. (12):[131]

$$\eta_{PV} = \eta_{TR}[1 - \beta_R(T_C - T_R) + \gamma log_{10} I_{PV} \quad (12)$$

where: η_{PV} is the PV module efficiency at room temperature; T_R (25ºC); β_R is the temperature coefficient for cell efficiency (~ 0.004 – 0.005/ºC); I_{PV} is the average hourly irradiation incident on the PV cell at normal operating temperature, T_C is the PV module temperature and γ is the radiation intensity coefficient for cell efficiency, which is usually assumed to be zero.[135] Thus, Eq. (12) can be rewritten as:

$$\eta_{PV} = \eta_{TR}[1 - \beta_R(T_C - T_R)] \quad (13)$$

A basic PV system integrated with utility grid (on-grid) and energy storage is shown in Fig. 6. The major components of a typical PV system are: (i) PV solar arrays collectors (ii) power conditioners, (iii) energy storage system and (iv) solar inverters. The solar energy of the sunlight is converted to DC power by PV arrays and the conversion rate depends on the insolation.[65] Blocking diode situated immediately after the arrays ensure the array generated power flows only towards the power conditioner and mitigate the backward flow of power which could occur during low insolation when the battery discharge back to the solar array.[65,112] The power conditioner consists of maximum power point tracker (MPPT), a battery charger and a discharger controller.[136] The MPPT ensure that maximum power generated by the PV array is extracted at all time, whereas the charge-discharge controller function as a charge regulator which prevent over-charging and over-discharging of the energy storage bank (batteries) necessary to store the electricity generated by the PV array conditioner.[65]

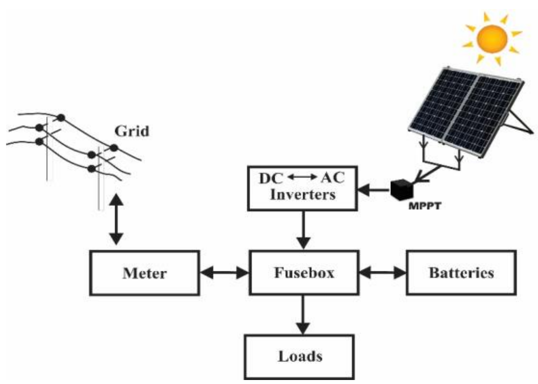

Figure 6: Schematic of a typical solar photovoltaic system

The first generation of PV cells consists of crystalline silicon (c-Si) and currently account for about 85–90% of the global PV module sales.[103,129,130] Their dominance in the market could be attributed to their low costs and best commercially available conversion efficiency.[67,127,129] Two main categories are currently present in market: (i) mono-crystalline (mc-Si) and (ii) poly-crystalline (pc-Si) PV cell. Although the PV technology is still evolving, c-Si PV cells have a wide range of well-established manufacturers all over the World. The c-Si PV cells have distinguished advantages because its basic material is Si, which is relatively abundant on the earth’s crust, non-toxic and semiconducting and it has natural oxide properties, low segregation coefficient for many metals and it is easily doped for P- and N-type junctions.[93,94,129] This has made the c-Si PV technology to achieve tremendous cost reductions in the last few years, even though the basic materials are still relatively expensive and it is still uncertain whether possible future supplementary cost reductions will be high enough to make it fully compete with modest solar resources in the wholesale power generation market.[94]

The second series is thin film (TF) PV technologies made of majorly chalcogenide nanocrystals – cadmium telluride (CdTe) and cadmium sulfide (CdS) and presently represent 10–15% of the global annual market.[129,137–139] CdTe has a band gap of 1.51 eV, which is very close to the solar spectrum for PV energy conversion, whereas CdS normally transmits visible spectrum and is usually used as window material for solar cell.[140,141] Both CdTe and CdS are very exciting technologies because they require low material and manufacturing cost, but have lower conversion efficiency as compared to c-Si and require higher land and cost of mounting.[141,142] The CdTe, copper indium (gallium) di-selenide (CIS/CIGS) and amorphous silicon (α-Si)/micromorph silicon (a-Si/μc-Si) are the three major groups of the TF PV technologies.[129,138,143] Some of the advantages of TF technologies include: low requirements of raw materials, high automation and production efficiency, easy of building integration and improved appearance, better efficiency at high ambient temperature and low sensitivity to overheating.[94,144] The major challenge of TF technologies, asides from efficiency and cost, is the limited experience on the lifetime performances on industrial scale.[129] However, several studies are still ongoing both in laboratory and industrial R&D to expose the TF technologies to market and create necessary “technical know-how” for industrial manufacturing and long-term service life. Additionally, the shortage of c-Si has pushed and accelerates the manufacturing of thin TF modules. Besides, it also faces challenge of material toxicity and availability, as well as durability of the cell.[129,138,145]

Concentrator photovoltaic, advanced TF and organic solar cells are the third categories of PV technologies. Although, these PV cells are not yet commercialized and still under laboratory and industrial R&D for improvement on both economic and environmental adaptability, they are potentially of higher efficiency solar cells with new conversion concepts and processes.[129,146,147]

3.1.2 PV design, array configuration, orientation and tilt angle

The PV cells collect photons emitted from sun light rays, which carry energy flow with disorder and fractal path.[62] The interaction between the photons and the cell could be described by the entropy generation related to open system because of the irreversible flow of photon energy.[62] The entropy of production of photons from the sun rays to the Earth is described according to Eq. (14).[148]

$$S_{g,v} = \frac{h\upsilon N_\upsilon}{T}\ln\left(\frac{d_{SE} - R_S}{R_S}\right) \tag{14}$$

where h is the Plank's constant (6.626×10^{-34}), υ is the frequency, N_υ is the number of photons emitted from the Sun, T is the temperature of the universe (2.7 K), d_{SE} is the distance between the Sun and Earth (1.49×10^{11} m) and R_S is the radius of the Sun (6.96×10^{8} m).

Several models are available in literature for PV design. Efficient modeling of the PV operating components such as the power generator, energy storage devices, power electronic interface and loading is necessary to improve the efficiency of the PV system. A summary of different design methodologies and models have been reported in literature.[129] It should be noted that to obtain maximum energy efficiency and ensure lowest energy lost in an ideal system conditions, the entropy generation must be minimum.

PV array is the complete power generation section of the whole solar photovoltaic assembles and it consists of numbers of photovoltaic panels. Each PV panel consists of one or more modules connected to form a unit. In each module, there are a numbers of solar cells, which are connect in parallel or series to generate higher energy. The arrangement of the solar arrays influences the current-voltage (I–V) output of the PV system. For instance, PV modules with series connection of arrays have increased open circuit voltage ($V_{oc, array}$) and constant short circuit current ($I_{sc, array}$), whereas increased $I_{sc, array}$ and constant $V_{oc, array}$ are obtained in a single PV panel with modules connected in parallel.[63] The amount of power generated in PV cell is mainly controlled by the PV array configuration and the power output of PV is related to number of panels (N) and modules (M) by the Eq. (15) and (16).[62]

$$V_{oc, array} = NV_{oc} \tag{15}$$

$$I_{sc, array} = MI_{sc} \tag{16}$$

The choice of series or parallel connection configuration depends on the desired voltage and load to be connected with the PV cell. In all cases, the design and configuration should be flexible to accommodate changes to the unpredicted solar irradiation fluctuations.

Aside from mounting the PV arrays on stable and durable structure that can support the array and withstand nature (i.e. rain-fall and wind) and corrosion, the orientation and the structure tilt angle is very important parameter to achieve maximum amount of Sun irradiation on the solar panel.[62,149] The structure tilt or tilt angle is determined by the electrical loading required, the location latitude and the orientation of the structure.[149] To obtain highest annual energy output, the solar panels are generally oriented toward equator with the modules pointed South in the Northern hemisphere and North in the Southern hemisphere, all incline at the same angle as the local latitude.[150,151] However, some authors have shown that to obtained maximum solar radiation, the tilt angle varies from location to location and optimum tilt angle depends on the local latitude as well as climate condition.[152]

It important to state that rack mounting is currently the most common type, because it is highly versatile, robust and easy to construct and install. Besides, for PV panel mounted on ground, tracking mechanisms may be employed which automatically rotate the panel to follow the sun movement, thus enhancing the energy output. Trackers are designed to be either single-axis which can track Sun from east to west or dual-axis which allows the panel to constantly face the Sun directly throughout the day.[153,154]

3.1.3 Optimization of PV power out (MPPT and electronic interface)

The power output of PV modules depends on insolation, temperature and voltage. Careful selection or variation of any of these parameters may ensure maximal power generation. Indeed, solar PV power fluctuates due to variations in radiation and temperature and its power output may also be influenced with loading, especially when the loads are connected directly to the modules.[65] There is always mismatch between the PV cell capacity and loading. Because of that, PV modules are required to be over-sized to meet the power demand during the low irradiation periods.[65,105] Besides, using tracker that tracks the direction of the Sun and some electronic circuits which can extract maximum power from the PV panel during different climate conditions can maximize the power output of PV modules. Such electronic devices, which are essentially DC to DC converters, are termed MPPT.[65] MPPT devices ensure that the PV modules run at the Maximum Power Point (MPP) by extracting the correct amount of current such that the load is always supplied with the maximum possible power generated under the given weather conditions.[65,105,129] Several MPPT electronic instruments and peripheral interface controller (PIC) are available in the market and the choice for a particular PV system depends on the cost and the gain in the power output when utilized. Relatively high cost MPPT/PIC may be a viable choice for high power PV system, where the cost of the gain in power output outweighs the price of the MPPT/PIC.[65]

3.2 Solar PV cells driven electrochemical separation technologies

Production of fresh/drinking water from sea/brackish water using electrodialysis powered by solar PV panels were the first set of renewable energy driven electrochemical technologies that was investigated in late 70's. This technology termed (PV- ED) was extensively developed and optimized and consequently, many pilot/field studies and installations were carried out in 80's using standalone PV modules (Fig. 7), especially in Asia.[155–159] For example, Adiga et al (1987)[160] studied the feasibility of utilizing a 450 peak-watt PV panel with operating voltage of 80 V to power an ED plant for the production of 1000 L of fresh water per day from feed water having a total dissolve solid concentration of about 5000 ppm. The PV-ED system was able to operate for 8 h during the day at a flow rate of 120 L h^{-1}. Similar studies were conducted by Kuroda et al. (1987)[161] with the electricity of the PV either directly connected to the ED plant or via battery system. Since then, many studies have been conducted on feasibility and potential of

PV-ED for the commercial production of the fresh/potable water from sea/brackish water.[162–164] In most of the early studies on PV-ED, the three critical challenges encountered in most installations were (i) fluctuating output of the electricity produced by the PV panels (ii) low output of each PV unit and (iii) cost of installation.

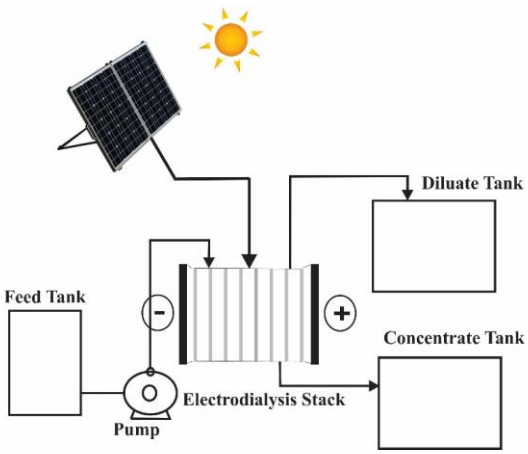

Figure 7: Schematic of typical standalone/off-grid electrodialysis plant. Adapted from ref.[165]

However, nowadays many PV-ED systems are installed with energy storage system especially batteries or using on-grid PV modules which not only ensure stable electricity supply to the ED units but also allow operation of the PV-ED over the nights and cloudy days, when the solar irradiation is negligible.[166] Besides, owing to the revolution and maturity of PV technologies, the issue of high cost of installations has been minimized and several units of PV can be mounted to achieved required electricity for driven ED. Additionally, several studies have been channeled towards the technical analyses, as well as financial, economic and social benefits of PV-ED technology especially in India and Arabian peninsula, where there is astronomic demand of fresh water production from sea and brackish ground water.[55,156,158,159,164,167] The PV-ED technology is maturing and ready for certification for commercial production of fresh water from desalination of brackish ground water. At present, there are many standalone/off-grid community-scale PV-ED desalination systems that serve as main source of portable water for many small communities and rural areas in India, Mediterranean, Gulf countries and Canary Islands.[156,164,168–170] Besides, many studies are still been conducted both on laboratory, pilot and field scale in order to optimize PV-ED system and ensure its full implementation on commercial scale. For instance, a Spanish research group[166] has investigated PV-ED system without batteries for the production of drinking water from brackish water in order eliminate the shortage of drinking water which is a major problem in Southern-Eastern part of Spain. It was reported that the PV-ED system was strongly influenced by the number and configuration of the PV modules, meteorological conditions, and characteristics of the ED reactor as well as the required volume of brackish water to be processed. Besides, the authors found that electric energy consumption of the ED system was proportional to the saline concentration of the brackish water and to reach irrigation water quality, lower energy was required as compared to the requirement of drinking water. Based on the results obtained, a standard model was proposed for effective prediction of the behavior of PV-ED system under different conditions. Other recent studies and advances on PV-ED system are summarized in Table 2. Moreover, some review papers are available on the solar power desalination processes using either electrodialysis or reversed osmosis membranes or both.[157–159]

In contrast, solar PV driven electrocoagulation is a relatively new technique and the pioneering evaluation was reported by Valero et al very recently (2008).[171] These authors investigated the EC treatment of synthetic textile effluent directly powered by PV modules. Two PV modules connected in either series or parallel were utilized as source of electricity. The PV modules with a power peak of 38.4 W and surface area of 0.5 m^2 were mounted at tilt angle of 55º with the modules facing south (0.4º W). Parameter J_v, which is the ratio between current density (j) and flowrate (Q), was maintained at constant value throughout the treatments by adjusting the flow rate. The obtained results for different effluent treated by EC using PV modules are summarized in Table 1.

Table 1: Results of different effluent conductivities EC experiments powered by PV modules

Conductivity (μS cm^{-1} at 20ºC)	G^a (W m^{-2})	V^a_{cell} (V)	I^a (A)	τ_{EC}^b (min)	T^a (ºC)	Decolorization efficiency (%)
Series PV array						
180	751	26.3	1.83	16	65	96.4
505	720	1.0	1.91	14	41	99.6
1997	777	4.6	2.13	13	31	99.1
Parallel PV array						
180	720	17.4	0.77	37		91.3
505	736	15.7	2.45	11	42	98.8
1997	745	7.3	3.91	7	32	99.1

Experimental conditions: $[RB]_0$ = 250 ppm, pH_0 = 6 and $J_v = 3 \times 10^8$ C m^{-2} m^{-3}.

[a]Average values of G, V_{cell} and I. Variation of the these parameters through all the tests were lower than 3%

[b]τ_{EC} was the time employed to treat three 80 mL samples.

As depicted in Table 1, over 90% removal of the Red Remazol 133 dye contained in the effluent was achieved in less than 20 min by EC treatment with either series or parallel PV modules array. Similarly, EC directly powered by solar PV modules has also been utilized for the removal of phosphate from landscape water.[172] The PV modules (30 W) mounted at 30 ºN facing south (15 ºW) and tilt angle of 30º had an I_{sc}, optimum operating current (I_{mp}), V_{oc} and optimum operating voltage (V_{mp}) of 1.93 A, 1.74 A, 21.6 V and 17.2 V, respectively. The total phosphate removal of 97.77 ± 2.13% was achieved at optimal experimental and climate conditions in less than 30 min of EC treatment. More recently, Hussain et al. (2017)[173] reported the removal of lead by EC powered by solar PV using novel perforated zinc electrode. The solar PV with an optimal I_{sc}, I_{mp}, V_{oc} and V_{mp} of 9.02 A, 8.3 A, 30.71 V and 30.2 V respectively was installed at 3º N latitude and 101º W longitude. The EC with solar PV was able to achieve 99.1%, 78.8%, and 74.4% lead removal after 1 h treatment at solar irradiation of 950, 410 and 165 W m^{-2} and temperatures of 33, 28 and 26ºC, corresponding to sunny, partly cloudy and cloudy weather respectively. In the same manner, García-García et al. (2015)[174] have studied the feasibility of EC powered by solar PV for the treatment of industrial wastewater collected from influent of treatment plant located at the outlet of an industrial park. The PV modules, which could provide up to 225 W, 17.02 V V_{oc} and 7.5 A I_{sc}, were mounted at 19 ºN, 99.7ºW and tilt angle of 18º. By using copper as electrode and 1–3 A current supply by solar PV, the EC was able to achieve 89%, 97%, 91% and 48% COD, color, turbidity and TOC removal efficiency respectively, in only 50 min. It is imperative to state that up to date, all studies on PV-EC utilized standalone/off-grid PV systems and have only been performed either on laboratory or pilot scale. As such, extensive works are still needed to optimize the PV-EC system both on small and pilot scale in order to adapt the technology for field/commercial usage.

Electrokinetic soil remediation powered by standalone/off-grid PV modules has been investigated both on laboratory and pilot scales for the treatment of organic and heavy metals/toxic anionic contaminated soils. A typical PV powered EKSR reactor developed by Rodrigo's group[175] is shown in Fig. 9a. The group[175] have reported the used of solar PV powered EKSR for the treatment of soil contaminated by 2,4-D herbicide. As depicted in Fig. 9b, the solar irradiation fluctuates in response to the day-night cycles, with maximum solar irradiation values during the noon time slot and minimum during the night. The maximum values obtained day by day also fluctuate (range from 275–513 W m^{-2}) as expected due to the changes in climatological conditions (alternation of sunny and cloudy days). As shown in Fig. 9c, the current intensity supplied by the PV was clearly influenced by the solar irradiation and similar trend was observed for current intensity profile with maximum daily peaks of intensity ranges from 0.59 to 0.77 A and almost null current during the nights. The 2,4-D removal efficiency of 73.6% was reached after 15 days of treatment using solar PV power (Fig. 9d), which was lower as compared to 90.2% obtained with continuous DC at similar experimental conditions because of the reversion of kinetic processes over night. Other studies on electrochemical separation powered by solar PV are summarized in Table 2.

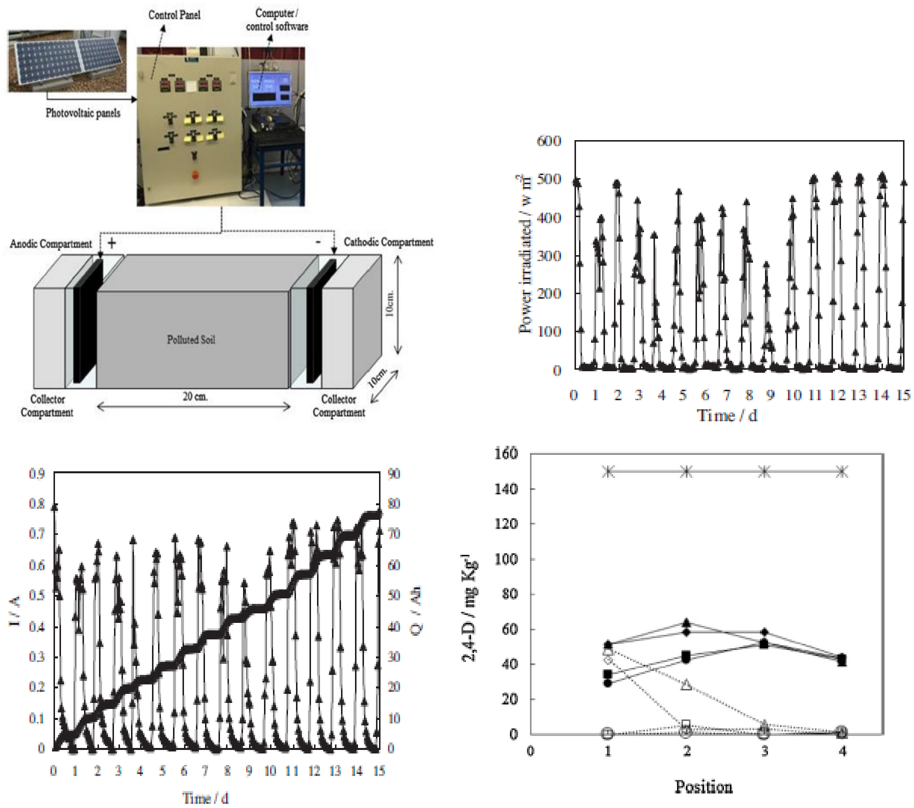

Figure 9: (a) schematic of solar PV–EKSR pre-pilot cell, (b) evolution in solar irradiation, (c) profile of supplied current intensity and total charge supplied to the EKSR cell and (d) 2,4-D pesticide map of the soil after the remediation tests powered by PV panels (full symbols) and DC power supply (empty symbols). Upper right position (●, ○), upper left position (■, □), bottom right position (♦, ◊) and bottom left position (▲, Δ). Printed with the permission of ref.[175]**(Prof. Rodrigo should please provide us with the soft copy of these figures)**

3.3 Solar PV cell driven electrochemical degradation technologies

Solar PV powered electrochemical degradation/oxidation is an emerging technology with an exciting potential and huge capacity of facilitating the adaptation of electrochemical oxidation processes on commercial scale. Although still under development for optimization and further improvement, many results have been reported on standalone/off-grid PV modules powered electrochemical oxidation of different organic pollutants on laboratory/pilot scale. Most of the studies on solar PV powered electrochemical degradation processes were performed by research groups from Spain, using electrooxidation with conductive boron-doped diamond electrode and autonomous solar photo-electro-Fenton process. However, an earlier study[64] investigated solar PV electrochemical oxidation of several phenolic compounds contaminated wastewater at the Bi–doped TiO_2 anode with simultaneous production of molecular hydrogen from water/proton reduction at the stainless steel cathode, as depicted in Fig. 10. Anodic current efficiencies in range of 3% to 17% were obtained for the complete oxidation of phenolic compounds, while the cathodic current and the energy efficiencies for hydrogen gas production ranged from 68% to 95% and 30% to 75%, respectively. Solar PV powered anodic Fenton has also been reported for decolorization of textile wastewater using a flow cell equipped with RVC cathode and gauze stainless steel anode with electricity directly supplied by solar panel (50 W, 17 V, 2.9 A, BP 350U cell).[176] Over 90% COD removal was reached after 2.33 h of treatment at cell current of 0.2 A. In another study, Ochia et al. (2010)[177] investigated solar PV driven sequential electrooxidation-photocatalysis processes for the treatment of river water using BDD electrode and TiO_2 photocatalyst. Three PV cells (V_{Pmax} = 17.4 V, I_{Pmax}= 7.2 A for each cell) with batteries were utilized to provide electric power for the mechanical system, the electrolytic reactor, as well as charging of the batteries for the use in cloudy/raining day or at night. Complete COD removal (450 mg L^{-1}) was attained by combined electrooxidation and photocatalysis process with pseudofirst kinetic rate of 5.1×10^{-3} observed for the COD decay during electrolysis with BDD electrode. Similarly, PV solar electro-oxidation (PSEO) was extensively studied by Alvarez-Guerra et al. (2010; 2011a,b)[178–180] using BDD electrode for the treatment of urban and lignosulfonate wastewater. The solar PV which consists of four monocrystalline silicon modules (SunTech STP 160) was mounted at tilt angle of 38º and south orientation (20º W) and was able to provide current densities in the range 10 – 60 mA cm^{-2} for the electrooxidation process. PSEO was found to be efficient for the mineralization of the organic in the wastewater with first order kinetic rate of $1.38–1.98 \times 10^{-3}$ min^{-1} attained for the decay of the TOC.

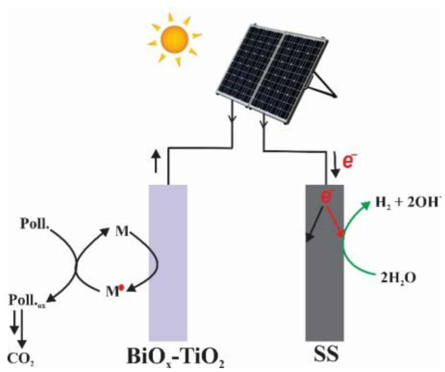

Figure 10: Schematic of a solar PV driven hybrid system for simultaneous electrochemical wastewater treatment and hydrogen production from water splitting. Adopted from ref.[64]

Valero et al. (2010, 2014)[63,181] demonstrated the feasibility of using an electrooxidation directly powered by solar PV for the treatment of wastewater from almond industry and textile effluent containing Remazol RB 133 dye. The solar PV module (PQ10/40/01-02 AEG) located at 38º 24' N, 0º 31' W, tilt angle of 55º facing south (0.4º W) and altitude 109 m above the sea level consists of polycrystalline silicon cells with peak power of 38.8 W and V_{OC} of 20 V. As expected, the current output of the PV varies with irradiation and complete decolorization of Remazol RB 133 and 75% COD removal from almond wastewater were reached after 400 min. Souza et al. (2015)[182] have also reported solar powered conductive diamond electrode oxidation for the treatment of herbicide 2,4-D. The PV module (38.59ºN, 3.55^0 W and oriented south) could supply current peak of 5.3–5.9 A at maximum irradiation of 450 W m^{-2} and average daily charge supply of 22.5 A h m^{-2} day^{-1} on a sunny day. Complete degradation of the herbicide 2,4-

D and its mineralization was attained by solar powered electrooxidation with BDD (Fig 11a) in a similar manner to that observed for convention power supplied (Fig.11b), even though the authors observed more accumulation of many intermediates in PV powered electrooxidation (Fig. 11c) as compared to the direct DC powered process (Fig. 11d), which was attributed to change in the operating conditions (irradiation and temperature) during the electrolysis.

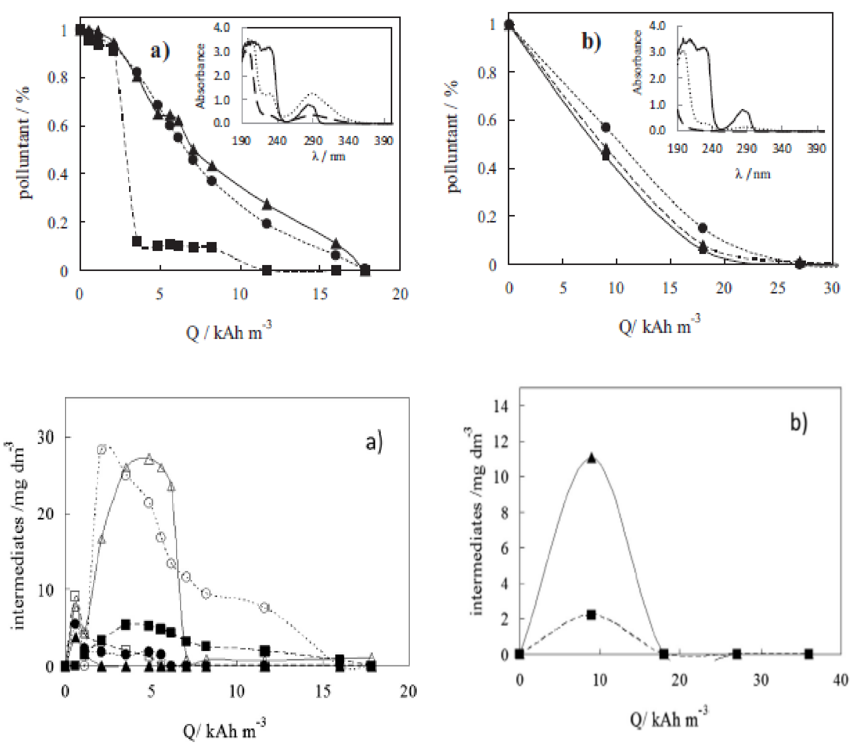

Figure 11: (a, b) decay of normalized (●) 2,4-D, (■) COD and (▲) TOC concentrations vs applied electric charge during the electrochemical treatment of synthetic wastewater polluted with 100 g dm^{-3} of 2,4-D using (a) solar panels and b) conventional power supply to power the electrochemical cell; and (c, d) evolution of the concentration of the main intermediates detected: (■) 4-chlororesorcinol, (□) 2-chlorophenol, (●) 4-chlorophenol, (○) 2,4-dichlorophenol, (▲) hydroquinone and (∆) benzoquinone vs applied electric charge during the electrochemical treatment of synthetic wastewater polluted with 100 g dm^{-3} of 2,4-D using (c) solar panels and

(d) conventional power supply to power the electrochemical cell. Printed with the permission of ref.[182] **(Prof. Rodrigo should please provide us with the soft copy of these figures)**

Brillas group[45,183] has recently developed an autonomous solar pre-pilot plant which utilized solar PV panel to power solar electro-Fenton process (SPEF). The pilot plant utilized electrochemical filter-press flow reactor system connected to the reservoir, pump, air pump and solar compound parabolic components (CPCs) to concentrate the solar radiation on the reactor (Fig. 12a). This process is highly versatile and efficient for complete mineralization of different classes of synthetic organic wastewater and can be easily scale-up for large scale treatment of organic contaminated wastewater.

(a)

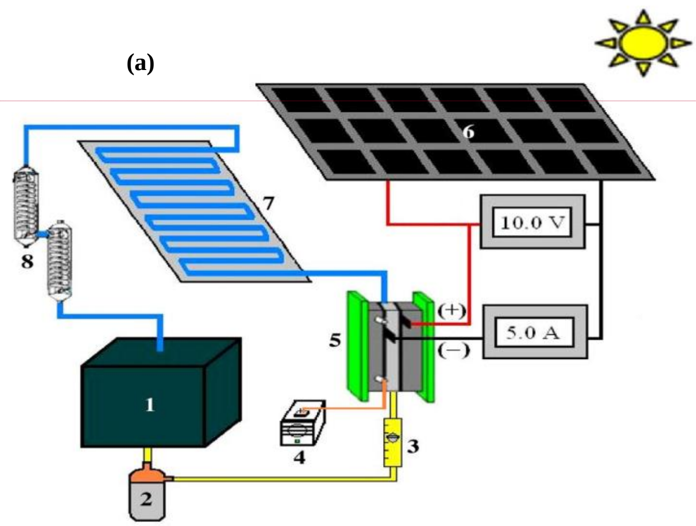

Comentado [MARR1]: Where is figure a?

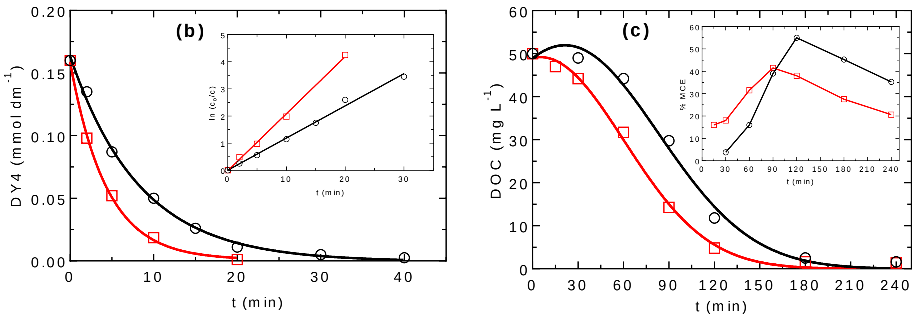

Figure 12: (a) Schematic diagram of autonomous solar pre-pilot plant: (1) Reservoir, (2) magnetic drive centrifugal pump, (3) flow meter, (4) air pump, (5) electrochemical filter-press reactor, (6) solar photovoltaic panel, (7) solar compound parabolic components and (8) heat exchanger, (b) color removal efficiency and (c) DOC decay obtained during the treatment of 0.16 mmol dm^{-3} Direct Yellow 4 (DY4) solution containing 0.05 mol dm^{-3} and 0.5 mmol dm^{-3} Fe^{2+} at pH 3 and 35 ºC by SPEF using the autonomous solar pre-pilot plant at a flow rate of 200 dm^{-3} h^{-1}. Average current: (○) 3 A and (Δ) 5 A. Inset panel of plot c present obtained mineralization current efficiency.

For example, Garcia-Segura and Brillas (2014)[45] utilized the autonomous pilot SPEF (Fig. 12a) for the decolorization and mineralization of Direct Yellow 4 diazo (DY4) dye solution. The pilot plant, which can treat up to 10 L of wastewater, was directly connected to PV modules that provided a maximum average current of 5.0 A. The filter-press reactor was equipped with Pt/GDE cathode and BDD anode and it was coupled to a CPCs photo-reactor of 1.57 dm^3 irradiation volume to illuminate the reactor. Complete decolorization of 0.32 mM DY4 was attained in less than 1 h and overall mineralization efficiency of about 96-97% was achieved in 4 h at 5 A applied current from PV cell (Fig. 12b and 12c). Similar results were achieved by the same authors for the treatment of monoazo, diazo and triazo dyes wastewater using the same pilot-plant at similar experimental conditions.[183]

Recently, a research group from US reported solar PV powered electrochemical disinfection of toilet wastewater from a pilot scale PV-powered self-contained mobile toilet system for possible reuse in toilet flushing and agricultural irrigation using wastewater electrolysis cell (WEC) (Fig. 13).[184] The solar PV modules simultaneously powered the toilet, electrochemical flow reactor and pumping system. The disinfection efficiency of the WEC was investigated with four microorganisms (Escherichia coli, Enterococcus, recombinant adenovirus serotype 5, and bacteriophage MS2) using real toilet and synthetic wastewater. Electrochemical production of ROS majorly $^{\bullet}OH$ and reactive chlorine species such as Cl_2, HOCl and ClO^- was ensured in the WEC by the application of current to the BiO_x/TiO_2 anode, as well as the presence of significant concentration of Cl^- ions (12 – 20 mM) in the real toilet wastewater. The authors showed that by application of cell voltage of +4 V, the WEC achieved 5-log_{10} reduction of all the seeded microorganisms in the real toilet wastewater within 60 min. In contrast, significant and rapid formation of chloramines was observed during the treatment of real toilet wastewater by chemical chlorination process, which reduces the efficiency of the disinfection process. Other relevant studies on solar PV driven electrochemical technologies are summarized in Table 2.

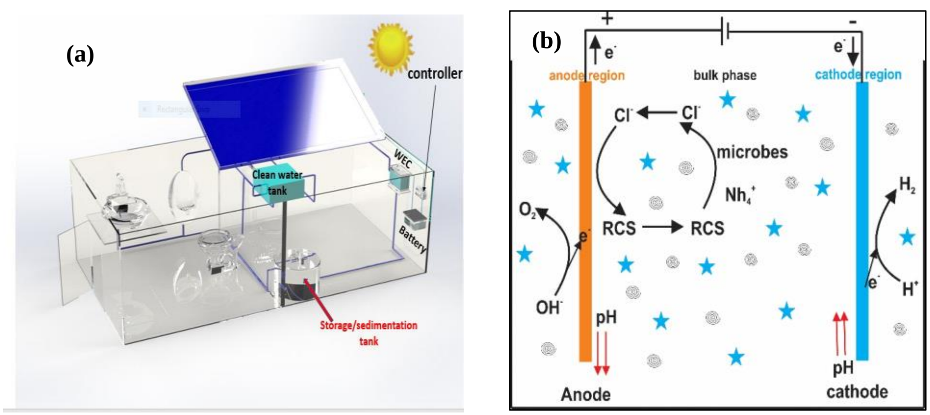

Figure 13: (a) schematic of the solar power mobile toilet and (b) wastewater electrolysis cell. Printed with permission of ref.[184]

Table 2: Summary of some relevant studies on solar PV driven electrochemical wastewater and soil treatment technologies

Pollutant	Technology	Solar PV energy	Experimental conditions	Efficiency
Saline groundwater	PV-ED	Peak output: 66 W, 24 V	Membrane stack: 24 ionic cell pairs of AR 204 SXZL 386 and CR 61 386 AM and CM respectively; feed saline water – 3300 ppm TDS; flow rate: 50 or 300 gal day^{-1}.	95% salt removal[165]
Brackish water	PV-ED	Peak output: 56 V, 14 A	EUR-2B-10P (EURODIA) pilot ED plant; membrane: ten 0.02 m^2 NEOSEPTA cell pairs; feed saline water: 1000 – 10,000 ppm TDS; flow rate 180 L h^{-1}	Salinity reduced to acceptable drinking water level[166]
ROC brine	PV-ED	Peak output: 160 W; 34.4 V	PCCell bench ED; Membrane stack: 2 ionic cell pairs of AM-PP RALEX and CM-PP RALEX AM and CM respectively; Fumasep FBM bipolar membrane; 1 mol L^{-1} NaCl ROC brine	~ 1 mol L^{-1} HCl production[185]
Cu	EKSR	Location: 48° 24' N, 89° 14' W; tilt angle: 48°; maximum output: 41 V and 5 A.	Cu concentration: 350 mg g^{-1} of dry soil; electrode: graphite; maximum applied V and I: 40 V and 0.6 A; time: 3 months	75% Cu removal from the soil and 92% Cu removal near the anode[186]
As	EKSR	Maximum output: 40 V	As concentration: 219.3 mg kg^{-1} of dry soil; electrode: iron; potential gradient: 0 – 1.33 V cm^{-1}; time: 35 days	27% and 32% As removal by solar PV and DC powered EKSR respectively[187]
Cd	EKSR	Location: 30° 37' N, 114° 21' E; maximum output: 5 W, 21 V and 0.34 A for V_{OC} and I_{SC} respectively; temp.: 11 – 27 °C;	Cd concentration: 140 mg kg^{-1} of dry soil; electrode: graphite sheet; time: 48 h	17.1% and 18.3% Cd removal for cloudy and sunny days respectively[188]
Cr/Cr(VI)	EE-EKSR	Location: 34.6° N, 112.4° E; nominal	Cr/Cr(VI) concentration: 1858/623 mg	43.65%, 91.88% and 19.32%

		output: 10 W, 22 V and 18% photoelectric conversion; temp.: 8 – 26 ºC.	kg^{-1} of soil; pH 8.3; electrode: graphite sheet; time: 144 h	Cr, Cr(VI) and Cr(III) removal efficiency respectively[189]
Fluorine	EKSR	Location: 34º 64'N, 112º 38' E; peak output: 10 W, 18 V and 18% photoelectric conversion	F concentration: 1,050 mg kg^{-1} of soil; pH 8.17; 20.51 g kg^{-1} of organic matter; electrode: graphite sheet; time: 96 h	22.3 % Fluorine removal efficiency[190]
Microalgae	EFL-F	Model: HONTEX-A830L; maximum output: 20 W, 5 V and 10 mA cm^{-2}.	20 L pond with inoculated algae; electrode: Zn, Al, Fe or Cu	95.83% algae removal using Al/C electrodes[191]
Trimethoprim (TMP)	SPEF	Location: 39º 57' 09'' N, 116º 29' 14'' E; working voltage and current: 18 V and 8.33 A	Undivided reactor, Ti/RuO_2 mesh/ACF electrodes; 125 mL of 200 mg L^{-1} solution of TMP 0.05 mM Na_2SO_4 at pH 3 and 0.1 mM Fe^{2+}	<80% TOC removal efficiency by SPEF after 360 min[192]
Industrial effluents	EO	Model: ERDM 225TP/6; location: 19.4^{0} N, 99.7^{0} W, tilt angle 18º power output: 225 W; V_{OC}: 17.02 V; I_{SC}: 7.5 A	Undivided batch cell, electrodes: BDD anode and Cu cathode; 125 mL of electrocoagulation treated industrial effluent at pH 2–7 and applied current 3 A	70.26% and 99.7% TOC and COD removal efficiency[174]
Methyl Orange	EO	Silicon solar cell	Undivided reactor; electrodes: birnessite, platinum and saturated calomel electrodes as working, counter and reference electrodes; 30 mL of 5 mg L^{-1} MO solution at pH 5.6; V = 2.0 V.	95.8 % decolorization with up to 91.4% after 10 cycle of reuse[193]

4 Wind energy driven electrochemical technologies

Wind is non-exhaustible, clean and environmental friendly source of energy found abundantly in most part of the World. Wind energy is one of the most rapidly advancing technologies in renewable and sustainable energy and has gained more popularity due to its low and stable cost compared to conventional fossil fuel.[194,195] It also has advantage of being available in remote and rural areas with limited access to the main electricity grid. Wind energy is suitable for location with wind speed greater than the cut-in speed. Indeed, the power generation rate in wind turbine depends mainly on the wind speed in a similar manner with the dependence of solar energy on sunlight irradiation intensity. The global wind energy capacity stands at 433 GW as at the end of year 2017, with over 52 GW installations in 2017 representing 10% capacity addition. China remain the leader in wind energy market with 15 GW installation in 2017 and total installation capacity of 114 GW,[101] while USA and Germany are the other major players in the wind energy market with installation capacities of 65 and 39 GW, respectively. The wind energy is forecasted to reach 666 GW by the end of 2019. Wind energy has been used for many applications such as windmills, water pumping, sealing boats and others.[106,196–198] As in the case of solar PV energy, it is not sustainable for long period of time. In particular, the energy output fluctuates time to time depending on the wind speed. Several reviews and books have been published on the principle of wind energy, wind turbines technologies, wind energy converters and harvester, wind farm locations and assemblage, wind energy policies and challenges, as well as it acceptability and rejection by citizen.[196,199–202] As such, it will only be discuss briefly in this paper.

4.1 Design, principle and operation of wind energy

Wind energy utilizes turbines which convert energy in wind speed to electricity. The major components of a typical wind turbine are shown in Fig. 13. The turbulent wind turns the propeller-like blades (two or more blades) around a rotor connected to the main shaft, which spins a generator to create electricity. In essence, wind turbines convert the kinetic energy in the wind into mechanical power in the shaft, which a generator can converts to electricity or can be used for specific purposes (such as grinding grain or pumping water).[200,203]

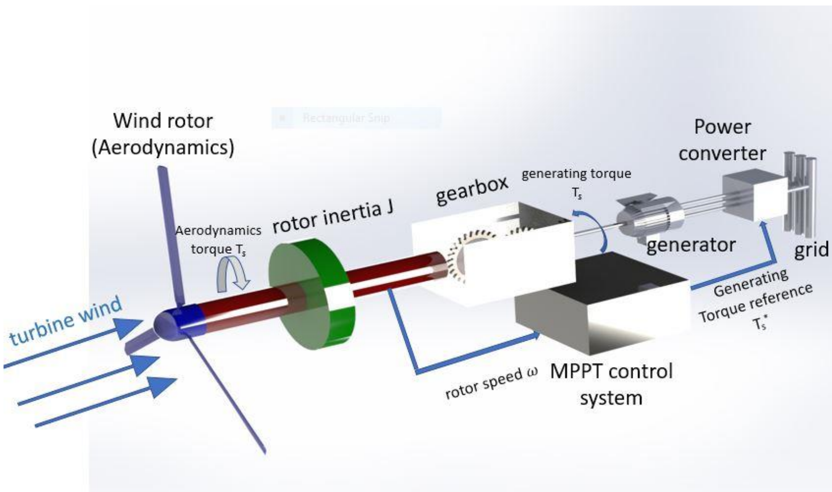

Figure 13: The major components of a typical wind turbine. Adapted from ref.[203] with modification

There are two main mechanisms for converting the kinetic energy of the wind into mechanical power of the shaft: drag and lift; both of which depend on retarding the wind and thereby extracting the kinetic energy (Fig. 14).[196,204,205] The drag is developed by obstructing the wind and the drag force is in the same direction as wind, whereas lift is produced when the wind is slightly deflected to extract the kinetic energy without turbulence and produced a large force (lift force) perpendicular to the direction of the wind with a smaller fraction of drag force.[205]

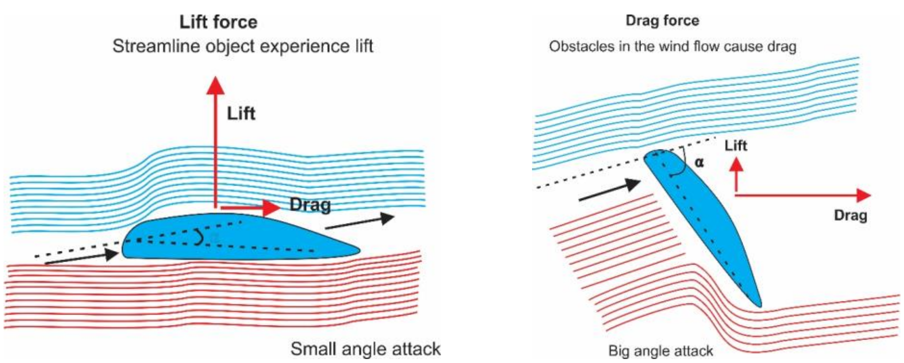

Figure 14: Principle of conversion of wind speeds in the wind turbine Adopted from ref.[205] with modification.

The power available in the wind is proportional to the wind speed and the area swept by the wind, and is given by:

$$P = \frac{1}{2}\rho A \upsilon^3 \qquad (17)$$

where ρ is the density of the air (1.2 kg m^{-3}), A is the cross-section or swept area of a windmill rotor and υ is the instantaneous free-stream wind velocity.

Considering the fluctuations in the wind speed, the energy in the wind can be express as:

$$E = PT = \frac{1}{2}\rho A \Delta t \sum \upsilon_i^3 \qquad (18)$$

where T is the actual torque and υ_i is the wind velocity at instantaneous torque Δt

Modern wind turbine can be categorized into two groups: the vertical-axis design and the horizontal axis design. Most windmills operate with horizontal axis wind turbines, which consist of two or three blades in upwind with the blades facing the wind.[200,206,207] However, research is still in progress for further optimization of vertical axis wind turbine to ensure full implementation on commercial scale. The advantage of the vertical axis wind turbine is that they do not require being oriented facing the wind because they present the same cross-sectional area to the wind from all directions; but this may constitute a major problem under storming conditions since the vertical axis rotor cannot be turn away from the wind to reduce the wind loading on it.[200,206]

Turbine blades are designed to meet the conflicting demands of structural capability (i.e. thicker airfoils) and aerodynamic efficiency (i.e. thinner airfoils). These competing demands are key considerations within turbine designs in order to optimize the aerodynamic blade shape for an enhanced power coefficient, increase the length of the turbine blades for increased swept rotor area and associated energy production as well as increase field reliability.[200] Turbine blades are designed based on the computationally predicted airfoils, which dictate the materials selection and structural features of the blades. Modern turbine blades are fabricated from fiber-reinforced composite material, which possess excellent specific modulus and stiffness values.[196,200,208]

Size of utility-scale wind turbines ranges from few kilowatts to several megawatts. Single small turbines with capacity less than hundred kilowatts are used for water pumping, homes and telecommunication dishes, whereas larger wind turbines are more cost-effective. Typically, they are installed in large numbers in wind farms to provide bulk electricity and they are connected directly to the grid. Low capacity turbines are most time used with energy storage devices like batteries or in conjunction with other renewable energy sources like photovoltaic and diesel generator in a hybrid wind system for off-grid application in remote locations.[207,209] Towers and foundations that support the wind turbines are a critical infrastructure in wind energy system and their design, assemblage and maintenance especial the offshore wind farms represent a unique challenge for structural engineers. A review on state-of-art on the design, structural and categories of towers and foundations for both onshore and offshore environment are available in literature.[200,208]

Wind farm installation and siting require careful consideration of many factors, even though wind is an inexhaustible and abundant resource. The technical aspects of wind farm location includes: (i) selection of the type of installation (i.e. on-shore or offshore), (ii) accessibility to sufficient wind speed at the height/depth at which the turbine is to be installed, (iii) good land topography and geological conditions (on-shore) for spaced installation of the turbines and rigid support of the towers and foundations, (iv) accessibility to grid lines and structures for easy transportation of generated electricity and (v) the type of turbine size in order to determine height/depth of the installation and the size of the tower/foundation as well as energy output. Economic factors such as capital cost, land cost, operation and management cost and electricity market should be considered before selecting suitable site for wind farm. Additionally, the possible effect of the wind farm on wildlife and endangered species, impact on human life (visual and noise), as well as electromagnetic interference are some of the environmental factors that should be considered in siting wind farm. Moreover, social considerations such as distance from residential areas, public acceptance, land and water use act and regulatory boundaries may affect the location of wind farm. Several research works and reviews are available on wind farm siting, cost, performance and challenges.[106,200,208,210,211]

4.2 Operating parameters optimization and energy storage

The optimization of the wind speed is the most crucial parameter for wind energy production and, in most cases; it is achieved by aerodynamic shape optimization of turbine blades design, as well as wind farm site location. Recently, variable-speed wind turbines have gradually become mainstreams of large-scale wind generation systems.[207,212] Several methods are employed for preliminary assessment of wind resources for a specific location using data obtained by meteorological stations. Among the existing methods, probabilistic mathematical functions such as Weibull and Rayleigh, wind atlas data, and indirect methods such as atmospheric boundary layer wind tunnel testing and numerical simulation with CFD (Computational Fluid Dynamics) are the prominent and most widely used for wind resources assessment.[203,207,213,214] In case of open areas like offshore with high mean wind speeds, Weibull and Rayleigh probabilistic functions are more effective, whereas the prediction of wind speed in the building environments is difficult owing to the varying roughness and obstacles in the path of the flow, which reduces the wind speed.[207] The reliable method for wind prediction in urban areas is by on-site direct measurement of the wind speed at the proposed position and altitude for the wind turbine installation, even though it is time consuming and expensive.[207]

Nowadays most wind turbines installations are usually equipped with MPPT control to regulate the rotor speed according to wind speed variations.[203] Wind turbines are controlled to operate at a specified window of wind speeds bounded by cut-in ($V_{cut\text{-}in}$) and cut-out ($V_{cut\text{-}out}$) speeds, operating outside this window is detrimental to both the turbine and the generator.[215] The wind turbines can be operated in three different regions, based on the prevailing wind speeds: (i) wind speed below $V_{cut\text{-}in}$, which should necessitate stoppage and disconnection from the grid (on-grid) to prevent it from being driven by the generator, (ii) moderate speed region that started from cut-in speed at which the turbine start working and ends at the rated speed (V_{rated}) at which the turbines produced rated (maximum) power and (iii) high speed region (between V_{rated} and $V_{cut\text{-}out}$) at which the turbine power is limited to avoid over-loading of the turbines and the generator, as well as ensure that the dynamic loads do not result in mechanical failure.[212,215,216] The MPPTs are applied in the moderate speed region to ensure maximum energy available is extracted from the generator of the wind turbines. Several types of MPPT control strategies, including tip speed ratio control, optimal torque control, power signal feedback control, perturbation and observation control and other MPPT methods which incorporates artificial intelligence algorithms like artificial neural network, fuzzy logic and neuro-fuzzy control have been utilized to optimize wind energy from turbines.[203,217,218]

The growths in quantities of electricity from renewable resources present a new set of technological challenges, such as the non-stability of the energy from renewable resources and distance of the installations from population centers, which are not previously encountered by the electricity grid.[219] For on-grid renewable resources, the uncertainty and variability can be dealt with by switching fast-acting reserves as needed on the basis of weather forecast, long distance transmission of the electricity, which ensures balancing of regional and local excesses/deficits or by installing large-scale storage facility on the grid.[220] The latter case is more applicable to standalone wind energy for building/urban installation.

4.3 Wind energy driven electrochemical separation technologies

Based on availability and extensive expansion in the wind energy market, some studies have investigated the feasibility of using electricity from wind turbine to power electrochemical wastewater/soil treatments. This is an exciting innovation considering the availability of wind in most regions and possibility of employing electrochemical treatments in remote village and locations, where accessibility to electricity grid is very limited. Standalone wind turbines driven ED (WT-ED) is the most prominent and commercially available wind energy power electrochemical separation process. Although most commercial renewable energy driven ED operates with solar PV, there are continuous growth and extensive researches on WT-ED due to remote locations of sea/brackish water as well as availability of wind resources in coastal areas. Besides, unlike solar energy, wind energy is readily available day and night, provided that the wind system is well-located. There are several pilot scales WT-ED systems that have been investigated and the technology is in advanced stage of R&D conditions mostly tested in Mediterranean region or Canary Islands. Commercial scale trials of WT-ED system have been carried out in Canary Islands.[221] Several progress studies are still being conducted on WT-ED using either on-grid or off-grid wind turbines (Fig. 15) in order to optimize the process for commercial purposes. For instance, Veza et al. (2001, 2004)[221,222] has investigated on-grid and off-grid WT-ED plant for the production of water in Gran Canaria Island (Spain). The ED plant was able to achieve between 3 and 8.5 $m^3\ h^{-1}$ production flow rate with power supply range from 4 to 19 kW, while the product water conductivity ranged from 200 to 500 $\mu S\ cm^{-1}$ and 100 to 280 $\mu S\ cm^{-1}$ for off-grid and on-grid WT-ED, respectively, using a medium size wind farm. Decentralized desalination of brackish water using electrodialysis directly powered by standalone wind energy has also been reported by Malek et al. (2016).[223] Water production and energy consumption increased with wind speed up till V_{rate} and the system produce good quality water with less than 600 mg L^{-1} NaCl. Several other studies on WT-ED has been summarized in some reviews and chapter of books.[224–226]

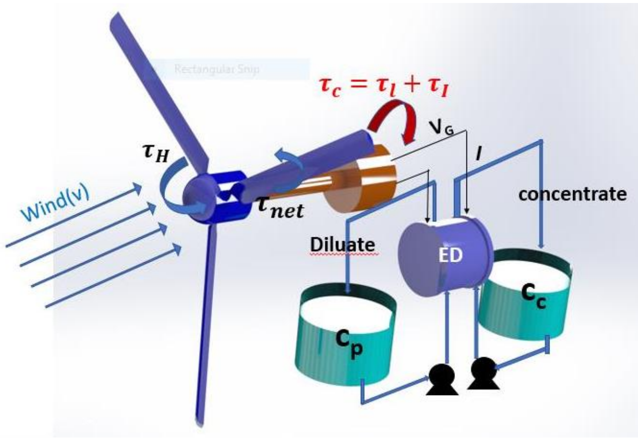

Figure 15: Standalone wind turbine powered ED plant. Reprinted with the permission of ref.[223]

Regarding soil remediation, Rodrigo's group[227] have reported the feasibility of EKSR directly powered by wind turbine for the removal of herbicide 2,4-D. The wind energy powered EKSR performed at both calm and near gale conditions and it was able to achieve 53.9% removal of 2,4-D in 15 days with charge supply of 49.2 Ah kg^{-1}, which was less efficient as compared to conventional DC powered process that reached 90.2% 2,4-D removal at 4.33 Ah kg^{-1} within the same treatment time. These results were explained in terms of the reversion in the transport processes when wind was not avaible. Although, the WT-EKSR is very promising, extensive studies are still needed to optimize its engineering parameters, as well as evaluate social-economic and environmental impact. Additionally, up to now, there are no studies available on wind energy powered electrocoagulation process.

4.4 Wind energy driven electrochemical degradation technologies

To the authors' knowledge, the only study on wind energy powered electrochemical degradation process was performed by group of Rodrigo.[126] The group investigated a wind powered BDD electrochemical oxidation process for the remediation of wastewater polluted with pesticide 2,4-D. A Bornay 600 power turbine (Bornay Aerogeneradores, Alicante-Spain) with two blade and controlled by electronic regulator (24 V, 30 A) was used to generate electricity at wind speed of 3.5 m s^{-1}, 11.0 m s^{-1}, 13.0 m $s^{-1}$and 60.0 m s^{-1} for turn-on, normal power, automatic brake system and work survival, respectively to run the electrochemical treatment system. A total charge of 18.75 Ah L^{-1} was passed to the electrolytic system in 20 h, which is much higher than the stoichiometric charge (0.36 Ah L^{-1}) required for the complete oxidation of a 100 mg L^{-1} solution of 2,4-D. Complete degradation and mineralization of the wastewater was achieved with the wind powered electrochemical oxidation system, however, some differences in performance profile (i.e. TOC removal) were observed when compared to DC powered EO, at similar conditions. The changes in performance were attributed to the changes in the profile of current intensity supplied from the turbine, which influences the concentration of the oxidants produced and in turn, the mediated oxidation process.

The two major criticisms, which may also be considered as challenges of coupling wind turbines with electrochemical wastewater/soil treatment technologies are: (i) large size of turbines and space required for its installation and (ii) wind turbines/farm location. The size of the turbines and need for solid based, as well as altitude required for effective operation of wind energy system, hinders the possibility of investigating wind turbines driven electrochemical technologies using bench/laboratory scale reactors. In fact, for successful laboratory scale experiment with wind turbines, long distance electricity transports or on-grid wind turbines are usually necessary because of the distance of the wind energy installation to city/buildings. Besides, wind farms are sited relatively far from settlements, thus most suitable for desalination plants but relatively difficult to connect to other electrochemical reactors like EC, EO and EF processes. Additionally, several technical, social and environmental issues are associated with wind turbine installations in residential area/urban centers, as such standalone wind turbine driven electrochemical wastewater and soil treatment reactors are less investigated compared to solar PV, which are easily installed in residential/building areas even though wind energy is independent of daylight.

5 Biomass Energy Driven Electrochemical Technologies: Promising results in lab-scale, perhaps the near future if scale-up is properly done.

Bioenergy is a renewable energy derived from biological/organic sources generally referred as "biomass". Biomass consists of organic materials such as wood, straw, sugarcane, manure and many other wastes that have stored chemical energy that can be converted to electrical energy. There are two categories of bioenergy: (i) traditional, which refers to the burning of biomass in organic matter such as wood, animal waste and charcoal and (ii) modern bioenergy technologies, which include liquid biofuels, bio-refineries, biogas generated from anaerobic digestion of wastes, as well as organic component of municipal and industrial solid/liquid wastes.[101] As depicted in Fig. 3b, bioenergy contributed about 5.5% (9 GW) of global renewable electricity capacity addition in 2017, of which the majority of the capacity expansion occurred in Asia (+ 5.9 GW) with Europe (+ 1.3 GW) and South America (+ 0.9 GW) being the other two regions with significant bioenergy capacity expansion in 2017.[100,101]

Among the modern bioenergy technologies, microbial fuel cells (MFCs) which convert the chemical energy of biomass/organic matters in wastewater (industrial, sewage treatment plants, municipal and household effluents etc.) to useful electricity is an emerging and exciting technology that combines clean energy production with wastewater remediation in one system. This is interesting, because in case of a successful full development of the technology, it may proffer simultaneous solutions to the challenges of energy shortage and water and environmental pollution. MFCs compose of two electrodes anode and cathode immersed in the electrolyte (wastewater). The degradation of the pollutants on the anode surface by anodiphilic bacterial colonies produces electrons which flow through the external circuit to cathode for the reduction of oxygen and concurrent production of electricity.[228–232] By careful selection of electrode materials and/or addition of Fenton catalyst (iron source) into the MFC system, the generated electric power could be easily enhanced and utilized in electrochemical treatment of the wastewater via the production of reactive oxygen species, mostly $^{\bullet}OH$. Extensive studies have been performed on lab-scale MFC with respect to configurations,[74,75,233] electrode materials[234–237] microbial communities and operating conditions,[78,238–242] all geared towards increasing the quantities of electricity generated and efficiency of degradation of the pollutants in the wastewater.

5.1 Principle and operation mechanism of MFC

Microbial fuel cell is an emerging technology that could systematically solve the two major challenges of the 21st century: energy production and water availability. After the pioneering studies about the production of electricity from biological degradation of organic matters,[243] this process has attracted much attention and interest from researchers across the globe in the last two decades. Till date, scientific works are continuously in progress to improve the efficiency of the MFC in terms of energy output and capacity for remediation of wastewater. This has led to extensive work on electrode materials selections and modification, discoveries of several anodiphilic bacteria and characterization of their colonies, different configuration of MFC, operation conditions, reliability and applications.[244] MFCs differs from the classical fuel cells (e.g. direct methanol fuel cells and proton exchange membrane fuel cell) in several ways because it: (i) utilizes biotic electrocatalyst (electroactive bacteria or proteins), (ii) operates at temperature range of 15 – 45ºC and neutral working pH, (iii) employ complex substrates (i.e. wastewater and effluent) as anodic fuel and (iv) has promising environmental impacts and moderate life cycles.[74,245–248] Briefly in MFCs, organic matter of wastewater is oxidized by microorganism, for which their metabolism results in production of electrons that are transferred to the anode (Fig. 16) via: (i) direct contact with the electrode through the conductive protein in the cell membrane of the microorganism and (ii) mediators-substance with redox properties which acts as communicators between the cell membrane and the anode.[77,233,244,249] These mediators may be excreted by the bacteria during metabolism or added externally to the system. Electrons generated then flow from anode through external electric circuit (bioelectricity) to the cathode where they are transferred to a high potential electron acceptor, such as oxygen. The flow of electrons means electricity production.[244,250,251]

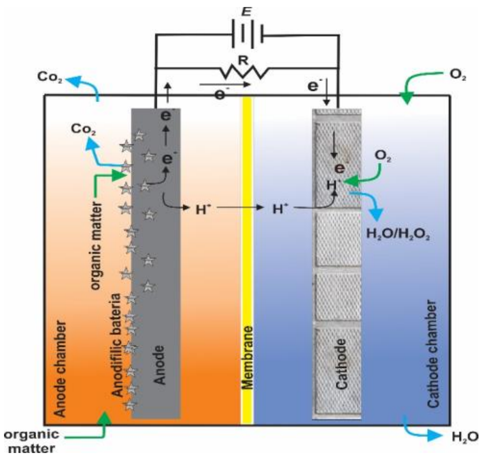

Figure 16: Schematic of basic principle of microbial fuel cells

Although simple substrates such methanol, acetate, glucose could be used as anolyte but one of the most interesting discoveries of this era is the possibility of generating electricity form complex substrates such as municipal or industrial wastewater.[233] The use of microbial oxidation to convert the chemical energy contained in wastewater into electrical energy has led to a new development in MFCs, with the process termed bioelectrochemical system (BES) or bioelectrochemical technology (BET). This has been the most widely studied MFCs in recent years.[233,244,250] Other BESs has been developed which can generate useful byproducts like hydrogen, formate, acetate, methane or desalinate water.[74,252–254] In this review, we are only interested in BESs that extract chemical energy from complex organic substrates and convert to useful electricity. MFCs are regarded as eco-friendly technologies with no energy requirement to operate and which do not generate pollutants during operation. However, like many other biologically-based techniques; they are inadequate alone for treatment of wastewater containing bio-recalcitrant organics like POPs.[3,9] As such, recent MFCs have been integrated with electrochemical treatments such as electro-Fenton, electrooxidation, or electrocoagulation process in the so-called MFC-mediated electro-Fenton (bioelectro-Fenton) or bio-electrocoagulation process, in order to enhance the concurrent abatement of biorefractory organic pollutants in anodic and cathode chambers, as well as busting the electricity output. In general, there are two configurations for which MFCs-BESs are used to drive electrochemical technologies: (i) BESs with in-situ electrochemical treatments and (ii) BESs powered ex-situ electrochemical treatments; both are discussed exhaustively in sections 5.3 and 5.4

5.2 Electrode materials in MFCs-BESs

The performance and economic feasibility of MFCs is directly related to the cost, durability and bioactivity of the electrode (anode) material used. New materials are being developed to improve the MFCs energy production, as well as enhance their commercial and industrial implementation. In MFCs, the selection of good anode materials takes precedence over the cathode since the degradation of the wastewater, as well as electrons production, occurs at the anode. However, in BESs both electrodes play crucial role in determining the efficiency of the system, because the production of reactive oxygen species (mostly $^{\bullet}OH$ for the degradation of recalcitrant organic pollutants) occurs at the cathode.

The selection of anode materials and its architecture plays a significant role in the performance of the MFC and it is the critical determining factor for the successful utilization of this technology for efficient energy conversion.[228,235,237,255] Different anode materials have been explored for MFCs over the last two decades. The early generation of MFCs utilized 2D carbon based materials such as graphite rods, graphite felt, carbon cloth, graphite sheet, graphite granules and activated carbon,[237,256,257] but recent studies have shown that 2D electrode materials have several limitations such as low surface area, high internal resistance, high activation and mass transfer over-potential which inhibits their capacity to achieve high efficiency in MFCs.[256] Due to recent progress in materials science and nanotechnology, 3D anode materials has attracted considerable attention for the development of high performance MFCs. Anode materials such graphite fiber brush, carbon felt and others have been utilized to overcome the limitation of 2D anode materials and enhance the energy conversion of MFCs.[256,258,259] In general, the anode materials in MFCs can be broadly grouped into three main classes: (i) carbonaceous, (ii) composite materials, and (iii) metal and metal oxides. Carbonaceous materials show good biocompatibility, excellent chemical stability, good electrical conductivity and they are inexpensive. Thus, they are the most widely studied anode materials in both MFCs and

MFCs-BESs.[256,260] Recent studies have utilized composite anode materials consisting two or more materials or surface modification of the original materials to enhance anodic kinetic performance and improve the anode properties. Composite materials such as graphite-polymer composite, polymeric-metals, graphene based anode, carbon nanotubes and multi-walled carbon nanotubes have been reported to show enhanced microbial development/attachment, microbial bioelectrocatalytic activity and extracellular electron transfer during the substrate metabolism.[255,261–266] Metal and metal oxides are much more conductive than carbon-based materials, but their application in MFCs is not so widespread. Many metals such as titanium, gold, copper and recently stainless steel have been considered for use in MFCs in recent years, but most of them are not very suitable because of their corrosive nature.[267–271] Some substantial reviews have summarized preparation, characterization, applications and challenges of anode materials used in MFCs/MFCs-BESs.[237,256]

Air-breathing cathodes are the most common configuration used in MFCs-BESs. These type of cathode materials are directly in contact with oxygen or air, which serves as electron acceptors and reduced to hydrogen peroxide (H_2O_2) or water.[237,256,272,273] The capacity of the cathode materials to produce large quantities of electrogenerated H_2O_2 is a very crucial factor in MFCs-BESs, since the catalytic activation of H_2O_2 in the cathode chamber leads to the formation of $^{\bullet}OH$ in the process termed BESs-EF or BET-EF. The electrodic materials should be highly conductive and corrosion resistant and they should have porous structure to permit substance/oxygen interchange with the surrounding electrolyte. Carbon based materials are the mostly used cathode/substrate, because of the excellent electrical conductivity, mechanical and chemical stability. They are the essential materials used in air-breathing cathode, commonly employed in BESs-EF system. Carbon cloth and paper were the first carbon-based air-breathing cathode that demonstrated satisfactory performance in MFCs; however, the expensive price mitigates their large-scale application.[228,235,256] Several other carbonaceous materials such carbon brush, carbon-fiber, activated carbon, graphite felt, carbon-felt and more recently bare/modified CNT has been studied as low-cost alternative and higher H_2O_2 production cathode in BESs-EF system.[256,261,274,275] Recently, more attention has been given to modified carbon substrate with air-diffused and catalyst layers for either oxygen reduction reaction (ORR) or Fenton's catalytic activation of H_2O_2 in BESs-EF system.[256,276] Air-diffusion layer is hydrophobic polymeric coatings in contact with the atmosphere, permitting oxygen diffusion to the cathode/catalyst layer but preventing water leakage. Polytetrafluoroethylene (PTFE) is the most widely used material to prepare air-diffusion layer of air-breathing cathode. The ORR catalytic activity of carbonaceous materials can also be enhanced through doping with other elements such as nitrogen, sulfur, boron, and phosphorus or chemical treatment with KOH or H_3PO_4.[272,277,278]

Additionally, iron and/or transition metal oxides have been used to modify carbon-based cathodes in order to couple cathodic (electro)-Fenton's reaction with anodic microbial oxidation in MFCs-BESs system. The iron/transition metal oxides ensure in-situ catalytic activation of H_2O_2 produced via ORR reaction to ROS especially $^{\bullet}OH$. Carbon based cathodic materials are essentially applied in BESs-EF system, because of their high potential for redox recycling of catalytic $M^{n+}/M^{(n+1)+}$ (M=transition metals, especially iron) on its surface, in addition to ORR reaction during electrolysis.

5.3 BESs coupled in-situ electrochemical technologies

Concurrent electricity generation and in-situ electrochemical oxidation of the complex organic wastewater has been investigated by many researchers using BESs. The remediation of the wastewater can be achieved by: (i) electro-Fenton degradation in the cathode chamber of MFCs-BESs system – bioelectro-Fenton, (ii) electrocoagulation with iron ions in the cathode region of MFCs-BESs and (iii) anodic oxidation at the anode region of the MFCs. However, BESs-bioelectro-Fenton has been the most efficient and widely investigated of all the integrated MFCs-electrochemical technologies.

In bioelectro-Fenton process (Fig. 17), the degradation of organics at the anode chamber by the metabolic activity of anodic microorganisms releases electrons that are transferred via the external circuit to the cathode, where the electrons are consumed to reduce the electron acceptor, mostly oxygen. The two-electron reduction of the oxygen at the cathode results in *in-situ* electrogeneration of H_2O_2 according to Eq. (19), provided a suitable cathode material (i.e. carbonaceous material) is used.[22,272,279]

$$O_2 + 2H^+ + 2e^- \rightarrow H_2O_2 \qquad (19)$$

The electrochemically produced H_2O_2 is catalytically decomposed to $^•OH$, hydroperoxyl ($HO_2^•$) or superoxide ($O_2^•$) radicals according to Eq. (5,20,21) by externally added iron dosage or iron loaded on the cathode via Fenton's (Fe^{2+}) or Fenton-like (Fe^{3+}) reaction in the cathode chamber aerated with O_2 or air. The produced radicals, especially $^•OH$, are non-selective oxidants and can completely mineralize any class of recalcitrant organic pollutants.[2,4,5] Interestingly, only catalytic quantities of iron source may be required because most of the Fe^{3+} ions produced in Eq. (5) are reduced to Fe^{2+} ions on the cathode by one electron transfer (Eq. (22)) when carbonaceous cathode materials, such as graphite-felt, activated carbon, carbon-felt or carbon cloth, are used.[3,44,280]

$$Fe^{3+} + H_2O_2 \rightarrow Fe^{2+} + HO_2^{\bullet} + H^+ \tag{20}$$

$$HO_2^{\bullet} \rightarrow H^+ + O_2^{\bullet} \tag{21}$$

$$Fe^{3+} + e^- \rightarrow Fe^{2+} \tag{22}$$

$$POPs + {}^{\bullet}OH \rightarrow [\text{organic byproducts}] + {}^{\bullet}OH \rightarrow CO_2 + H_2O \tag{23}$$

Additionally, the use of heterogeneous solid iron catalysts may provoke the surface-catalyzed mechanism of H_2O_2 activation to $^•OH$. Particularly, this is the case when relatively insoluble iron sources like natural iron-containing minerals – goethite, pyrite, limonite and pyrrhotite or synthetic iron-containing nanoparticles such as $Fe@Fe_2O_3$ or Fe_3O_4 are added to the cathode chamber of MFCs-BESs either as solid iron source or loaded on the cathode as functionalized electrode. In this case, the mechanisms of H_2O_2 usually involve two situation depending on the pH at which the EF is being performed and, to some extent, on the physicochemical properties of the solid catalyst.[22,281] At acidic pH (i.e. pH < 4) the catalytic activation of H_2O_2 is controlled by the redox cycling of dissolved Fe^{3+}/Fe^{2+} (from the partial dissolution of the solid catalyst/iron-functionalized cathode) and surface Fe^{III}/Fe^{II} redox couple. As such, the predominant process depends on the rate and quantities of dissolved Fe^{3+}/Fe^{2+} leached into the solution.[19,22,281] The homogeneous decomposition of H_2O_2 has been presented in Eq. (5,19–23). In contrast, at neutral or basic pH (i.e. pH > 6), the decomposition of H_2O_2 is expected to be predominantly by surface catalyzed process, because Fe^{III} is insoluble at these pH values.[22,282,283] The surface catalyzed mechanisms has been extensively summarized in the literature.[22]

In addition, similar catalytic decomposition of H_2O_2 via either homogeneous or surface mechanism can be achieved by other transition metals like V, Co, Mn and Cu, depending on the pH, as well as the source and properties of the catalyst dosage. Homogeneous activation of H_2O_2 by these transition metals proceeds in similar manner to that of Fe^{2+} in a Fenton-like reaction Eq. (24). In a situation where both iron and one or more other transition metals co-exist in the treated solution, the transition metal can cause the regeneration of Fe^{2+} by reduction of Fe^{3+} formed via Fenton's oxidation in the bulk solution (Eq. (25)) in addition to activation of the H_2O_2.[22,281]

$$M^{n+} + H_2O_2 + H^+ \rightarrow M^{(n+1)+} + {}^{\bullet}OH + H_2O \qquad (24)$$

$$Fe^{3+} + M^{n+} \rightarrow Fe^{2+} + M^{(n+1)+} \qquad (25)$$

Where M^{n+} is Cu^+, V^{4+}, or Co^{2+} and $M^{(n+1)}$ is Cu^{2+}, V^{5+} or Co^{3+}

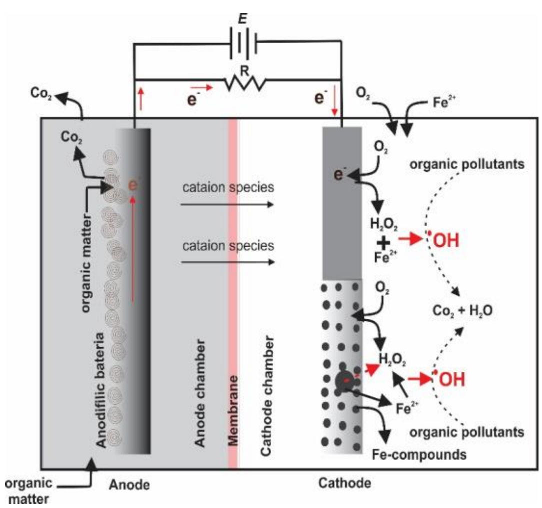

Figure 17: Schematic of bioelectrochemical/bioelectro-Fenton technology coupling anodic biological organic degradation and cathodic Fenton oxidation

Pioneer studies on bioelectro-Fenton remediation of refractory pollutants in MFCs-BESs system were conducted by several Chinese research groups. For instance, Zhu et al. (2009)[284] reported simultaneous electricity generation and degradation of p-nitrophenol in a MFC equipped with carbon-felt cathode, capable of in-situ electrogeneration of H_2O_2 and scrap iron added to cathode chamber as Fe^{2+} dosage source. The electrogenerated H_2O_2 was catalytically decomposed to $^{\bullet}OH$ by Fe^{2+} leached from iron scrap. Complete p-nitrophenol destruction was achieved after 12 h and up to 85% of the TOC was removed after 96 h in the cathode chamber of the MFC. The destruction of the p-nitrophenol was attributed to the oxidation activity of H_2O_2, $^{\bullet}OH$ and redox reaction of the iron scrap. At the same time, a maximum power density of 143 mW m^{-3} was generated by the microbial activity in the anode chamber. Similar studies were conducted using natural pyrrhotite as a cathodic heterogeneous Fenton catalyst for the degradation of biorefractory organics in landfill leachate.[285] The MFC equipped with pyrrhotite–coated graphite cathode generated a maximum power density of 4.3 Wm^{-3}, which was 133% higher than that reached by the graphite cathode. The authors showed that the pyrrhotite-coated graphite cathode achieved an in-situ electrogeneration of Fenton's reagents (Fe^{2+} + H_2O_2) as demonstrated by cyclic voltammetry measurements. Additionally, $^{\bullet}OH$, $HO_2^{\bullet}$ and $(O_2^{\bullet})^-$ were detected in cathode chamber, and they contributed importantly to the power output of the MFC. Approximately, 77% of color and 78% of COD were removed when treating old landfill leachate in the cathode chamber of the MFC, demonstrating the efficiency of the MFC equipped with pyrrhotite-graphite cathode for the remediation of biorefractory pollutants.

Feng et al. (2010)[286] have also achieved complete degradation and mineralization of azo dye Orange II in a bio-electro-Fenton system driven by MFC operating at neutral pH and using carbon-nanotubes (CNTs)–γ-FeOOH composite cathode, with the simultaneous generation of electricity (up to 230 mW m^{-3} of maximum power density output). In-situ generation of Fenton's reagents ($H_2O_2 + Fe^{2+}$) was attained in the aerated cathode chamber by simultaneous reduction of O_2 at the CNTs surface (Eq. (19)) and reductive leaching of Fe^{2+} from γ-FeOOH in the composite cathode. The same authors[287] have studied a polypyrrole/anthraquinone-2,6-disulfonate conductive film modified anode and cathode in dual chamber MFCs for cathodic mineralization of azo dye Orange II in neutral EF. The performance of the MFC in terms of power output and H_2O_2 production was markedly improved by using modified cathode, as shown by the increase in maximum power density from 633 to 823 mW cm^{-2} and H_2O_2 concentration from 0.63 to 2.79 mg L^{-1}. The improvements in efficiency of the MFC were due to the increased surface area of the electrode after modification, which multiplies the number of sites for microbial colonization at the anode and O_2 reduction at the cathode. Complete degradation and mineralization of Orange II was achieved within 30 min and 60 h, respectively, for all modified electrode studied. Similarly, Zhuang et al. (2010)[288] have investigated bioelectro-Fenton system in a dual chamber MFCs using Fe@Fe_2O_3/carbon-felt cathode for simultaneous microbial oxidation of wastewater at the anode and cathodic degradation of biorefractory pollutant by Fenton's reaction. The authors achieved 95% decolorization of Rhodamine blue, and 90% TOC removal in 12 h using short circuit conditions (0 Ω external resistance), whereas lower decolorization efficiency (75%) was attained in 24 h with closed circuit system (1000 Ω external resistance). The higher efficiency obtained in closed circuit MFCs system was attributed to increases in cathodic current density, which were favorable for H_2O_2 production. Besides, it was showed that using Fe@Fe_2O_3/carbon-felt in MFCs as cathode achieved better decolorization (95%) and higher TOC removal (90%) as compared to non-catalyzed carbon-felt with Fe^{2+} (64% and 78% decolorization and TOC removal, respectively) or without Fe^{2+} solution (49% and 40% decolorization and TOC removal, respectively) under short-circuit conditions. Additionally, the system produced steady currents of 0.32, 0.44 and 0.61 mA; and achieved maximum power densities of 56, 142 and 307 mW m^{-3} when using non-catalyzed carbon felt, Fe^{2+}/non-catalyzed carbon felt and Fe@Fe_2O_3/carbon-felt cathodes, respectively. The same group[289] have used similar MFC systems to demonstrate enhanced power output as a result of Fenton's reaction that develops in the cathode chamber. The more interesting results were obtained with Fe@Fe_2O_3/carbon-felt with a sustainable increase in the cathodic current density for more than 15 days and a total decomposition of generated H_2O_2 into ROS, especially $^{\bullet}OH$.

Luo et al. (2011)[290] utilized similar dual chamber MFC equipped with carbon-cloth anode and carbon-felt cathode for the simultaneous degradation of refractory contaminants in both anode and cathode chambers, as well as production of electricity up to a maximum current density of 15.9 W m^{-3}. Furfural solution of 300 mg L^{-1} was used as sole substrate in the anode chamber, while azo-dye Acid Orange II (AO7) was the biorefractory organic pollutants in the cathode chamber. Approximately 100% furfural and 96% COD were removed by the microbial oxidation in the anode chamber, whereas 89% and 81% AO7 and COD were removed in the cathode chamber by heterogeneous bioelectro-Fenton-like system, using 1 g $FeVO_4$ powder as catalyst source. The oxidation of AO7 and COD removal were enhanced in the cathode chamber by Fenton-like reaction catalyzed with $FeVO_4$ and the optimal pH value and $FeVO_4$ dosage towards AO7 degradation were found to be around 3.0 and 0.8 g, respectively.

An eco-friendly fuel cell-Fenton system for zero energy depollution was recently reported for the degradation of AO7 without any external power supply.[291] A dual MFC with carbon-felt modified by porous carbon (CF@pC) was used as cathode and the anode was CF modified by Au nanoparticles (CF@Au) (Fig. 18). The CF@Au was fabricated by electrodeposition of a gold layer onto the surface of a commercial carbon-felt. Electrodeposition was performed using cyclic voltammetry by running 70 scans from – 0.9 to 0.0 V versus SCE, in a N_2 saturated solution of 0.05 mg L^{-1}chloroauric acid.

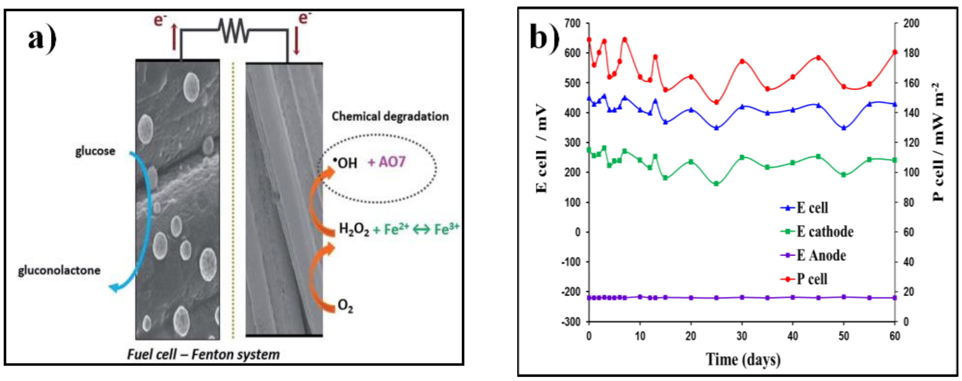

Figure 18: Schematic of microbial fuel cell –Fenton system and (b) cell voltage recorded over sixty days (60) of operation. Printed with the permission of ref.[291]

The catholyte of the MFC-Fenton system was 0.1 mM AO7 containing $FeSO_4$ (0.2 mM) in 50 mM Na_2SO_4 at pH 3, while the anolyte was mainly a glucose aqueous solution. As shown in Fig. 18b, an average current density output of 360.3 ± 51.5 mA m^{-2} corresponding to average power density of 170 mW m^{-2} was continuously produced for at least two months, thus providing enough electrons for the ORR at the cathode where the $^{\bullet}OH$ were formed. The authors achieved up to 90% degradation of AO7 in 10 h (Fig. 19) with high production rate of H_2O_2 (9.2 mg L^{-1} h^{-1}) at the porous cathode.

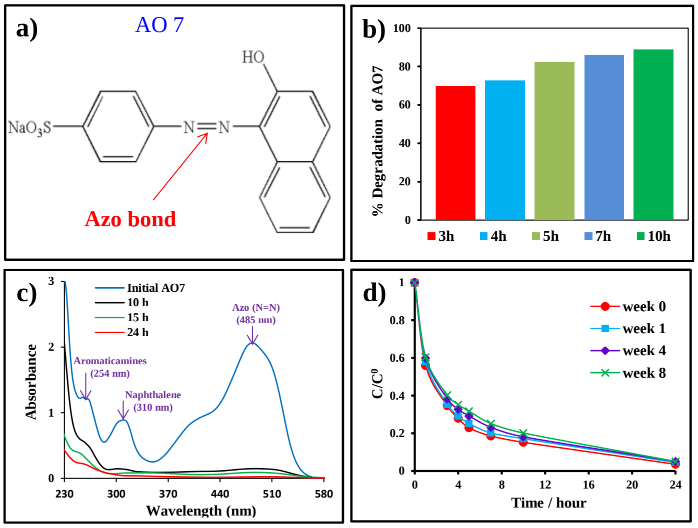

Figure 19: (a) structure of methyl orange (AO7), (b) degradation efficiency of AO7 at different time, (c) spectrophotometric spectra of the treated AO7 and (d) normalized decay of AO7 vs electrolysis time obtained in MFC-Fenton system. Printed with the permission of ref.[291]

Recently, emerging biorefractory pollutants such as pharmaceuticals has also been studied as model pollutant in bioelectro-Fenton system using dual chamber MFC. For instance, Zhang et al. (2015)[292] studied bioelectrochemical degradation of paracetamol in a dual chamber MFC using porous graphite felt and graphite plate as anode and cathode respectively, with $FeSO_4.7H_2O$ directly added as iron source. The Fenton's reagents – H_2O_2 and Fe^{2+} required for the production of $^{\bullet}OH$ were continuously electrogenerated and regenerated respectively at the cathode by bio-electrons produced at the anode and transferred to cathode chamber. At optimal conditions of 5 mg L^{-1} of total iron, initial solution pH value of 2 and 20 Ω external resistance, the removal and mineralization efficiency of paracetamol solution were found to be 70% and 25% respectively within 9 h of treatment along with concurrent generation of a maximum power density of 217.27 ± 23.24 mW m^{-2}. Wang et al. (2017)[293] reported enhanced degradation of emerging contaminants like estrone, bisphenol A, triclocarban and sulfamethazine from wastewater using MFC-bioelectro-Fenton system. The MFC equipped with graphite electrodes demonstrated high potential for in-situ H_2O_2 electrogeneration when glucose solution was used in the anolyte in both batch and continuous experiments with maximum power density generation of 625 and 784 mW m^{-3}, respectively. By adjusting the pH of the catholyte to 3.0, the produced H_2O_2 was catalytically activated to $^{\bullet}OH$ in the presence of 1.25 mM $FeSO_4$ and the formation of $^{\bullet}OH$ in the cathode chamber was confirmed by the degradation of salicylic acid and the formation of its hydroxyl byproducts. Effective removal of the emerging contaminants was attained in both batch and continuous MFC-BESs system within 24 h of treatment and the removal was attributed to both adsorption of the contaminants onto the graphite electrodes and degradation by $^{\bullet}OH$ produced Fenton's reaction. Several other studies have also investigated bioelectro-Fenton system for the degradation of different classes of biorefractory organic pollutants especially in the last 3 years and the main results obtained in such studies are summarized in Table 3.

Table 3: Summary of some recent studies on MFC-BES for simultaneous pollutants degradation and electricity production

pollutants	technology	MFC description and experimental conditions	Power/current density	Main results
Sanitary landfill leachate	MFC-BEF	Dual chamber MFC separated by cation exchange membrane and granular activated carbon-graphite electrodes; anode and cathode chamber net vol. 600 and 500 mL respectively; leachate contained 2401±562 mg COD L^{-1}, 237±57 mg BOD_5 L^{-1} and 24.05±8.42 cm^{-1} UV_{254}; T=25°C, pH=3; time=1–35 days; 300 mg L^{-1} $FeSO_4$ added to catholyte iron source	43.5 ± 2.1 A m^{-3}	1077–1244 mg L^{-1} day^{-1} COD removal rate was attained with concomitant renewable electricity production[294]
	MFC-BEF	Dual chamber MFC; anode and cathode chamber=280 mL; carbon-felt electrode; leachate 2152±624 mg L^{-1} COD, 166.9±29.2 mg L^{-1} BOD_5, 24.1±8.4 cm^{-1} UV_{254}; 300 mg L^{-1} $FeCl_3.6H_2O$ or $FeSO_4.7H_2O$ added to catholyte as iron source; pH = 3	1.7 A m^{-3}	77–81% and 34.6–40.7 COD removal efficiency at 300 mg L^{-1} $FeSO_4$ for synthetic leachate and real leachate respectively; Better COD removal achieved with $FeSO_4$ compared to $FeCl_3$[295,296]
Methyl orange	MFC-BEF	Dual chamber MFC; working volume of the chambers=550 mL; graphite fiber as anode and $Fe@Fe_2O_3$/ACF as cathode; 5 mg L^{-1} of methyl orange in 0.05 mM Na_2SO_4 as catholyte; O_2 flow rate = 750 mL min^{-1}; pH = 3	268.1 mW m^{-3}	88.63 μM of steadily produced H_2O_2 at external resistance of 100 Ω; 73.9%–86.7% methyl orange removal efficiency was attained for eight repeated cycle[297]
Phenol	MFC-BPES	Single chamber MFC; volume=175 mL; Ag/AgCl, carbon and electrochemically active TiO_2/Ti as reference, counter and working electrodes respectively; 20 mg L^{-1} of phenol in 0.1 mM Na_2SO_4; pH = 7	8.4×10^{-2} mA cm^{-2}	62% phenol removal after 4 h[298]
Triphenyltin	MFC-BEF	Dual chamber MFC; working volume of the	57.25 mW m^{-2}	135.96 μM of H_2O_2 production was

chloride		chambers=30 mL; carbon cloth or graphite felt as anode and $Fe@Fe_2O_3$/graphite felt composite as cathode; 100 µM of triphenyltin chloride in 2% NaCl; air flow rate=100 mL min^{-1}; pH = 3		achieved with $Fe@Fe_2O_3$/graphite felt cathode; 78.32 ± 2.07% removal of triphenyltin efficiency in 100 h[299]
Tetracycline hydrochloride	MBR/MFC-BEF	Continuous flow dual chamber MFC; 23 mL and 78.75 mL working volume for anode and cathode chamber respectively; graphite particles as anode and PVDF/carbon cloth as cathode; 180 mg L^{-1} tetracycline at 0.055 mL min^{-1} flow rate;10 g of FeOOH/GAC or FeOOH/TiO_2/GAC added to cathode chamber	60 mW m^{-2}	90% tetracycline removal efficiency, 90% and 80% COD and NH_4-N removal efficiency respectively with FeOOH/TiO_2/GAC[300]
Orange G	MFC-BEF/ED	Dual chamber MFC; working volume of the chambers=50 mL; carbon fiber brush as anode and graphite plate cathode; 40 mL of 100–500 mg L^{-1} orange G; air flow rate=8 mL min^{-1}; 10 mM Fe^{2+} added to catholyte pH=2	2.0 A m^{-2}	Complete decolorization and mineralization of 400 mg L^{-1} Orange G in 6 and 12 h respectively at first order rate constant of 1.15±0.06 and 0.26±0.03 h^{-1}, respectively[301]
Medicinal herb wastewater	MFC-BEF	Dual chamber MFC; working volume of the chambers=450 mL ; graphite plate as anode and $Fe@Fe_2O_3$/graphite composite as cathode; wastewater contain 4423±221 mg L^{-1} COD and 2250±112 mg L^{-1} BOD; air flow rate=300 mL min^{-1}; pH=3	49.76 mW m^{-2}	78.05% and 84.02% COD removal was achieved in anaerobic anode chamber and aerobic BEF cathode chamber respectively[302]
Amaranth	MFC-BEF	Dual chamber MFC; working volume of the chambers=80 mL; granular graphite as anode and pure graphite as cathode; 70 mL of 75 mg L^{-1} amaranth; pH=3	28.3 W m^{-3}	82.59% and 76.43% removal efficiency achieved in 1 h with the addition of 0.1 mM Fe^{2+} and 0.5 mM Fe^{3+} respectively[303]
p-nitrophenol (p-NP)	MFC-BEF	Dual chamber MFC; cathode chamber volume=50 mL; carbon-felt as anode and	237.5 mA m^{-2}	96% p-NP removal in 6 h; seven cycles of reusability of limonite with

		cathode; 50 mL of 0.25 p-NP; 112 mg of limonite as Fe dosage; air-injection rate of 100 mL min^{-1}; 35 ºC and pH = 2		> 94% p-NP removal[304]
-	MFC-BES	Dual chamber MFC flow reactor; net volume of the chamber = 28 mL; carbon black and graphite hybrid air-cathodes and carbon fiber brush as anode; electrolyte feed to cathode at 10 mL min^{-1} from aerated thank	12.3 mA cm^{-2}	11. 9 mg L^{-1} h^{-1} cm^{-2} production of H_2O_2[305]
Swine wastewater	MFC-BEF	Dual chamber biochemical reactor; cathode chamber volume = 350 mL; graphite as anode and Fe@Fe_2O_3/Carbon-felt as cathode; feeding rate = 3.1 and 1.24 L day^{-1}; O_2-injection rate of 300 mL min^{-1}; 30ºC and cathodic chamber at pH = 3	3 – 8 W m⁻3	62.2–95.7% BOD_5, COD, NH_3-N and TOC removal[306]
17β-estradiol(E2) and 17 α-ethyinyl estradiol (EE2)	MFC-BEF	Dual chamber biochemical reactor; anode/cathode e chamber volume=75 mL; carbon as anode and Fe@Fe_2O_3/NCF as cathode; 20 µg L^{-1} of E2 and EE2 in 0.1 M NaCl as cathode solution; O_2-injection rate of 100 mL min^{-1} 30ºC and cathodic chamber at pH=3	4.35 W m⁻3	81% and 56% of E2 and EE2 respectively in 10 h[307]

The bio-electrocoagulation cell using MFC operates in a similar manner than the electrocoagulation process (Fig. 20a). It uses a sacrificial iron anode and bioactive cathode in different chambers, separated by anion exchange membrane. The bio-production of electricity via the microorganism actions initiates the dissolution of the iron into Fe ions, which can acts as coagulant for the removal of pollutants. Studies on bio-electrocoagulation cell are very scarce, especially with respect to removal of organic pollutants. However, a recent study by Dong et al. (2017)[308] used these processes for the simultaneous treatment of algae-polluted wastewater and electricity generation. The author employed a dual chamber MFCs equipped with nitrifying bio-cathode made of carbon graphite fiber brush and sacrificial iron mesh anode. Continuous aeration was achieved by connecting air diffuser to be bottom of the cathode. The system was operated by first injecting the algae-polluted wastewater into the anode chamber and the supernatant injected to the cathodic chamber. The resident times of the wastewater were 3 h and 6 h, respectively, in anode and cathode chamber. More than 80% of the algae population was removed after 1 h, at solution conductivity of 4.94 mS cm^{-1}, whereas the process merely attained algae removal efficiency of 55.4% at the same treatment time when the solution conductivity was reduced to 2.33 mS cm^{-1}. Three different mechanisms were suggested for the removal of the algae from the wastewater: (i) electrostatic attraction between the positively charged iron ions and negatively charged algae cell, which can breaks the electrostatic repulsive force between algae cells and decreases the system dispersion stability, as well as favors algae sedimentation, (ii) sweeping and enmeshment effect due to the interaction between the algae and generated iron hydroxides in the cathode chamber and (iii) biological deactivation of the algae cells. The coagulation effect of iron ions was obvious from the settled algae flocs with its color changing gradually from yellowish green to reddish brown, while the supernatant remained transparent. In addition, maximum power densities of 8.41 and 11.33 mW m^{-3} were produced at solution conductivities of 2.33 and 4.94 mS cm^{-1}, respectively.

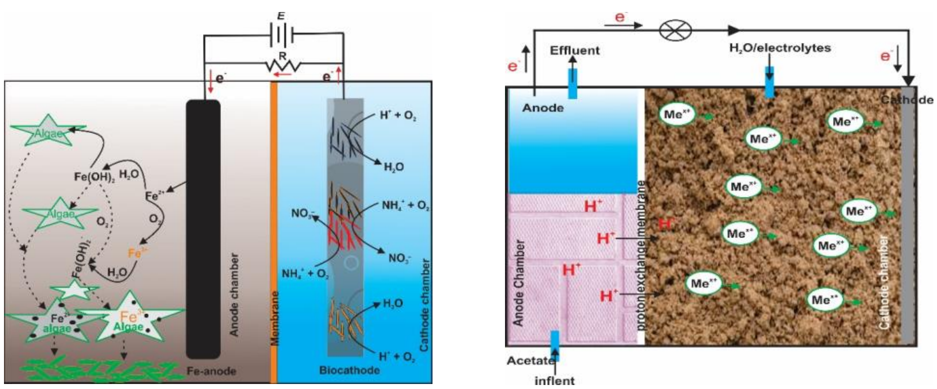

Figure 20: Schematic of a typical (a) MFC- electrocoagulation and (b) MFC-electrokinetic soil remediation system. Adopted from ref.[308] and[309] respectively with modification.

In-situ electrooxidation of organic pollutants is a very rare case in MFCs since the anode materials must be biocompatible to ensure high interaction between its surface and electroactive microorganism in the anode chamber. Carbonaceous and metallic-based materials are the most common type of electrode adopted in MFCs owing to their distinguish characteristics as explained in Section 5.3. These classes of electrodes like, graphite, stainless steel and platinum are “active electrodes” with respect to ROS production and the oxidation of organics on the surface of such electrodes is very slow with limited mineralization, since the primary oxidants are chemisorbed oxygen species.[1] This is the situation of most cases of degradation of organic substrate at anode chamber of MFCs, which is most by biological activity of the microbes or electron-transfer.

In-situ EKSR driven by electric field derived from electricity generated by MFC has also been recently proposed by a Chinese group.[309] The study investigated the removal of Cd and Pb from contaminated soil in a dual chamber MFC equipped with granular graphite as the anode and carbon-felt as cathode using graphite rod for electrical contact and proton exchange membrane as separator (Fig. 20b). The anode chamber, containing the electrochemically active microorganisms, was continuously pumped with 396 mL day^{-1} of a synthetic nutrient solution, whereas the cathode chamber was filled with 230 g sieved dried contaminated soil, flooded with

200 mL of deionized water and watered every two days from top of cathode chamber with deionized water during the experiment. Titanium wires were woven through the carbon-felt cathode, which was placed at the far edge of the cathode chamber. A copper wire was used as current collector. The obtained results showed that the weak electricity generated in MFCs (3.6 and 7.5 mW m^{-3} of maximum power density for Cd and Pb contaminated soil, respectively) could power the EKSR effectively. The removal efficiencies of 31% and 44.1% for Cd and Pb respectively, were achieved in the cathode region after 143 and 108 days of treatment of soil contaminated with Cd and Pb, respectively. Soil properties such as pH and conductivity were also observed to be significantly redistributed from anode to cathode regions after remediation.

5.4 MFCs – ex-situ EAOPs

As explained in Section 1, the principal challenge of electrochemical environmental technologies are the high power investment required, which has limited it application in commercial scale, as well as the access to electricity grids in many rural areas specifically of developing countries. In case of a future successful scale-up of the BES technology, power generated from this renewable source may be an alternative source of energy to power electrochemical technologies.

In this view, recently, few studies have investigated the feasibility of using the power generated in MFCs as energy source to power externally electrochemical wastewater treatment cells (Fig. 21). For instance, Liu et al. (2012)[310] developed a novel anodic Fenton (AFT) system for the treatment of AO7 solution using electricity produced by MFCs. The MFC-AFT couple consists of dual chamber MFC and AFT electrolytic cell with the anode and cathode chamber of both MFC and AFT separated by proton exchange membranes. The anode (iron) and cathode (Pt) of the AFT were externally connected to the anode and cathode of the MFC. Tests were conducted using a 400 mL solution of AO7 in 0.16 M NaCl at pH 3 as anolyte and same volume of 0.16 M NaCl as catholyte and H_2O_2 solution of 2 mM was introduced into the anode chamber using an injector. In the MFC-AFT couple, electrons were produced in the anode chamber of MFC by microbial activity and then, they were transferred via external circuit to the anode (iron) of the AFT, where they cause the release of iron as the iron ions (Fe^{2+}) required for Fenton's reaction. The MFC-AFT achieved over 85% AO7 removal efficiency within 30 min, which was higher as compared to the 2% and 28% AO7 removal obtained with only H_2O_2 and Fe ions, respectively.

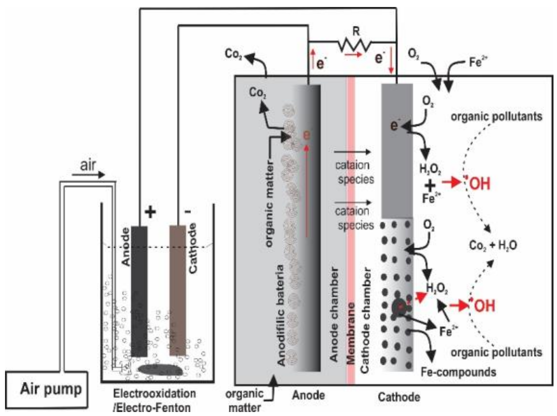

Figure 21: Schematic of a typical external electrochemical reactor powered by MFC-BES

A Spanish group has reported in-situ and ex-situ decolorization of Lissamine green B using electro-Fenton's oxidation in the cathode chamber of a MFC and the stable electricity generated by this MFC was used to externally power another EF reactor.[311] The microbial activity at the anode chamber produced electrons which were transferred to the cathode via external circuit and utilized to generate H_2O_2 from ORR reaction. A controlled air flow rate of 2 L min^{-1} was introduced into the cathode chamber, which contained10 mg L^{-1} Lissamine green B and crystal violet at pH 2. 10 g of iron alginate (150 mg L^{-1}of Fe) beads were added to the cathode chamber to activate the decomposition of H_2O_2 to $^{\bullet}OH$ and oxidize the Lissamine green B and crystal violet. The MFC was able to produce stable electricity, which was directly connected to mini electrochemical cell of 4 mL volume containing Lissamine green B, Na_2SO_4 and $FeSO_4$ at pH 2 for batch EF experiments using graphite sheet electrodes. After 9 hours of operation, approximately 94% of Lissamine green B and 83% of crystal violet were removed by in-situ bioelectro-Fenton oxidation in cathode chamber, with corresponding TOC removals of about 82% and 70% for Lissamine green B and crystal violet, respectively. On the other hand, the ex-situ mini EF cell was able to reach 98.3% decolorization and 80% of TOC removal at the optimum applied voltage of 700 mV supplied by MFC, which demonstrated that the connection between both systems is feasible. The same group[312] has used benthonic MFC for the same application. The cathode compartment (equipped with graphite cathode and continuously aerated with air) of the hybrid system with a working volume of 150 mL was filled with dyes solution, iron-alginate beads and Na_2SO_4. Almost complete degradation of dyes solution (88-98.2%) was achieved in 15 min along with over 1000 mV power generation. In addition, the ex-situ EF batch experiment with the electricity generated in benthonic MFC reached over 98% reactive black 5 removal in 120 min when treating a 70 mg L^{-1} dye solution.

Other authors have successfully powered EF process by directly connecting the output of a MFC to an electrolytic cell. For example Zhu et al. (2013)[313] studied a single chamber low voltage MFC as a renewable electricity source to power EF process for degrading phenol solution. The MFC produced a stable voltage of 0.2–0.3 V at pH 3, which was able to achieve 75% TOC removal in EF reactor in 22 h of single cycle with complete transformation of phenol into simple and biodegradable organic acids. Similar studies have been reported by Wang et al. (2015)[314] in which the output of single MFC and two stacked MFCs (connected in series) were used to power EF process for degradation of pyridine. A degradation efficiency of 82.9% for pyridine was achieved in 6 h, during the treatment of a waste containing an initial concentration of 200 mg L^{-1} at pH 3 and 700 mV applied voltage supplied by the MFC system. Electrooxidation with H_2O_2 production (EO-H_2O_2) powered by single chamber MFC has also been studied for the decolorization of MO.[315] The electrolytic cell equipped with carbon-felt electrodes was able to achieve 90.4% color removal within 6 h, when treating 50 mg L^{-1} MO solution at pH 3 and powered by 700 mV output of MFC. Recently, alternate switching between MFC and microbial electrolysis cell (MEC) assemble was developed for regulating the H_2O_2 produced in the cathode chamber and enhancing the degradation of the organic pollutants.[316] It was shown that during the MEC mode, the H_2O_2 was catalyzed by Fe^{2+} to produce the $^{\bullet}OH$ needed for the degradation of organic pollutants. Upon switching to MFC mode, the unused H_2O_2 (residual H_2O_2) was removed as electron acceptor. The residual H_2O_2 is capable of quenching the generated $^{\bullet}OH$, thus reducing the efficiency of the BEF process. Complete decolorization and mineralization of 50 mg L^{-1} Methylene Blue (MB) was achieved in MEC mode with first order rate constant of 0.43 and 0.22 h^{-1} for MB degradation and TOC decay respectively, and total removal of residual H_2O_2 (180 mg L^{-1}) was attained in MFC mode at a removal rate of 4.61 mg $L^{-1}h^{-1}$ with the generation of a maximum current density of 0.49 A m^{-2}.

6 New Approaches for renewable energy driven electrochemical technologies: What is it still starting to be cooked in the laboratories?

6.1 Triboelectric nanogenerators powered electrochemical technologies

The most abundant energy associated with human is mechanical energy, because of body motion. A nanogenerator was first introduced to harvest human energy from work, breathing, talking and many others via two effects: piezoelectricity[79,317,318] and triboelectricity.[79,319,320] Triboelectric nanogenerator produces electricity based on the mechanical force between two dissimilar materials in contact with each other. When two dissimilar materials are brought into physical contact, electrostatic charges are created; the induced triboelectric charges can generate a potential when the two materials are separated by mechanical force, which can drive electrons to flow between two electrodes built on top and bottom surface of the dissimilar material.[79] This is the working principle of triboelectric nanogenerator (TENG).[321,322] The area power density and volume power density of TENG has reaches 500 W m^{-2323} and 15 W m^{-3} with over 70% instantaneous conversion efficiency[323], since January 2012, when the first TENG was reported. TENG can be used to harvest any kind of mechanical energy that are available but wasted in our daily life and can also serve as self-power sensor for actively detecting the static and dynamic processes arising from mechanical agitation using the current and voltage output of the TENG, respectively.[324] It is important to state that the output of TENGs is usually an AC voltage, therefore it is necessary to connect a rectifier to change it to DC required for different applications.[79] By incorporating TENGs as an electricity source, several types self-powered system has been successfully achieved such as wireless sensor networks,[81,325,326] electrochemical reactions,[82] chemical sensors and electronic systems[327–329], corrosion sensor[330,331] and, recently, self-sustained electrochemical wastewater treatments.[82] There are four fundamental working modes of TENG vis á vis vertical contact-separation, lateral sliding, single electrode and freestanding triboelectric-layer modes.[79] Comprehensive reviews and fundamental theory of

TENGs are available in literature,[79,81,82,86,326] and, as such, will not be discussing further in this review.

Since TENGs was developed less than six years ago, studies on its application as self-sustainable energy source for electrochemical wastewater treated were first reported in 2013 by Yang et al.[332] The authors utilized silicon solar cell and TENG (Fig. 22) as a hybrid energy cell for simultaneous harvesting of solar and mechanical energies. The TENG was incorporated into the solar cell by replacing the protective layer of Si solar cell with a thin layer film of polydimethysiloxane, which in conjunction with the conductive layer on the surface of the wavy Si constitutes a TENG. A rectified voltage output of about 2.5 V was generated by the TENG using single solar cell with the series connection of TENG and solar cell ensures that there is always current/voltage output when either the solar or mechanical energy is available. The output was significantly enhanced (12 V) when the interlayer distance of the TENG was increased and when it was used an integrated system consisting of five solar cells connected in series. By applying the energy from hybrid solar cell and TENG and using Pt electrode, the authors were able to reach 98% RhB degradation in 10 min. The degradation of the RhB was by both $^{\bullet}OH$ and ClO^{-}, produced from water and Cl^{-} oxidation at the anode. The same authors[333] have used a hybrid cell of TENG and a pyroelectric nanogenerator (PENG) as a self-powered electrocatalytic process for the degradation of MO. The hybrid cell, which can simultaneous or individually harvest mechanical and thermal energies, could achieve an output current density of 0.17 mA m^{-2} and 0.33 mA m^{-2} for TENG and PENG, respectively. It was found that the energy generated by TENG could be stored in batteries for subsequent powering of the degradation of MO by electrocatalytic oxidation, while direct electrolysis of MO using PENG energy was able to reach 80% degradation in 144 h.

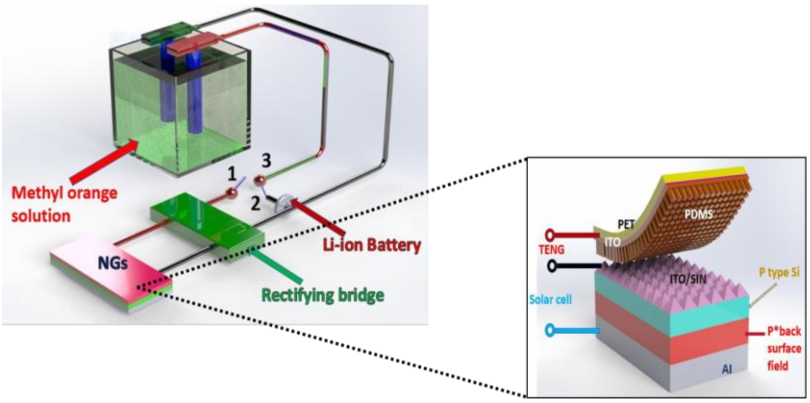

Figure 22: Schematic diagram of self-powered (TENG) electrochemical degradation of methyl orange. Printed with the permission of ref.[333]

Other authors[334] have investigated TENG for self-powered phenol detection and electrochemical degradation, using β-cyclodextrin to enhance the triboelectrification. The fabricated energy harvester, equipped with a Ti/PbO_2 anode and a Ti cathode, was vertically fixed in wastewater tank with the TENG using the wave energy of the water to generate electricity. At water wave velocity of 1.4 m s^{-1}, the current density and voltage of 20 μA cm^{-2} and 70 V, respectively, could be generated by the TENG. A phenol detection sensitivity of 0.01 μM^{-1} was demonstrated in the sensing range of 10 – 100 μM, whereas at 1.4 m s^{-1} water wave velocity the phenol degradation efficiency of 90% was attained in 320 min using a fix initial phenol concentration of 80 mg L^{-1}. The Wang's group has also reported the application of rolling friction enhanced TENG (RF-TENG) in self-powered electrochemical recovery of Cu^{2+} from wastewater[335] and a rotating TENG (R-TENG)[336] for self-powered wastewater treatment system with simultaneous degradation of RhD and Cu^{2+} recovery. Four unit of RF-TENG connected in parallel were able to generate a combined short circuit current of 240 μA and transfer a charge quantity of 380 nC, which could attained a collection removal efficiency of 80% of Cu^{2+} ions in the wastewater. The R-TENG, on the other hand, was able to produce 1.8 mA after rectifying the output when rotation rate was 450 rpm, which could be enhanced up to 12.5 mA by using a conventional transformer (reducing the voltage from 150 V to 13 V). By connecting the rectified and transformed R-TENG current to the electrochemical reactor, the authors were able to reach

100% degradation of 100 mg L^{-1} RhB in 15 min and 97.3% removal efficiency of 150 mg L^{-1} Cu^{2+} ion in 3 h (Fig. 23).

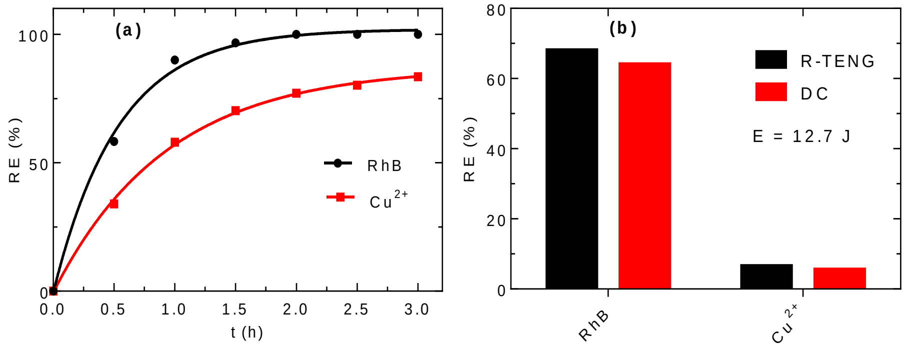

Figure 23: Removal efficiency of RhB and Cu^{2+} after 3 h and (b) comparison of performances of the electrochemical reactor driven by DC and R-TENG at 12.7 J energy consumption obtained during the treatment of 100 and 150 ppm of RhB and Cu^{2+}, respectively. Reprinted with the permission of ref.[335]

Recently, the same group[80] has also used a similar R-TENG with higher rotation (200–1000 rpm) for self-powered electrochemical oxidation of 4-aminoazobenzene solution. The I_{SC} of the TENG sharply increased from 50 μA to 200 μA when the rotation of the disc was increased from 200 to 1000 rpm, whereas the V_{OC} and the transfer charge was observed to remain almost unchanged at 600 V and 0.4 μC respectively. Decolorization efficiency of up to 99.9% of 4-aminoazobenzene solution was achieved in 12 min with the TENG. Similar, self-powered Pt-free carbon electrode electrochemical system using a multi-layer linkage TENG (ML-TENG) (Fig. 24) has been reported for the degradation of methyl red (MR).[337] The carbon electrodes provided an added advantage due to its low cost, as compared to Pt electrode commonly used in TENG powered electrochemical process. The peak V_{OC}, I_{SC} and peak power of the ML-TENG could reach and kept stable at 1300 V, 1.2 mA and 7.4 W m^{-2}, respectively, by using sponge as the buffer layer and pre-charged injection. Using the electricity generated by ML-TENG, complete decolorization of MR solution (100%) was attained in 160 min, demonstrating the efficiency of the electrochemical system powered by TENG. Other studies have investigated different configuration of TENG to power electrochemical reactors for the degradation of degumming wastewater,[338] wastewater sterilization and algae removal.[339]

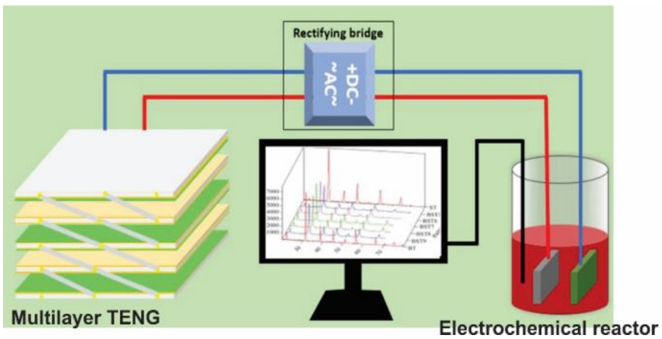

Figure 24: Schematic diagram of MT-TENG driven electrochemical reactor. Printed with the permission of ref.[337]

Recently, EF process powered by robust and flexible multilayer TENG (RFM-TENG) and flexible multilayer TENG (FM-TENG) have been reported as self-powered electrochemical technology for the degradation and mineralization of azo dye Basic Orange II[340] and 4-methylaminoazobenzene,[341] respectively. The I_{SC}, Q_t, V_{OC} and maximum power density of 960 µA, 2.8 µC, and 1050 V and 650 µA, 1.7 µC, and 750 V corresponding to 5.5 W m^{-2} (1 MΩ) and 2.6 W m^{-2} (500 kΩ) were achieved for the RFM-TENG and FM-TENG, respectively. In both studies, biomass derived carbon material was utilized as electrocatalyst (electrodes) for the oxygen reduction reaction and H_2O_2 production. The produced H_2O_2 was catalytically decomposed by Fe^{2+} (added as $FeSO_4$) via Fenton's reaction to form $^{\bullet}OH$, which oxidizes basic orange II and 4-methylaminoazobenzene. It was also demonstrated that undivided single electrochemical cells showed higher efficiency.

The feasibility of self-power electro-coagulation (SPEC) system using TENG for de-centralized water treatment has also been reported in literature.[342] The SPEC, which utilized pair of Al-electrodes, successfully removes pollutants from water. Thus, after 72 h of operation, the SPEC system reached 90% and 97% removal of algae and organic dyes, respectively.

6.2 Photocatalytic fuel cells driven electrochemical technologies

Photoelectrochemical cells (PECs) using solar visible or UV light developed for splitting water molecules into hydrogen and oxygen is a very promising technology that has found application in many fields, especially energy conversion and wastewater treatment.[85,343] In PECs wastewater treatment, organic molecules are oxidized until final degradation to CO_2 by excited holes, which is fundamentally an oxidation process on the photoanodic half-cell with external flow of electrons to the cathode.[85,344] This has led to the development of a novel wastewater treatment reactor known as photocatalytic fuel cells (PFCs). PFCs as a novel and exciting technology for organic pollutants degradation and simultaneous electricity production have drawn increasing attention,since their invention few years ago.[344,345] In a typical PFC system (Fig. 25), the photo-excitation of electrons at the anode surfaces create excited holes, which interact with H_2O/OH^- to produced ROS majorly $^{\bullet}OH$ that oxidizes organic pollutants in anode chamber, while the external flows of the released electrons to the cathode produces the electricity.[85,346,347] The operation of PFCs can be conceptualize as the cold combustion of organic substances in the wastewater on the photocatalyst surface under clean solar energy to generate recyclable electricity power, thus contributing to both environmental pollution remediation and energy recycling. In essence, the waste chemical energy of the pollutants can be recycled and reused via the PFCs system. Pioneering studies on PFCs were reported by Kaneko et al. (2006),[348] who used a nanoporous TiO_2 film photoanode and O_2-reducing cathode to construct a PFC. Since then, several studies have successfully achieved efficient electricity production and simultaneous wastewater treatment, using different TiO_2 or other photoanodes in PFCs system.[83,84,349–352]

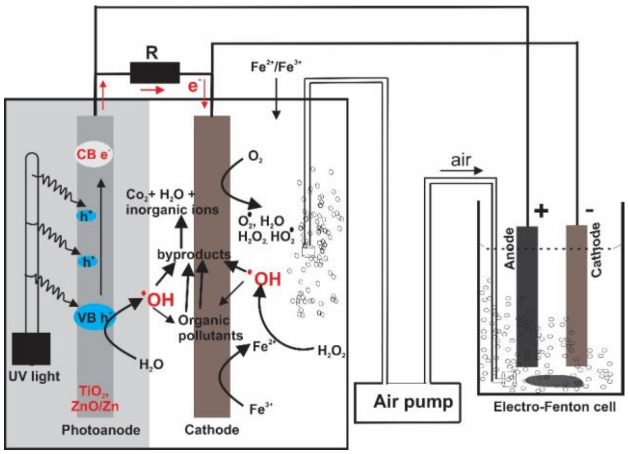

Figure 25: Schematic representation of the mechanism of a typical PFC

TiO_2 is the most widely used semiconductors for wastewater treatment, thanks to its high stability, suitable band gaps and acceptable separation properties of the electrons-holes during the organic oxidation, even though it requires UV illumination because of its 3.0–3.2 eV bandgap. Most PFCs uses bare or doped TiO_2 containing photoanodes. However, several new semiconductor photoanodes such as n-type Si, GaAs, CdSe, ZnS/ZnO, Fe_2O_3,WO_3, $BiVO_4$, and Cu_2O/Cu,[347,353] have recently been designed to enhance light adsorption, electron-hole pairs separation or surface area, which can partly improve the PFC's performance in organic pollutants degradation and simultaneous electricity generation. Majority of these new generation photoanodes especially BiOCl, BiOBr, $BiVO_4$ and others,[347] have been proven to be suitable for solar energy conversion due to their relatively small band gap. In order to reduce electron-hole combination, dual absorber photoanodes such as WO_3/TiO_2, $BiVO_4/TiO_2$ and $BiVO_4/WO_3$ with two semiconductors connected by solid junctions have also been investigated.[353] The combinations of bi-absorber with different band gaps and valence/conductive band positions help to inhibit electron-hole recombination and also to improve the solar adsorption and interface reactions.

Recently, some researchers have investigated the feasibility of using in-situ generated electric energy in PFCs to power electrochemical oxidation processes (mostly EF), in order to increase the performance of system for the degradation of recalcitrant organic pollutants. Indeed, one of the major limitations of PFCs in wastewater treatment is that the holes (oxidant) which causes the degradation of organic molecules are produced and localized at the surface of the photoanode/photocathode, thus making the system being diffusion controlled and limiting the extent of the main radical reactions to the nearness of the anode. Although, increase in surface area of photoanode/photocathode will enhance the efficiency of the process, the area cannot be indefinitely increased.[353] This has become a bottleneck that limits the organic degradation in the existing PFC systems, but could easily be overcome by enhancing the efficiency of radical reactions/production (i.e. $^{\bullet}OH$) in the bulk of the solution, rather than on the surface of the electrodes. By using air/O_2 breathing cathode capable of in-situ production of H_2O_2 and prior addition of iron source dosage in the wastewater, strong oxidants, especially $^{\bullet}OH$, could be generated in the solution in PFCs via Fenton's reaction (Eq. (9)), which has led to the so called (electro)Fenton-photocatalytic fuel cells (EF-PFCs) system.

The mechanism of radical production in EF-PFC is initiated at the electrodes surfaces. At the photoanode, electron-hole pairs are generated in the conduction and valence band upon UV irradiation. The photo-produced holes (h^+) oxidize water to $^{\bullet}OH$ according to Eq. (26) and (27).[353]

$$TiO_2 + h\nu \rightarrow h^+ + e^- \qquad (26)$$

$$H_2O + h^+ \rightarrow {}^{\bullet}OH + H^+ \qquad (27)$$

The photo-excited electrons are transferred via the external circuit to O_2-reducing cathode and, at the same time, the H^+ ions produced via photooxidation are diffused through the electrolyte to the cathode. The transport of the photo-excited electrons generates electricity in the external circuit due to the potential difference and continuous consumption of electrons. This is accompanied by the O_2 reduction at the cathode surface with the formation of radicals and hydrogen peroxide as reported by Zhao et al. (2017)[353] (Eq. (28– 31)):

$$O_2 + e^- \rightarrow O_2^{-\bullet} \qquad (28)$$

$$O_2 + 2H^+ \rightarrow H_2O_2 \qquad (29)$$

$$O_2^{-\bullet} + H^+ \rightarrow HO_2^{\bullet} \qquad (30)$$

$$H_2O_2 + {}^{\bullet}OH \rightarrow HO_2^{\bullet} + H_2O \qquad (31)$$

In the presence of iron sources (i.e. recycling Fe^{3+}/Fe^{2+} redox couple) in the solution, the in-situ generated H_2O_2 (Eq. (40) is catalytically decomposed to $^{\bullet}OH$ via Fenton's reaction (Eq. (9)). The Fe^{2+} is continuously regenerated in the solution via the reduction of Fe^{3+} formed in Eq. (9) by radicals ($O_2^{-\bullet}$, $HO_2^{\bullet}$, H_2O_2) or at the cathode surface (Eq. (22)) depending on the cathode materials used. As stated in Section 5.2, carbonaceous cathode materials such as ACF, carbon-felt and graphite felt are very efficient in both in-situ generation of H_2O_2 as well as electro-regeneration of Fe^{2+} from Fe^{3+}. [5] The regeneration of Fe^{2+} in the bulk solution in typical EF-PFCs is summarized in Eq. (32–34):

$$Fe^{3+} + O_2^{-\bullet} \rightarrow Fe^{2+} + O_2 \qquad (32)$$

$$Fe^{3+} + HO_2^{\bullet} \rightarrow Fe^{2+} + H^+ + O_2 \qquad (33)$$

$$Fe^{3+} + H_2O_2 \rightarrow Fe^{2+} + HO_2^{\bullet} + H^+ \qquad (34)$$

At the end, the generated oxidants (h^+, $^{\bullet}OH$ (via Fenton's reaction and water photooxidation), $O_2^{-\bullet}$, $HO_2^{\bullet}$ and H_2O_2) can easily oxidize the organic pollutants in wastewater even until their final mineralization to CO_2.

Two relevant studies have been conducted on EF-PFCs for simultaneous wastewater treatment and electricity generation using two different configurations. Zhao et al. (2017)[353] used EF-PFC system with TiO_2 nanotubes array photoanode and addition of ferrous ions for the degradation of refractory organic mixtures containing dyestuffs and pharmaceuticals using an in-situ EF coupled with PFC . The EF-PFC ensures radical reactions, both at the surface of the photoanode and in the bulk of the solutions with efficient degradation of the pollutants by h^+, $^{\bullet}OH$, $O_2^{-\bullet}$, and $HO_2^{\bullet}$ generated by photoexcitation and electrochemical assisted Fenton's reaction, respectively. It was observed that the degradation rate of organics such as methyl orange, methyl blue, congo red and tetracycline was significantly enhanced in EF-PFC as compared to conventional PFC as depicted in Fig 26. Besides, current densities up to 2.47 mA cm^{-2} were produced by the EF-PFC system, which were 1.2–2.4 times higher than those produced in traditional PFC.

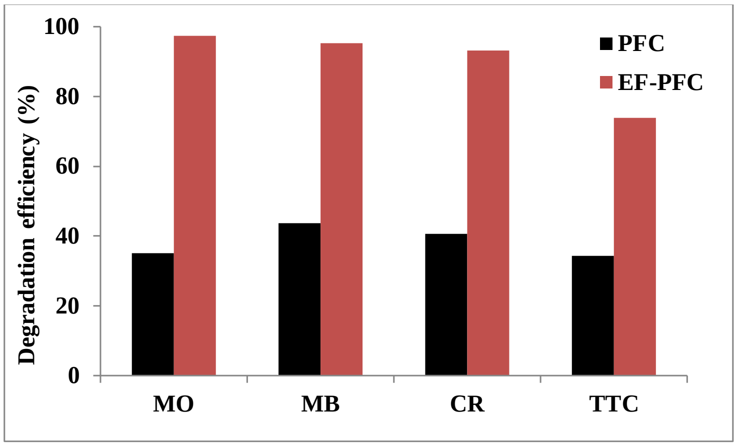

Figure 26: Comparison degradation efficiency of EF-PFC using 0.2 mM Fe^{2+} and PFC treatment of 20 mg L^{-1} of methyl orange (MO), methyl blue (MB), congo Red (CR) and tetracycline (TTC) solution containing 0.10 mg L^{-1} Na_2SO_4 as electrolyte at pH 3 and 60 min treatment time. Printed with the permission of ref.[353]

In a related study, Nordin et al. (2017)[87] investigated the feasibility of harnessing electricity generated in a PFC for ex-situ driving of EF process using Reactive Black 5 as model pollutants. The PFC reactor equipped with ZnO/Zn photoanode and carbon plate cathode was able to generate 11.39 mW cm^{-2} and 15.37 mW cm^{-2} when coupled in a hybrid system with EF reactor containing Reactive Black 5 dye and distilled water, respectively. Higher degradation efficiency of Reactive Black 5 (> 80%) was achieved in the Fenton's reactor as compared to PFC reactor (< 30%) of the hybrid system.

7 Challenges for connection of electrochemical devices and green energy source

7.1 Batteries and energy storages system driven electrochemical technologies

Standalone renewable energy sources, most especially solar photovoltaics and wind turbines has been fully integrated into many economic sectors and, nowadays, efficient and cost-effective energy storage systems are using with them not only to stabilize the power output but also to store the excess energy generated during the peak period. Energy storage based on electrochemical reactions such as batteries and redox flow cells are the most widely utilized storage system with PV and wind energy, however, in most cases the selected energy system depends on the end-time use.[354]

Batteries and redox flow cells are suitable for both AC and DC end-use applications. The rechargeable batteries allows the conversion of electricity produced by renewable sources such as solar PV and wind energy to storable chemical energy, hence ensure the interchange conversion/storage between electrical and chemical energies (Fig. 27).[355–357] High energy-capacity rechargeable batteries have found several applications in different fields such as portable electronic equipment, electrical vehicles, aerospace and other important areas. Recently, rechargeable batteries have been investigated as electricity source for powering electrochemical processes for the remediation of polluted water/wastewater.

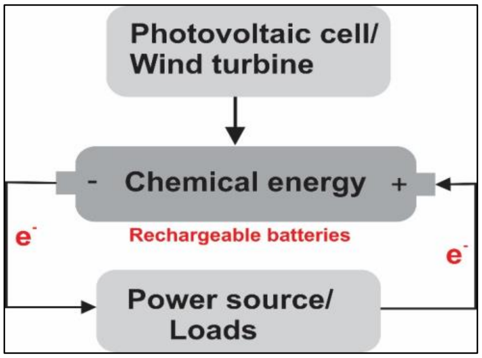

Figure 27: Energy storage mechanism of rechargeable batteries connected to renewable energy sources. Adopted from ref.[355] with modification

Batteries are made of one or more electrochemical cells. Typical electrochemical cell in battery system comprised of electrolyte (paste, liquid or solid) together with anode (positive electrode) and cathode (negative electrode). Electrochemical reactions occur at the electrodes during discharging, generating a flow of electrons via an external circuit (electricity). Interestingly, by applying external voltage across the electrodes, the reactions are reversed allowing the battery to be recharged.[355,358] Presently, there are several categories of electrochemical storage devices that can be used for storing renewable energy. The most important are: (i) redox flow batteries (ZnBr, Vanadium and PSB), (ii) Sodium-sulfur batteries (NaS), (iii) Lithium-ion batteries (Li-ion), (iv) Nickel-Cadmium batteries (Ni-Cd), (v) Lead-acid batteries and (vi) Metal-air batteries. In addition, the storage of hydrogen produced by water electrolysis is also a very studied system.

Among these systems, Redox Flow Batteries (RFB) especially VRFB has a distinguish advantage since their power and energy storage can be easily increased.[354]. Because of that they are the only category that will be discussed in detail in this work. An extended literature about the use of other energy storage devices can be found elsewhere.[356,257]

VRFB energy storage system utilizes VO^{2+}/VO_2^+ and V^{3+}/V^{2+} redox couples in H_2SO_4 aqueous solution as positive and negative electrolyte respectively (Fig. 28), and the energy storage capacity of the VRFB strongly depends on the concentration and volume of the electrolyte. The positive and negative electrodes are separated by ion-exchange membrane, which should possess low permeation rates of vanadium ions (V^{2+}, V^{3+}, VO^{2+}, VO_2^+) and membrane resistance, in order to minimize loss of energy capacity caused by the migration of the vanadium ions and the voltage efficiency, respectively.[357,359,360] Carbonaceous materials mostly graphite felt and carbon-felt are the common electrode materials used in VRFB, because they exhibits excellent stability in acidic media, and provide large reactive surface areas and sufficient numbers of sites for redox reaction.[356,358,361] The power output of VRFB is dependent on the number of unit cells and on the surface area of the electrodes.[358,362] Essentially, there are two configurations vis-á-vis series and parallel connections for stacking individual cell to one another and the power of VRFB is directly proportional to stack size and configuration used.

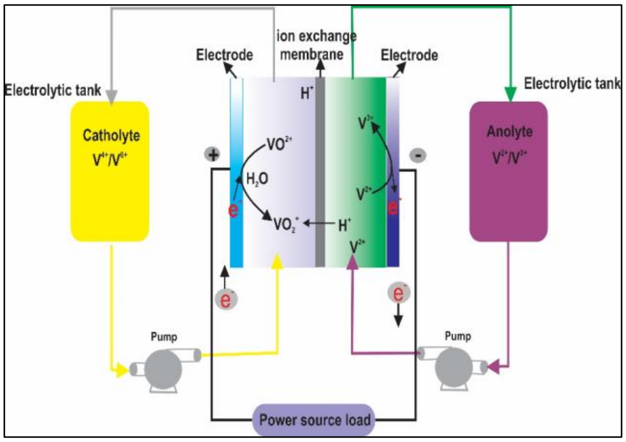

Figure 28: Schematic of operation mechanism of vanadium redox flow batteries. Adopted from ref.[357] with modification

In most cases, typical initial solution used in VRFB is vanadyl sulfate ($VOSO_4$) at concentration of 1.6–2.0 M dissolved in 2 M H_2SO_4. The electrolytes are modified to the appropriate oxidation state during the first full charging. The discharging and charging reactions on the half-cell in VRFB are as follows:[362,363]

$$\text{Anodic: } VO^{2+} + H_2O \leftrightarrow VO_2^{+} + 2H^{+} + e^{-} \quad (35)$$

$$\text{Cathodic: } V^{3+} + e^{-} \leftrightarrow V^{2+} \quad (36)$$

The overall discharging reaction of a typical VRFB is

$$VO_2^{+} + 2H^{+} + V^{2+} \rightarrow VO^{2+} + H_2O + V^{3+} \quad (37)$$

A fully charged VRFB unit cell with half-cells of V (II) and (V), each of concentrations of 2.0 M in 2.0 M H_2SO_4 has an open circuit potential (without loading) of 1.6 V and energy density of around 25 W h kg^{-1}. However, the current density depends on the system configuration and it can reach between 10–130 mA cm^{-2}, as well as operate effectively in the temperature range 10–40ºC.[364,365]

Research work on the feasibility of using VRFB charged by renewable energy, such as solar PV and wind energy as electricity source for driven electrochemical wastewater technologies were conducted by Rodrigo's group. Preliminary studies were conducted on the potential and efficiency of bench-scale VRFB charged under galvanostatic conditions and highly variable conditions of electricity produced by wind turbines.[70] The VRFB used consist of soft carbon-felt electrodes separated by cation exchange membrane and 200 mL each of positive and negative electrolytes containing 2.0 M vanadium (VO^{2+} in positive electrolyte and V^{3+} in negative electrolyte) in 3.0 M H_2SO_4 and circulated at a flow rate of 20 mL min^{-1} with the aid of a peristatic pump. It was shown that the VRFB operated in wind-charging mode performed slightly worse than the VRFB operated in galvanostatic mode, even though similar efficiency and charge/discharge capacities were achieved. The same group[366] has reported similar results for solar PV-charging VRFB, which achieve similar efficiency and charge/discharge capacities with VRFB charged under galvanostatic condition, but do not affect in the same way to the accelerated degradation of the performance of the electrochemical cell. Recent studies by this group[367] has also compared the efficiency of electrocoagulation process powered by galvanostatic current and combined or individual solar PV – VRFB for the treatment of synthetic wastewater polluted with 100 mg L^{-1} of pharmaceutical oxyfluorfen. Although, the electrocoagulation was not efficient for the removal of the pharmaceutical with only 25% of the pollutant accumulated in the flocs, the potentiality of VRFB for regulating and powering the electrochemical cell was found to be very promising and it promoted further investigation for possible applications in other electrochemical environmental technologies.

7.2 Scale-up of solar PV and electrochemical cells

Scale-up of renewable energy driven electrochemical technologies from laboratory/bench scale to industrial/field scale is a very important issue in commercialization of electrochemical treatment technologies. The use of on-grid solar PV (the most convenient source nowadays) can facilitate the scale-up and industrial application of renewable energy driven electrochemical technologies owing to the availability of large amount of electricity that can power any kind of technologies. As pointed out in previous sections, the output power of single unit standalone solar PV may be very low for driving large-scale electrochemical technologies. There are two main key areas for the scale-up of renewable energy driven electrochemical technologies: stacking of several units of renewable energy sources and scale-up of the electrochemical reactors.

Regarding the stacking of several units of renewable energy sources, no great obstacle is found in their design and construction, except that desirable configuration (i.e. series or parallel connections between the units) should be selected based on the required current and voltage to drive the electrochemical reactor. Several successes have been recorded in this aspect owing to the high technology know-how in PV and wind energy technologies, obtained with their application in several other key sectors. For instance, commercial PV-EDs using several stacked units of solar PVs are currently in use in Arabian Peninsula, Spain, India and Mediterranean for the production of fresh water from sea water.[156,168,170,368,369] Many pilot plant scale studies based on electrooxidation and electrocoagulation have also be conducted using stack units of standalone PV, though there are no commercial/industrial implementations of such technology up to now. The main concern in such stacking units should be related to the management of over-heating especially in solar PV modules. Concerning this heating, several research works and some reviews papers[131,370,371] have reported different techniques to overcome it, such as evaporative chimney, coupling different cooling technologies with the PV modules, solar panels built with phase change materials, water immersion cooling technique, photonic crystal cooling using transparent coating on PV panels, and solar PV panels with thermoelectric cooling.

On the other hand, the scale-up of electrochemical wastewater treatment technologies can be achieved in two ways, by either stacking of electrochemical cells or by increasing the size of the electrodes in the electrolytic cell. In the case of stacking electrochemical cells, the designs and configurations are less difficult. However, only few studies have reported results on pilot plant scale treatment of organic pollutants.[8,372–375] The two potential issues/challenges with stack reactors/cells are: controlling the heat and hydrogen gas evolution within the stacked cells. Heat transfer either in wires or into the electrolytes is a serious challenge in large-scale plants because of huge amount of heat that must be dissipated. The use of heat exchangers and cooling jackets can assist in eliminating or diminishing the over-heat of the wires and reactors but more importantly is the designs of stack cells that allows easy dissipation of heat and avoid overheating caused by ohmic drops.[8] On the other hand, hydrogen gas evolution at the cathode is a key and unresolved challenge in electrochemical environmental technologies because this gas is expected to be generated in large quantities during the electrochemical treatment of wastewater on large-scale. In undivided electrochemical reactors, a mixture of H_2 and O_2 are produced in the bulk electrolyte, which may represent hazardous working conditions if not properly handled. This problem is minimal on small bench-scale reactors normally used in laboratory studied, owing to the small amount of total H_2 produced, which can be eliminated by incorporating appropriately dissipation systems such as extractors and purge valves during the design and fabrication of the reactors. In contrast, the elimination of H_2 is very much difficult in a large scale experiment; as such it becomes a significant problem.[376] Hydrogen recovery and valorization has been hypothesized,[377,378] but up till date, the idea has only been implemented on small devices owing to its complexity and low cost-effectiveness. Alternatively, the use of divided cells with membrane separator may reduce the problem but such assemble requires higher potential and higher operation cost.[8]

The size of electrode plays a major role in determining the efficiency of electrochemical wastewater treatment technology. However, it is well known that potential and current distribution patterns are not uniform but depends on many factors such as uniformity of electrode surface, flow patterns, the current feeders, presence of turbulence promoters and others. It is important to state that electrochemical wastewater treatment processes are diffusion-controlled, which implies that the efficiency of the process is limited by the rate of the mass transport of pollutants towards the electrode surface. The maximum efficiency is obtained when the electric charge transfer rate and the pollutant's mass transport are balanced. Otherwise, the rate of side reactions such as water oxidation and hydrogen evolution becomes significant at the expense of organic pollutants removal.[8] Therefore, as much as maximum size of electrode needed for industrial application is of great importance, the difficulty of achieving even current and potential distribution on its surface, and working close to maximum efficiency, decreased with increased electrode size.

Scale up of electrochemically-assisted soil remediation processes is even more tricky. In this case the controlling mechanisms change when increasing the scale from electrokinetic to thermic, meaning that this scale-up is a very complex issue that should be very much further studied.[379–381] thus, we are very far still from a commercial implementation of green energy powering of electrochemically assisted soil remediation processes.

7.3 Main barriers to be removed for the new powering technologies

Regarding future applications, electricity produced by single unit of MFCs, TENG and PFCs is still very low for successful electrochemical wastewater treatment even at the bench scale. In fact, the current power density generated from wastewater in MFCs is frequently less than 40 W m^{-2} under optimum conditions,[382] the average power density of a unit TENG is less than 50 mW cm^{2} [79] while a unit PFC has power density below 500μA cm^{-2}.[353] The lower power density has limited the applications of electricity from these sources for powering electrode based electrochemical wastewater technologies. Except TENGs, which have been used for electrooxidation of organic pollutant with reactive chlorine production, MFCs and PFCs have only been limited to power Fenton based electrochemical wastewater treatment. Electrooxidation usually requires the application of higher current density, especially when high oxygen overpotential electrodes such as BDD is used, because the energy is required both for the water discharge reaction and oxidation of organic pollutants. Thus, studies on MFCs, TENGs and PFCs powered electrooxidation with non-active anodes are yet to be reported in literature. Therefore, future studies should be directed towards amplifying the output electricity from these sources, either by stacking several units or combine of two or more different sources.

Also because of their low technology readiness level, the relative costs associated to MFCs and TENGs are very high. The design and application of these energy sources/technologies are yet to record landmark commercial success both in driving electrochemical wastewater technology and other application because of cost arising from its configuration and output capacities, which are higher, as compared to existing energy sources. For example, the high cost in MFCs principally arises from the use of expensive electrodes like platinum, catalyst and membrane separator materials. On the other hand, TENGs requires transformers to convert the generated AC to DC current which constitutes additional cost, even though the transformer has added advantage of step-up the generated electricity and reduce the voltage.

7.4 Main environmental concerns

There are still general environmental barriers on the application of renewable energy sources, most importantly the disposal of non-functional and used cases and components of the solar PV cells, wind turbines, MFCs, TENGs and PFCs, which should be taken into consideration before commercial success of the renewable energy technology driven electrochemical wastewater. This may constitute serious environmental pollution issue, since the metal frames (PV and wind turbine), chamber cases (MFCs and PFCs) require proper disposal; else it causes aesthetic/visual pollution.

More importantly, some of these renewable energy sources utilize materials or chemicals with questionable environmental compatibility, as such their deterioration or wearing can cause serious hazardous and toxicological effect in ecosystem, and less attention has been given to this aspect. For instance, new generation PV cells are made from CdS and CdTe, which implies that disposal of non-functioning and broken cells of such PVs, requires utmost attention because Cd is one of the most toxic heavy metal on planet. Besides, if CdTe/CdS PV cells are left exposing to harsh weather conditions, especially where there is possibility of acidic rain, both Cd contaminated soil and surface water may occur in such environment. Similarly, some PFCs utilize GaAs, CdSe, and ZnS/ZnO photoanodes, which means that the deterioration or wearing of such photoanodes possess serious hazardous issue, because of the toxicity of Cd, As, Se and Zn. Therefore, extra attentions are required when utilizing such materials in PFCs and the treated solution must be properly analyzed for possible contamination by either of the hazardous heavy metals and anions. Alternatively, such materials should be avoided to eliminate possible hazardous pollution from those toxic substances.

7.4 Cost-effectiveness of electrochemical technologies: The last barrier.

The real application of new technologies depends not only on their technical feasibility but also, and even more importantly, on their cost- effectiveness. Since there are several existing environmental treatment technologies currently in use, the acceptability of a new technology will be strongly influenced by both its technical and economic viability and in electrochemical processes; cost of electricity is a factor of the major relevance. In renewable energy driven electrochemical technologies, the electricity produced from the source can power electro-mechanic devices such as pump, agitators and DC devices. Thus, for PV-ED systems which are current being applied on commercial scale, there are substantial studies and reviews on the economic analysis of this process based on the specific product cost (fresh water) analysis. For instance, the water cost of a PV-ED unit ranges from 1.6 to 5.8 US$/m^3.[164] The major advantage of PV-ED is the ability to develop a small-scale desalination plants. Indeed, it has been demonstrated that relatively high cost of solar PV is the main barrier for successful diffusion of solar energy, particularly as regards to powering electrochemical treatment technology such as

ED.[156] As explained in Section 3, the cost of unit solar PV is still very high, even though it continuously fall yearly due to continuous revolution in the solar energy sector.

As for other electrochemical technologies which are yet to available on commercial scales, cost analysis of the bench and pilot-scale are not well-studied or reported in literature, though few studies are available on the energy consumption per cubic meter of treated wastewater. It is not easy to obtain cost data for electrochemical cells, as well as operational cost since both operational and reactor costs depend on many factors such as reactor configurations, electrode materials, operational parameters, efficiency desired and others. Additionally, the cost of electricity per unit kW varies for different countries, as such it is easier to compare energy consumption per unit volume of treat solution rather than cost. It was reported that in many cases the cost of electrochemical cells itself could be between 30 and 60% of the total treatment cost, so, may be as important as energy cost.[8] Table 4, summarize some calculated energy cost per cubic meter of treated effluent reported for different electrochemical technologies.

Table 4: Summary of some recent studies on energy and cost analysis of renewable energy driven electrochemical wastewater and soil treatment technologies

Effluent	**Technology**	**Energy consumption/cost**	**Remark**
Cd contaminated soil	PV-EKSR	208 W m^{-3} (¥250/m^{-3})	PV cost = ¥35 W^{-1}; E_C = ¥0.56 $(kWh)^{-1}$.[188]
phosphate	PV-EC	0.71 kWh m^{-3}/15.75 kWh kg^{-1}.[172]	
Pb	PV-EC	0.219 kWh m^{-3}	Lower energy compared to conventional electricity.[173]
Cr	PV-EKSR	3.472 kWh m^{-3} (US$1.04 m^{-3})	PV cost = US$473.5 m^{-3}; E_C = ¥0.56 $(kWh)^{-1}$.[189]
River water	PV-EO/PC	¥26 L^{-1} of drinking water	Low production cost compared to conventional electricity.[177]
Textile wastewater	PV-EF	0.717 – 2.65 kWh m^{-3}.[176]	
Lignosulfonate	PV-EO	100 – 571 kWh m^{-3}.[373]	

wastewater

9 Concluding remarks

A review of research studies made over the last three decades on renewable energy driven electrochemical water/wastewater and contaminated soil treatment technologies has been conducted. The fundamental principles and methodologies of different electrochemical technologies like electrodialysis, electrokinetic remediation, electrocoagulation, electrooxidation and electro-Fenton processes were discussed. Different renewable energy sources like solar PV, wind turbine, MFCs, TENGs and PFCs were presented by describing their concepts of electricity production and mode of application in driving electrochemical wastewater/soil treatment reactors using different experimental works and results reported by reliable authors. It has been revealed that solar PV and wind energy powered electrodialysis is currently the only commercially available renewable energy driven electrochemical technology used for the production of fresh water from sea/brackish water, whereas other renewable energy driven electrochemical technologies have only been tested on either laboratory or pilot-scale and they are waiting for further studies in order to be commercialized, though they show huge promising inputs for environmental remediation.

The critical aspects of scale-up of renewable energy driven electrochemical technologies which includes stacking several units of renewable energy sources to produce higher amount of electricity for driving the electrochemical reactors, as well as scale-up of the electrochemical reactors via enlarging of electrodes and stacking of several unit cells were examined along with difficulty and challenges associated with each aspect. The non-stability and availability of the energy output at all time, low outputs of unit renewable energy sources, as well as environmental issues concerning using of toxic materials for production solar cells and photoanodes were some of barriers needed to be overcome for successful implementation of renewable energy driven electrochemical technologies. Economic analysis and data on cost and energy consumption of bench-scale and pilot plant of typical renewable energy driven electrochemical technologies were reviewed and it was concluded that further elaborate studies are necessary in this aspect for easy comparison with existing industrial remediation techniques and commercial adaptation of the technologies.

Finally, it is envisaged that this review aims to constitute a reference document in the field of renewable energy and wastewater and soil remediation, and help those searching about green, available and low cost electricity for driving electrochemical reactors. It will help researchers to launch new ideas and technological tools, as well as facilitate the implementation and commercial adaptation of electrochemical environmental processes for industrial-scale water/wastewater and contaminated soil treatments.

Acknowledgement

Financial support of CAPES under PNPD post-doctoral grant and National Council for Scientific and Technological Development (CNPq) are gratefully acknowledged. Also financial support from the Spanish Ministry of Economy, Industry and Competitiveness and European Union through projects CTQ2017-91190-EXP and CTM2016-76197R (AEI/FEDER, UE) is gratefully acknowledged

Reference

1 M. Panizza and G. Cerisola, *Chemical Reviews*, 2009, **109**, 6541–6569.

2 P. V. Nidheesh, M. Zhou and M. A. Oturan, *Chemosphere*, 2018, **197**, 210–227.

3 S. O. Ganiyu, E. D. van Hullebusch, M. Cretin, G. Esposito and M. A. Oturan, *Separation and Purification Technology*, 2015, **156**, 891–914.

4 M. A. Oturan and J.-J. Aaron, *Critical Reviews in Environmental Science and Technology*, 2014, **44**, 2577–2641.

5 E. Brillas, I. Sires and M. A. Oturan, *Chem. Rev.*, 2009, **109**, 6570–6631.

6 I. Sirés, E. Brillas, M. A. Oturan, M. A. Rodrigo and M. Panizza, *Environmental Science and Pollution Research*, 2014, **21**, 8336–8367.

7 M. A. Rodrigo, N. Oturan and M. A. Oturan, *Chem. Rev.*, 2014, **114**, 8720–8745.

8 C. A. Martínez-Huitle, M. A. Rodrigo, I. Sirés and O. Scialdone, *Chemical Reviews*, 2015, **115**, 13362–13407.

9 I. Sirés and E. Brillas, *Environment International*, 2012, **40**, 212–229.

10 C. A. Martínez-Huitle and S. Ferro, *Chemical Society Reviews*, 2006, **35**, 1324.

11 C. A. Martínez-Huitle and E. Brillas, *Angewandte Chemie International Edition*, 2008, **47**, 1998–2005.

12 L. Feng, E. D. van Hullebusch, M. A. Rodrigo, G. Esposito and M. A. Oturan, *Chemical Engineering Journal*, 2013, **228**, 944–964.

13 H. Särkkä, A. Bhatnagar and M. Sillanpää, *Journal of Electroanalytical Chemistry*, 2015, **754**, 46–56.

14 B. P. Chaplin, *Environmental Science: Processes & Impacts*, 2014, **16**, 1182.

15 F. C. Moreira, R. A. R. Boaventura, E. Brillas and V. J. P. Vilar, *Applied Catalysis B: Environmental*, 2017, **202**, 217–261.

16 K. V. Plakas and A. J. Karabelas, Springer Berlin Heidelberg, Berlin, Heidelberg, 2017.

17 M. A. Oturan, *Environ. Sci. Pollut. Res.*, 2014, **21**, 8333–8335.

18 S. Vasudevan and M. A. Oturan, *Environmental Chemistry Letters*, 2014, **12**, 97–108.

19 P. V. Nidheesh, H. Olvera-Vargas, N. Oturan and M. A. Oturan, Springer Berlin Heidelberg, Berlin, Heidelberg, 2017.

20 H. Lin, N. Oturan, J. Wu, M. A. Oturan and H. Zhang, Springer Berlin Heidelberg, Berlin, Heidelberg, 2017.

21 C. A. Martínez-Huitle and E. Brillas, *Applied Catalysis B: Environmental*, 2009, **87**, 105–145.

22 S. O. Ganiyu, M. Zhou and C. A. Martínez-Huitle, *Applied Catalysis B: Environmental*, 2018, **235**, 103–129.

23 J. Farrell, J. Wang and R. LeBlanc, in *Pesticide Decontamination and Detoxification*, American Chemical Society, 2003, vol. 863, pp. 99–112.

24 K. E. Carter and J. Farrell, *Environ. Sci. Technol.*, 2008, **42**, 6111–6115.

25 C. Comninellis, *Electrochimica Acta*, 1994, **39**, 1857–1862.

26 B. Marselli, J. Garcia-Gomez, P.-A. Michaud, M. A. Rodrigo and C. Comninellis, *Journal of The Electrochemical Society*, 2003, **150**, D79.

27 C. Zanta, P. A. Michaud, C. Comninellis, A. R. De Andrade and J. F. C. Boodts, *J. Appl. Electrochem.*, 2003, **33**, 1211–1215.

28 S. O. Ganiyu, N. Oturan, S. Raffy, M. Cretin, R. Esmilaire, E. van Hullebusch, G. Esposito and M. A. Oturan, *Water Research*, 2016, **106**, 171–182.

29 F. E. Durán, D. M. de Araújo, C. do Nascimento Brito, E. V. dos Santos, S. O. Ganiyu and C. A. Martínez-Huitle, *Journal of Electroanalytical Chemistry*, 2018, **818**, 216–222

30 M. Panizza and G. Cerisola, *Applied Catalysis B: Environmental*, 2007, **75**, 95–101.

31 Y. Yang and M. R. Hoffmann, *Environ. Sci. Technol*., 2016, **50**, 11888–11894.

32 J. Radjenovic, V. Flexer, B. C. Donose, D. L. Sedlak and J. Keller, *Environ. Sci. Technol.*, 2013, **47**, 13686–13694.

33 A. M. Sales Solano, C. K. Costa de Araújo, J. Vieira de Melo, J. M. Peralta-Hernandez, D. Ribeiro da Silva and C. A. Martínez-Huitle, *Applied Catalysis B: Environmental*, 2013, **130–131**, 112–120.

34 M. A. Rodrigo, P. Cañizares, C. Buitrón and C. Sáez, *Electrochimica Acta*, 2010, **55**, 8160–8164.

35 K. Cho and M. R. Hoffmann, *Environ. Sci. Technol.*, 2014, **48**, 11504–11511.

36 K. Cho and M. R. Hoffmann, *Chem. Mater.*, 2015, **27**, 2224–2233.

37 A. Y. Bagastyo, D. J. Batstone, K. Rabaey and J. Radjenovic, *Water Res.*, 2013, **47**, 242–250.

38 S. O. Ganiyu, N. Oturan, S. Raffy, M. Cretin, C. Causserand and M. A. Oturan, *Separation and Purification Technology*, 2019, **208**, 142–152.

39 J. M. Barazesh, C. Prasse and D. L. Sedlak, *Environ. Sci. Technol.*, 2016, **50**, 10143–10152.
40 J. T. Jasper, Y. Yang and M. R. Hoffmann, *Environ. Sci. Technol.*, 2017, **51**, 7111–7119.
41 L. Chen, P. Campo and M. J. Kupferle, *Journal of Hazardous Materials*, 2015, **283**, 574–581.
42 J. Radjenovic and D. L. Sedlak, *Environmental Science & Technology*, 2015, **49**, 11292–11302.
43 A. Dirany, I. Sirés, N. Oturan, A. Özcan and M. A. Oturan, *Environmental Science & Technology*, 2012, **46**, 4074–4082.
44 S. O. Ganiyu, N. Oturan, S. Raffy, G. Esposito, E. D. van Hullebusch, M. Cretin and M. A. Oturan, *Electrochimica Acta*, 2017, **242**, 344–354.
45 S. Garcia-Segura and E. Brillas, *Electrochimica Acta*, 2014, **140**, 384–395.
46 E. Brillas, *Journal of the Brazilian Chemical Society*, 2014, **25**, 393–417.
47 E. Neyens and J. Baeyens, *Journal of Hazardous Materials*, 2003, **98**, 33–50.
48 J. Šima and J. Makáňová, *Coordination Chemistry Reviews*, 1997, **160**, 161–189.
49 J. J. Pignatello, *Environmental Science & Technology*, 1992, **26**, 944–951.
50 C. Weller, S. Horn and H. Herrmann, *Journal of Photochemistry and Photobiology A: Chemistry*, 2013, **268**, 24–36.
51 P. Cañizares, F. Martínez, C. Jiménez, J. Lobato and M. A. Rodrigo, *Environ. Sci. Technol.*, 2006, **40**, 6418–6424.
52 E. Brillas and C. A. Martínez-Huitle, *Applied Catalysis B: Environmental*, 2015, **166**–**167**, 603–643.
53 A. Fernandes, M. J. Pacheco, L. Ciríaco and A. Lopes, *Applied Catalysis B: Environmental*, 2015, **176**–**177**, 183–200.
54 A. Campione, L. Gurreri, M. Ciofalo, G. Micale, A. Tamburini and A. Cipollina, *Desalination*, 2018, **434**, 121–160.
55 C. Fernandez-Gonzalez, A. Dominguez-Ramos, R. Ibañez and A. Irabien, *Renewable and Sustainable Energy Reviews*, 2015, **47**, 604–615.
56 H. Strathmann, *Desalination*, 2010, **264**, 268–288.
57 K. Tado, F. Sakai, Y. Sano and A. Nakayama, *Desalination*, 2016, **378**, 60–66.
58 A. T. Yeung and Y.-Y. Gu, *Journal of Hazardous Materials*, 2011, **195**, 11–29.
59 H. I. Gomes, C. Dias-Ferreira and A. B. Ribeiro, *Chemosphere*, 2012, **87**, 1077–1090.

60 Reddy Krishna R., Maturi Kranti and Cameselle Claudio, *Journal of Environmental Engineering*, 2009, **135**, 989–998.

61 E. Vieira dos Santos, C. Sáez, P. Cañizares, C. A. Martínez-Huitle and M. A. Rodrigo, *Journal of Hazardous Materials*, 2017, **322**, 413–420.

62 W. T. Mook, M. K. Aroua and G. Issabayeva, *Renewable and Sustainable Energy Reviews*, 2014, **38**, 36–46.

63 D. Valero, J. M. Ortiz, E. Expósito, V. Montiel and A. Aldaz, *Environ. Sci. Technol.*, 2010, **44**, 5182–5187.

64 H. Park, C. D. Vecitis and M. R. Hoffmann, *J. Phys. Chem. A*, 2008, **112**, 7616–7626.

65 G. K. Singh, *Energy*, 2013, **53**, 1–13.

66 J. Khan and M. H. Arsalan, *Renewable and Sustainable Energy Reviews*, 2016, **55**, 414–425.

67 M. Roeb, M. Neises, N. Monnerie, C. Sattler and R. Pitz-Paal, *Energy Environ. Sci.*, 2011, **4**, 2503–2511.

68 B. Coelho, A. C. Oliveira and A. Mendes, *Energy Environ. Sci.*, 2010, **3**, 1398–1405.

69 M. Millán, M. A. Rodrigo, C. M. Fernández-Marchante, S. Díaz-Abad, M. C. Peláez, P. Cañizares and J. Lobato, *Electrochimica Acta*, 2018, **270**, 14–21.

70 E. Mena, R. López-Vizcaíno, M. Millán, P. Cañizares, J. Lobato and M. A. Rodrigo, *International Journal of Energy Research*, **42**, 720–730.

71 F. Cucchiella, I. D'Adamo and M. Gastaldi, *Journal of Cleaner Production*, 2016, **131**, 460–474.

72 J. Hoppmann, J. Volland, T. S. Schmidt and V. H. Hoffmann, *Renewable and Sustainable Energy Reviews*, 2014, **39**, 1101–1118.

73 G. Merei, J. Moshövel, D. Magnor and D. U. Sauer, *Applied Energy*, 2016, **168**, 171–178.

74 A. Escapa, R. Mateos, E. J. Martínez and J. Blanes, *Renewable and Sustainable Energy Reviews*, 2016, **55**, 942–956.

75 H. Wang, J.-D. Park and Z. J. Ren, *Environ. Sci. Technol.*, 2015, **49**, 3267–3277.

76 M. Sun, L.-F. Zhai, W.-W. Li and H.-Q. Yu, *Chem. Soc. Rev.*, 2016, **45**, 2847–2870.

77 U. Schröder, F. Harnisch and L. T. Angenent, *Energy Environ. Sci.*, 2015, **8**, 513–519.

78 W.-W. Li, H.-Q. Yu and Z. He, *Energy Environ. Sci.*, 2014, **7**, 911–924.

79 Z. L. Wang, J. Chen and L. Lin, *Energy Environ. Sci.*, 2015, **8**, 2250–2282.

80 S. Gao, J. Su, X. Wei, M. Wang, M. Tian, T. Jiang and Z. L. Wang, *ACS Nano*, 2017, **11**, 770–778.
81 Z. L. Wang, *Faraday Discuss.*, 2015, **176**, 447–458.
82 X. Cao, Y. Jie, N. Wang and Z. L. Wang, *Advanced Energy Materials*, **6**, 1600665.
83 L. Li, G. Wang, R. Chen, X. Zhu, H. Wang, Q. Liao and Y. Yu, *Lab Chip*, 2014, **14**, 3368–3375.
84 Z. Wu, G. Zhao, Y. Zhang, J. Liu, Y. Zhang and H. Shi, *J. Mater. Chem. A*, 2015, **3**, 3416–3424.
85 Y. Liu, J. Li, B. Zhou, H. Chen, Z. Wang and W. Cai, *Chem. Commun.*, 2011, **47**, 10314–10316.
86 F. Invernizzi, S. Dulio, M. Patrini, G. Guizzetti and P. Mustarelli, *Chem. Soc. Rev.*, 2016, **45**, 5455–5473.
87 N. Nordin, L.-N. Ho, S.-A. Ong, A. H. Ibrahim, Y.-S. Wong, S.-L. Lee, Y.-S. Oon and Y.-L. Oon, *Separation and Purification Technology*, 2017, **177**, 135–141.
88 A. Sapkota, H. Yang, J. Wang and Z. Lu, *Environ. Sci. Technol.*, 2013, **47**, 1184–1185.
89 J. Baxter, Z. Bian, G. Chen, D. Danielson, M. S. Dresselhaus, A. G. Fedorov, T. S. Fisher, C. W. Jones, E. Maginn, U. Kortshagen, A. Manthiram, A. Nozik, D. R. Rolison, T. Sands, L. Shi, D. Sholl and Y. Wu, *Energy Environ. Sci.*, 2009, **2**, 559–588.
90 V. Daioglou, A. P. C. Faaij, D. Saygin, M. K. Patel, B. Wicke and D. P. van Vuuren, *Energy Environ. Sci.*, 2014, **7**, 482–498.
91 *C&EN Global Enterp*, 2016, **94**, 17–17.
92 *C&EN Global Enterprise*, 2016, **94**, 17–17.
93 B. Hartweg, in *Climate Change Literacy and Education Social Justice, Energy, Economics, and the Paris Agreement Volume 2*, American Chemical Society, 2017, vol. 1254, pp. 81–90.
94 O. OCDE, *World Energy Outlook 2014.*, Organisation for Economic Co-operation and Development, Washington, 2014.
95 H. Zou, H. Du, D. C. Broadstock, J. Guo, Y. Gong and G. Mao, *Journal of Cleaner Production*, 2016, **112**, 1475–1485.
96 E. Csefalvay and I. T. Horvath, *ACS Sustainable Chem. Eng.*, 2018, **6**, 8868–8874.
97 C. McGlade and P. Ekins, *Nature*, 2015, **517**, 187–190.

98 F. Cucchiella and I. D'Adamo, *Clean Techn Environ Policy*, 2015, **17**, 1929–1944.
99 B. CHAPMAN, in *Understanding the Global Energy Crisis*, Purdue University Press, 2014, pp. 27–72.
100 Renewables 2017, https://www.iea.org/publications/renewables2017/, (accessed May 29, 2018).
101 Renewable Capacity Statistics 2018, /publications/2018/Mar/Renewable-Capacity-Statistics-2018, (accessed May 29, 2018).
102 *C&EN Global Enterp*, 2017, **95**, 23–23.
103 F.-J. Haug and C. Ballif, *Energy Environ. Sci.*, 2015, **8**, 824–837.
104 J. A. Carta, J. González and V. Subiela, *Solar Energy*, 2003, **75**, 153–168.
105 R. Tang, *Solar Energy*, 2017, **157**, 614–628.
106 M. R. Shaner, S. J. Davis, N. S. Lewis and K. Caldeira, *Energy Environ. Sci.*, 2018, **11**, 914–925.
107 N. Armaroli and V. Balzani, *Energy Environ. Sci.*, 2011, **4**, 3193–3222.
108 Y. Hu and H. Cheng, *Environ. Sci. Technol.*, 2013, **47**, 3044–3056.
109 N. Armaroli and V. Balzani, *Chemistry – A European Journal*, **22**, 32–57.
110 N. K. Sidda, B. Espejo-Garcia, F. J. Lopez-Pellicer, M. Á. Latre and F. J. Zarazaga-Soria, *Environ. Sci. Technol.*, 2014, **48**, 15–16.
111 F. Cucchiella and I. D'Adamo, *Renewable and Sustainable Energy Reviews*, 2012, **16**, 5245–5259.
112 Y. Zhang, A. Lundblad, P. E. Campana and J. Yan, *Energy Procedia*, 2016, **88**, 455–461.
113 G. Li, Y. Jin, M. W. Akram and X. Chen, *Renewable and Sustainable Energy Reviews*, 2017, **79**, 440–458.
114 V. C. Sontake and V. R. Kalamkar, *Renewable and Sustainable Energy Reviews*, 2016, **59**, 1038–1067.
115 P. Periasamy, N. K. Jain and I. P. Singh, *Renewable and Sustainable Energy Reviews*, 2015, **43**, 918–925.
116 D. H. Muhsen, T. Khatib and F. Nagi, *Renewable and Sustainable Energy Reviews*, 2017, **68**, 70–86.
117 B. Ali, *Renewable and Sustainable Energy Reviews*, 2018, **81**, 413–420.

118 S. Mohammed Wazed, B. R. Hughes, D. O’Connor and J. Kaiser Calautit, *Renewable and Sustainable Energy Reviews*, 2018, **81**, 1206–1225.
119 S. S. Chandel, M. Nagaraju Naik and R. Chandel, *Renewable and Sustainable Energy Reviews*, 2015, **49**, 1084–1099.
120 J. Settino, T. Sant, C. Micallef, M. Farrugia, C. Spiteri Staines, J. Licari and A. Micallef, *Renewable and Sustainable Energy Reviews*, 2018, **90**, 892–909.
121 N. Monghasemi and A. Vadiee, *Renewable and Sustainable Energy Reviews*, 2018, **81**, 2714–2730.
122 Y. Choi and J. Song, *Renewable and Sustainable Energy Reviews*, 2017, **75**, 1386–1391.
123 N. Kannan and D. Vakeesan, *Renewable and Sustainable Energy Reviews*, 2016, **62**, 1092–1105.
124 L. García-Rodríguez, *Wind Engineering*, 2004, **28**, 453–463.
125 Y. Zhang, M. Sivakumar, S. Yang, K. Enever and M. Ramezanianpour, *Desalination*, 2018, **428**, 116–145.
126 F. L. Souza, M. R. V. Lanza, J. Llanos, C. Sáez, M. A. Rodrigo and P. Cañizares, *Journal of Environmental Management*, 2015, **158**, 36–39.
127 J. Jean, P. R. Brown, R. L. Jaffe, T. Buonassisi and V. Bulović, *Energy Environ. Sci.*, 2015, **8**, 1200–1219.
128 World Energy Outlook 2015, https://webstore.iea.org/world-energy-outlook-2015, (accessed May 30, 2018).
129 C. Lupangu and R. C. Bansal, *Renewable and Sustainable Energy Reviews*, 2017, **73**, 950–965.
130 C. Battaglia, A. Cuevas and S. D. Wolf, *Energy Environ. Sci.*, 2016, **9**, 1552–1576.
131 J. Siecker, K. Kusakana and B. P. Numbi, *Renewable and Sustainable Energy Reviews*, 2017, **79**, 192–203.
132 T. Ikegami, T. Maezono, F. Nakanishi, Y. Yamagata and K. Ebihara, *Solar Energy Materials and Solar Cells*, 2001, **67**, 389–395.
133 A. R. Jordehi, *Renewable and Sustainable Energy Reviews*, 2016, **61**, 354–371.
134 J. A. Duffie and W. A. Beckman, *Solar engineering of thermal processes*, New York Wiley, 2nd ed., 1991.
135 D. L. Evans, *Solar Energy*, 1981, **27**, 555–560.

136 T. Esram, J. W. Kimball, P. T. Krein, P. L. Chapman and P. Midya, *IEEE Transactions on Power Electronics*, 2006, **21**, 1282–1291.

137 J. Ramanujam and U. P. Singh, *Energy Environ. Sci.*, 2017, **10**, 1306–1319.

138 Y. Zhao and C. Burda, *Energy Environ. Sci.*, 2012, **5**, 5564–5576.

139 H. Fu, *J. Mater. Chem. C*, 2018, **6**, 414–445.

140 S. G. Kumar and K. S. R. K. Rao, *Energy Environ. Sci.*, 2013, **7**, 45–102.

141 M. Tsuji, T. Aramoto, H. Ohyama, T. Hibino and K. Omura, *Journal of Crystal Growth*, 2000, **214**–**215**, 1142–1147.

142 O. Stroyuk, A. Raevskaya and N. Gaponik, *Chem. Soc. Rev.*, 2018, **47**, 5354–5422.

143 T. Surek, *Journal of Crystal Growth*, 2005, **275**, 292–304.

144 Technology Roadmap Solar Photovoltaic Energy - 2014 edition, P60.

145 M.-E. Ragoussi and T. Torres, *Chem. Commun.*, 2015, **51**, 3957–3972.

146 B. Parida, S. Iniyan and R. Goic, *Renewable and Sustainable Energy Reviews*, 2011, **15**, 1625–1636.

147 V. V. Tyagi, N. A. A. Rahim, N. A. Rahim and J. A. /L. Selvaraj, *Renewable and Sustainable Energy Reviews*, 2013, **20**, 443–461.

148 U. Lucia, *Physica A: Statistical Mechanics and its Applications*, 2013, **392**, 3912–3919.

149 A. Z. Hafez, A. Soliman, K. A. El-Metwally and I. M. Ismail, *Renewable and Sustainable Energy Reviews*, 2017, **77**, 147–168.

150 A. Gharakhani Siraki and P. Pillay, *Solar Energy*, 2012, **86**, 1920–1928.

151 K. Bakirci, *Renewable and Sustainable Energy Reviews*, 2012, **16**, 6149–6159.

152 E. Abdeen, M. Orabi and E.S. Hasaneen, *Solar Energy*, 2017, **155**, 267–280.

153 H. Fathabadi, *Solar Energy*, 2016, **138**, 67–76.

154 A. Bahrami, C. O. Okoye and U. Atikol, *Renewable Energy*, 2017, **113**, 563–579.

155 E.-E. Delyannis, *Desalination*, 1987, **67**, 3–19.

156 T. Abraham and A. Luthra, *Desalination*, 2011, **268**, 238–248.

157 P. Compain, *Procedia Engineering*, 2012, **46**, 220–227.

158 M. Shatat, M. Worall and S. Riffat, *Sustainable Cities and Society*, 2013, **9**, 67–80.

159 H. Sharon and K. S. Reddy, *Renewable and Sustainable Energy Reviews*, 2015, **41**, 1080–1118.

160 M. R. Adiga, S. K. Adhikary, P. K. Narayanan, W. P. Harkare, S. D. Gomkale and K. P. Govindan, *Desalination*, 1987, **67**, 59–66.

161 O. Kuroda, S. Takahashi, S. Kubota, K. Kikuchi, Y. Eguchi, Y. Ikenaga, N. Sohma, K. Nishinoiri, S. Wakamatsu and S. Itoh, *Desalination*, 1987, **67**, 33–41.

162 N. Ishimaru, *Desalination*, 1994, **98**, 485–493.

163 A. Al-Karaghouli, D. Renne and L. L. Kazmerski, *Renewable Energy*, 2010, **35**, 323–328.

164 N. C. Wright and A. G. Winter, *Desalination*, 2014, **352**, 82–91.

165 H. M. N. AlMadani, *Renewable Energy*, 2003, **28**, 1915–1924.

166 J. Uche, F. Círez, A. A. Bayod and A. Martínez, *Energy*, 2013, **57**, 44–54.

167 A. Gonzalez, M. Grágeda and S. Ushak, *Applied Energy*, 2017, **206**, 1643–1652.

168 J. M. Ortiz, E. Expósito, F. Gallud, V. García-García, V. Montiel and A. Aldaz, *Solar Energy Materials and Solar Cells*, 2008, **92**, 1677–1688.

169 J. M. Ortiz, E. Expósito, F. Gallud, V. García-García, V. Montiel and A. Aldaz, *Desalination*, 2007, **208**, 89–100.

170 J. M. Ortiz, E. Expósito, F. Gallud, V. García-García, V. Montiel and A. Aldaz, *Journal of Membrane Science*, 2006, **274**, 138–149.

171 D. Valero, J. M. Ortiz, E. Expósito, V. Montiel and A. Aldaz, *Solar Energy Materials and Solar Cells*, 2008, **92**, 291–297.

172 S. Zhang, J. Zhang, W. Wang, F. Li and X. Cheng, *Solar Energy Materials and Solar Cells*, 2013, **117**, 73–80.

173 F. Hussin, F. Abnisa, G. Issabayeva and M. K. Aroua, *Journal of Cleaner Production*, 2017, **147**, 206–216.

174 A. García-García, V. Martínez-Miranda, I. G. Martínez-Cienfuegos, P. T. Almazán-Sánchez, M. Castañeda-Juárez and I. Linares-Hernández, *Fuel*, 2015, **149**, 46–54.

175 F. L. Souza, C. Saéz, J. Llanos, M. R. V. Lanza, P. Cañizares and M. A. Rodrigo, *Electrochimica Acta*, 2016, **190**, 371–377.

176 S. Figueroa, L. Vázquez and A. Alvarez-Gallegos, *Water Research*, 2009, **43**, 283–294.

177 T. Ochiai, K. Nakata, T. Murakami, A. Fujishima, Y. Yao, D. A. Tryk and Y. Kubota, *Water Research*, 2010, **44**, 904–910.

178 E. Alvarez-Guerra, A. Dominguez-Ramos and A. Irabien, *Chemical Engineering Research and Design*, 2011, **89**, 2679–2685.

179 E. Alvarez-Guerra, A. Dominguez-Ramos and A. Irabien, *Chemical Engineering Journal*, 2011, **170**, 7–13.
180 A. Dominguez-Ramos, R. Aldaco and A. Irabien, *Journal of Chemical Technology & Biotechnology*, 2010, **85**, 821–830.
181 D. Valero, V. García-García, E. Expósito, A. Aldaz and V. Montiel, *Separation and Purification Technology*, 2014, **123**, 15–22.
182 F. L. Souza, C. Saéz, J. Llanos, M. R. V. Lanza, P. Cañizares and M. A. Rodrigo, *Chemical Engineering Journal*, 2015, **277**, 64–69.
183 S. Garcia-Segura and E. Brillas, *Applied Catalysis B: Environmental*, 2016, **181**, 681–691.
184 X. Huang, Y. Qu, C. A. Cid, C. Finke, M. R. Hoffmann, K. Lim and S. C. Jiang, *Water Research*, 2016, **92**, 164–172.
185 M. Herrero-Gonzalez, P. Diaz-Guridi, A. Dominguez-Ramos, R. Ibañez and A. Irabien, *Desalination*, 2018, **433**, 155–163.
186 I. Hassan, E. Mohamedelhassan and E. K. Yanful, *Electrochimica Acta*, 2015, **181**, 58–67.
187 E.-K. Jeon, S.-R. Ryu and K. Baek, *Electrochimica Acta*, 2015, **181**, 160–166.
188 S. Yuan, Z. Zheng, J. Chen and X. Lu, *Journal of Hazardous Materials*, 2009, **162**, 1583–1587.
189 M. Zhou, J. Xu, S. Zhu, Y. Wang and H. Gao, *Separation and Purification Technology*, 2018, **190**, 297–306.
190 M. Zhou, S. Zhu, Y. Liu and X. Wang, *Environ Sci Pollut Res Int*, 2013, **20**, 5806–5812.
191 A. Rahmani, D. Zerrouki, L. Djafer and A. Ayral, *International Journal of Hydrogen Energy*, 2017, **42**, 19591–19596.
192 Y. Zhang, A. Wang, X. Tian, Z. Wen, H. Lv, D. Li and J. Li, *Journal of Hazardous Materials*, 2016, **318**, 319–328.
193 G. Ren, M. Sun, Y. Sun, Y. Li, C. Wang, A. Lu and H. Ding, *RSC Adv.*, 2017, **7**, 47975–47982.
194 F. Fazelpour, E. Markarian and N. Soltani, *Renewable Energy*, 2017, **109**, 646–667.
195 C. Diyoke, M. Aneke, M. Wang and C. Wu, *RSC Adv.*, 2018, **8**, 22004–22022.
196 J. A. Carta, in *Comprehensive Renewable Energy*, ed. A. Sayigh, Elsevier, Oxford, 2012, pp. 569–622.
197 S.-Y. Liu and Y.-F. Ho, *Renewable and Sustainable Energy Reviews*, 2016, **59**, 39–55.

198 M. Wang, P. Ullrich and D. Millstein, *Renewable Energy*, 2018, **127**, 242–257.
199 G. C. van Kooten, in *Comprehensive Renewable Energy*, ed. A. Sayigh, Elsevier, Oxford, 2012, pp. 541–568.
200 D. J. Willis, C. Niezrecki, D. Kuchma, E. Hines, S. R. Arwade, R. J. Barthelmie, M. DiPaola, P. J. Drane, C. J. Hansen, M. Inalpolat, J. H. Mack, A. T. Myers and M. Rotea, *Renewable Energy*, 2018, **125**, 133–154.
201 Y. Zhang, N. Tang, Y. Niu and X. Du, *Renewable and Sustainable Energy Reviews*, 2016, **66**, 322–344.
202 C. Jung, D. Schindler and L. Grau, *Energy Conversion and Management*, 2018, **173**, 383–398.
203 M. Yin, Z. Yang, Y. Xu, J. Liu, L. Zhou and Y. Zou, *Applied Energy*, 2018, **221**, 508–521.
204 E. Hau, in *Wind Turbines: Fundamentals, Technologies, Application, Economics*, ed. E. Hau, Springer Berlin Heidelberg, Berlin, Heidelberg, 2013, pp. 79–87.
205 V. Quaschning, *Understanding renewable energy systems*, Earthscan, London ; Sterling, VA, 2005.
206 *A Wind Turbine Recipe Book 2014 English Units Edtion by Hugh Piggott by Hugh Piggott - Read Online*, .
207 T. Stathopoulos, H. Alrawashdeh, A. Al-Quraan, B. Blocken, A. Dilimulati, M. Paraschivoiu and P. Pilay, *Journal of Wind Engineering and Industrial Aerodynamics*, 2018, **179**, 146–157.
208 *Wind Energy Engineering by Trevor M. Letcher by Trevor M. Letcher - Read Online*, .
209 Y. Kumar, J. Ringenberg, S. S. Depuru, V. K. Devabhaktuni, J. W. Lee, E. Nikolaidis, B. Andersen and A. Afjeh, *Renewable and Sustainable Energy Reviews*, 2016, **53**, 209–224.
210 İ. Talinli, E. Topuz and E. A. and S. Kabakcı, *Wind Farm - Technical Regulations, Potential Estimation and Siting Assessment*, , DOI:10.5772/17311.
211 P. Enevoldsen, S. V. Valentine and B. K. Sovacool, *Energy Policy*, 2018, **120**, 1–7.
212 S. M. Muyeen, R. Takahashi, T. Murata and J. Tamura, *IEEE Transactions on Power Systems*, 2010, **25**, 331–340.
213 M. S. Adaramola, M. Agelin-Chaab and S. S. Paul, *Energy Conversion and Management*, 2014, **77**, 61–69.

214 T. F. Ishugah, Y. Li, R. Z. Wang and J. K. Kiplagat, *Renewable and Sustainable Energy Reviews*, 2014, **37**, 613–626.

215 M. A. Abdullah, A. H. M. Yatim, C. W. Tan and R. Saidur, *Renewable and Sustainable Energy Reviews*, 2012, **16**, 3220–3227.

216 S. Marmouh, M. Boutoubat and L. Mokrani, in *2016 8th International Conference on Modelling, Identification and Control (ICMIC)*, 2016, pp. 296–302.

217 M. Cirrincione, M. Pucci and G. Vitale, *IEEE Transactions on Industry Applications*, 2011, **47**, 861–872.

218 W.-M. Lin and C.-M. Hong, *Energy*, 2010, **35**, 2440–2447.

219 G. Crabtree, J. Misewich, R. Ambrosio, K. Clay, P. DeMartini, R. James, M. Lauby, V. Mohta, J. Moura, P. Sauer, F. Slakey, J. Lieberman and H. Tai, *AIP Conference Proceedings*, 2011, **1401**, 387–405.

220 B. Dunn, H. Kamath and J.-M. Tarascon, *Science*, 2011, **334**, 928–935.

221 J. Veza, B. Peñate and F. Castellano, *Desalination*, 2004, **160**, 211–221.

222 J. M. Veza, B. Peñate and F. Castellano, *Desalination*, 2001, **141**, 53–61.

223 P. Malek, J. M. Ortiz and H. M. A. Schulte-Herbrüggen, *Desalination*, 2016, **377**, 54–64.

224 V. Montiel, D. Valero, F. Gallud, V. García-García, E. Expósito and J. Iniesta, in *Electrochemical Water and Wastewater Treatment*, eds. C. A. Martínez-Huitle, M. A. Rodrigo and O. Scialdone, Butterworth-Heinemann, 2018, pp. 513–541.

225 E. Tzen, in *Renewable Energy Powered Desalination Handbook*, ed. V. G. Gude, Butterworth-Heinemann, 2018, pp. 91–139.

226 B. S. Richards and A. I. Schäfer, in *Sustainability Science and Engineering*, Elsevier, 2010, vol. 2, pp. 353–373.

227 F. L. Souza, J. Llanos, C. Sáez, M. R. V. Lanza, M. A. Rodrigo and P. Cañizares, *Journal of Environmental Management*, 2016, **171**, 128–132.

228 A. Rinaldi, B. Mecheri, V. Garavaglia, S. Licoccia, P. D. Nardo and E. Traversa, *Energy Environ. Sci.*, 2008, **1**, 417–429.

229 Y. Fan, S.K. Han and H. Liu, *Energy Environ. Sci.*, 2012, **5**, 8273–8280.

230 X.-W. Liu, W.-W. Li and H.-Q. Yu, *Chem. Soc. Rev.*, 2014, **43**, 7718–7745.

231 B. E. Logan, M. J. Wallack, K.-Y. Kim, W. He, Y. Feng and P. E. Saikaly, *Environ. Sci. Technol. Lett.*, 2015, **2**, 206–214.

232 Z. Ge, J. Li, L. Xiao, Y. Tong and Z. He, *Environ. Sci. Technol. Lett.*, 2014, **1**, 137–141.
233 B. E. Logan, B. Hamelers, R. Rozendal, U. Schröder, J. Keller, S. Freguia, P. Aelterman, W. Verstraete and K. Rabaey, *Environ. Sci. Technol.*, 2006, **40**, 5181–5192.
234 T. Saito, T. H. Roberts, T. E. Long, B. E. Logan and M. A. Hickner, *Energy Environ. Sci.*, 2011, **4**, 928–934.
235 S. Chen, H. Hou, F. Harnisch, S. A. Patil, A. A. Carmona-Martinez, S. Agarwal, Y. Zhang, S. Sinha-Ray, A. L. Yarin, A. Greiner and U. Schröder, *Energy Environ. Sci.*, 2011, **4**, 1417–1421.
236 M. Rimboud, D. Pocaznoi, B. Erable and A. Bergel, *Phys. Chem. Chem. Phys.*, 2014, **16**, 16349–16366.
237 M. Zhou, M. Chi, J. Luo, H. He and T. Jin, *Journal of Power Sources*, 2011, **196**, 4427–4435.
238 F. Zhao, R. C. T. Slade and J. R. Varcoe, *Chem. Soc. Rev.*, 2009, **38**, 1926–1939.
239 H. Song, M.-Z. Ding, X.-Q. Jia, Q. Ma and Y.-J. Yuan, *Chem. Soc. Rev.*, 2014, **43**, 6954–6981.
240 J. R. Trapero, L. Horcajada, J. J. Linares and J. Lobato, *Applied Energy*, 2017, **185**, 698–707.
241 B. E. Logan and J. M. Regan, *Trends in Microbiology*, 2006, **14**, 512–518.
242 J. Wang, X. Song, Y. Wang, B. Abayneh, Y. Ding, D. Yan and J. Bai, *Bioresource Technology*, 2016, **221**, 697–702.
243 M. C. Potter, *Proc. R. Soc. Lond. B*, 1911, **84**, 260–276.
244 F. J. Hernández-Fernández, A. Pérez de los Ríos, M. J. Salar-García, V. M. Ortiz-Martínez, L. J. Lozano-Blanco, C. Godínez, F. Tomás-Alonso and J. Quesada-Medina, *Fuel Processing Technology*, 2015, **138**, 284–297.
245 A. P. Borole, G. Reguera, B. Ringeisen, Z.-W. Wang, Y. Feng and B. H. Kim, *Energy Environ. Sci.*, 2011, **4**, 4813–4834.
246 Y. Fan, H. Hu and H. Liu, *Environ. Sci. Technol.*, 2007, **41**, 8154–8158.
247 D. Pant, A. Singh, G. Van Bogaert, Y. A. Gallego, L. Diels and K. Vanbroekhoven, *Renewable and Sustainable Energy Reviews*, 2011, **15**, 1305–1313.
248 D. Pant, A. Singh, G. V. Bogaert, S. I. Olsen, P. S. Nigam, L. Diels and K. Vanbroekhoven, *RSC Adv.*, 2012, **2**, 1248–1263.
249 M. Safdar, J. Jänis and S. Sánchez, *Lab Chip*, 2016, **16**, 2754–2758.

250 C. Santoro, C. Arbizzani, B. Erable and I. Ieropoulos, *Journal of Power Sources*, 2017, **356**, 225–244.
251 Y. Qiao, S.J. Bao and C. M. Li, *Energy Environ. Sci.*, 2010, **3**, 544–553.
252 K. Rabaey and R. A. Rozendal, *Nat. Rev. Microbiol.*, 2010, **8**, 706–716.
253 X. Cao, X. Huang, P. Liang, K. Xiao, Y. Zhou, X. Zhang and B. E. Logan, *Environ. Sci. Technol.*, 2009, **43**, 7148–7152.
254 C. W. Marshall, D. E. Ross, E. B. Fichot, R. S. Norman and H. D. May, *Environ. Sci. Technol.*, 2013, **47**, 6023–6029.
255 K. Katuri, M. L. Ferrer, M. C. Gutiérrez, R. Jiménez, F. del Monte and D. Leech, *Energy Environ. Sci.*, 2011, **4**, 4201–4210.
256 J. M. Sonawane, A. Yadav, P. C. Ghosh and S. B. Adeloju, *Biosensors and Bioelectronics*, 2017, **90**, 558–576.
257 J. Wei, P. Liang and X. Huang, *Bioresource Technology*, 2011, **102**, 9335–9344.
258 Y. Hindatu, M. S. M. Annuar and A. M. Gumel, *Renewable and Sustainable Energy Reviews*, 2017, **73**, 236–248.
259 W. Yang, K.-Y. Kim, P. E. Saikaly and B. E. Logan, *Energy Environ. Sci.*, 2017, **10**, 1025–1033.
260 H. O. Mohamed, M. Obaid, A. S. Yasin, J. H. Kim and N. A. M. Barakat, *RSC Adv.*, 2016, **6**, 111657–111665.
261 X.W. Liu, X.F. Sun, Y.-X. Huang, G.P. Sheng, S.G. Wang and H.Q. Yu, *Energy Environ. Sci.*, 2011, **4**, 1422–1427.
262 Y. Zhao, K. Watanabe and K. Hashimoto, *Phys. Chem. Chem. Phys.*, 2011, **13**, 15016–15021.
263 X. Xie, M. Ye, L. Hu, N. Liu, J. R. McDonough, W. Chen, H. N. Alshareef, C. S. Criddle and Y. Cui, *Energy Environ. Sci.*, 2012, **5**, 5265–5270.
264 X. Xie, G. Yu, N. Liu, Z. Bao, C. S. Criddle and Y. Cui, *Energy Environ. Sci.*, 2012, **5**, 6862–6866.
265 H. Yuan and Z. He, *Nanoscale*, 2015, **7**, 7022–7029.
266 Y.Q. Wang, H.X. Huang, B. Li and W.S. Li, *J. Mater. Chem. A*, 2015, **3**, 5110–5118.
267 S. F. Ketep, A. Bergel, A. Calmet and B. Erable, *Energy Environ. Sci.*, 2014, **7**, 1633–1637.

268 D. Pocaznoi, A. Calmet, L. Etcheverry, B. Erable and A. Bergel, *Energy Environ. Sci.*, 2012, **5**, 9645–9652.
269 M. Ma, S. You, G. Liu, J. Qu and N. Ren, *J. Mater. Chem. A*, 2016, **4**, 18002–18007.
270 X. Peng, S. Chen, L. Liu, S. Zheng and M. Li, *Electrochimica Acta*, 2016, **194**, 246–252.
271 P. Ledezma, B. C. Donose, S. Freguia and J. Keller, *Electrochimica Acta*, 2015, **158**, 356–360.
272 Z. Wang, G. D. Mahadevan, Y. Wu and F. Zhao, *Journal of Power Sources*, 2017, **356**, 245–255.
273 E. Zhang, F. Wang, Q. Yu, K. Scott, X. Wang and G. Diao, *Journal of Power Sources*, 2017, **360**, 21–27.
274 L. Feng, Y. Yan, Y. Chen and L. Wang, *Energy Environ. Sci.*, 2011, **4**, 1892–1899.
275 X. Xie, M. Pasta, L. Hu, Y. Yang, J. McDonough, J. Cha, C. S. Criddle and Y. Cui, *Energy Environ. Sci.*, 2011, **4**, 1293–1297.
276 X. Tang, H. Li, W. Wang, Z. Du and H. Y. Ng, *RSC Adv.*, 2014, **4**, 12789–12794.
277 Z. Chen, K. Li, P. Zhang, L. Pu, X. Zhang and Z. Fu, *Chemical Engineering Journal*, 2015, **259**, 820–826.
278 X. Wang, N. Gao, Q. Zhou, H. Dong, H. Yu and Y. Feng, *Bioresource Technology*, 2013, **144**, 632–636.
279 X. Li, S. Chen, I. Angelidaki and Y. Zhang, *Chemical Engineering Journal*, 2018, **354**, 492–506.
280 I. Sirés, J. A. Garrido, R. M. Rodríguez, E. Brillas, N. Oturan and M. A. Oturan, *Applied Catalysis B: Environmental*, 2007, **72**, 382–394.
281 V. Poza-Nogueiras, E. Rosales, M. Pazos and M. Á. Sanromán, *Chemosphere*, 2018, **201**, 399–416.
282 S. O. Ganiyu, T. X. Huong Le, M. Bechelany, N. Oturan, S. Papirio, G. Esposito, E. van Hullebusch, M. Cretin and M. A. Oturan, *Chemical Engineering Journal*, 2018, **350**, 844–855.
283 Y. Wang, G. Zhao, S. Chai, H. Zhao and Y. Wang, *ACS Applied Materials & Interfaces*, 2013, **5**, 842–852.
284 X. Zhu and J. Ni, *Electrochemistry Communications*, 2009, **11**, 274–277.

285 Y. Li, A. Lu, H. Ding, X. Wang, C. Wang, C. Zeng and Y. Yan, *Electrochemistry Communications*, 2010, **12**, 944–947.

286 C.H. Feng, F.B. Li, H.J. Mai and X.Z. Li, *Environ. Sci. Technol.*, 2010, **44**, 1875–1880.

287 C. Feng, F. Li, H. Liu, X. Lang and S. Fan, *Electrochimica Acta*, 2010, **55**, 2048–2054.

288 L. Zhuang, S. Zhou, Y. Yuan, M. Liu and Y. Wang, *Chemical Engineering Journal*, 2010, **163**, 160–163.

289 L. Zhuang, S. Zhou, Y. Li, T. Liu and D. Huang, *Journal of Power Sources*, 2010, **195**, 1379–1382.

290 Y. Luo, R. Zhang, G. Liu, J. Li, B. Qin, M. Li and S. Chen, *Bioresource Technology*, 2011, **102**, 3827–3832.

291 T. X. H. Le, R. Esmilaire, M. Drobek, M. Bechelany, C. Vallicari, D. L. Nguyen, A. Julbe, S. Tingry and M. Cretin, *J. Mater. Chem. A*, 2016, **4**, 17686–17693.

292 L. Zhang, X. Yin and S. F. Y. Li, *Chemical Engineering Journal*, 2015, **276**, 185–192.

293 Y. Wang, C. Feng, Y. Li, J. Gao and C.P. Yu, *Chemical Engineering Journal*, 2017, **307**, 679–686.

294 M. Hassan, N. Pous, B. Xie, J. Colprim, M. D. Balaguer and S. Puig, *Chemical Engineering Journal*, 2017, **328**, 57–65.

295 M. Hassan, N. Pous, B. Xie, J. Colprim, M. D. Balaguer and S. Puig, *Bioresource Technology*, 2017, **243**, 949–956.

296 M. Hassan, H. Wei, H. Qiu, Y. Su, S. W. H. Jaafry, L. Zhan and B. Xie, *Bioresource Technology*, 2018, **247**, 434–442.

297 T. Ling, B. Huang, M. Zhao, Q. Yan and W. Shen, *Bioresource Technology*, 2016, **203**, 89–95.

298 Y. Bennani, M. C. F. M. Peters, P. W. Appel and L. C. Rietveld, *Electrochimica Acta*, 2015, **182**, 604–612.

299 X.Y. Yong, D.Y. Gu, Y.D. Wu, Z.Y. Yan, J. Zhou, X.Y. Wu, P. Wei, H.H. Jia, T. Zheng and Y.C. Yong, *Journal of Hazardous Materials*, 2017, **324**, 178–183.

300 Y. Li, L. Liu and F. Yang, *Journal of Membrane Science*, 2017, **525**, 202–209.

301 X. Li, X. Jin, N. Zhao, I. Angelidaki and Y. Zhang, *Bioresource Technology*, 2017, **228**, 322–329.

302 N. Birjandi, H. Younesi, A. A. Ghoreyshi and M. Rahimnejad, *Journal of Environmental Management*, 2016, **180**, 390–400.
303 L. Fu, S.-J. You, G. Zhang, F.-L. Yang and X. Fang, *Chemical Engineering Journal*, 2010, **160**, 164–169.
304 H.-C. Tao, X.-Y. Wei, L.-J. Zhang, T. Lei and N. Xu, *Journal of Hazardous Materials*, 2013, **254**–**255**, 236–241.
305 N. Li, J. An, L. Zhou, T. Li, J. Li, C. Feng and X. Wang, *Journal of Power Sources*, 2016, **306**, 495–502.
306 N. Xu, S. Zhou, Y. Yuan, H. Qin, Y. Zheng and C. Shu, *Bioresource Technology*, 2011, **102**, 7777–7783.
307 N. Xu, Y. Zhang, H. Tao, S. Zhou and Y. Zeng, *Bioresource Technology*, 2013, **138**, 136–140.
308 Y. Dong, Y. Qu, C. Li, X. Han, J. J. Ambuchi, J. Liu, Y. Yu and Y. Feng, *Journal of Hazardous Materials*, 2017, **340**, 104–112.
309 Z. Chen, B.K. Zhu, W.F. Jia, J.H. Liang and G.X. Sun, *Environmental Technology & Innovation*, 2015, **3**, 63–67.
310 X.W. Liu, X.F. Sun, D.B. Li, W.W. Li, Y.X. Huang, G.P. Sheng and H.Q. Yu, *Water Research*, 2012, **46**, 4371–4378.
311 M. Á. Fernández de Dios, A. G. del Campo, F. J. Fernández, M. Rodrigo, M. Pazos and M. Á. Sanromán, *Bioresource Technology*, 2013, **148**, 39–46.
312 M. A. F. de Dios, O. Iglesias, E. Bocos, M. Pazos and M. A. Sanromán, *Journal of Industrial and Engineering Chemistry*, 2014, **20**, 3754–3760.
313 X. Zhu and B. E. Logan, *Journal of Hazardous Materials*, 2013, **252**–**253**, 198–203.
314 Z. Wang, B. Zhang, A. G. L. Borthwick, C. Feng and J. Ni, *Chemical Engineering Journal*, 2015, **280**, 99–105.
315 B. Zhang, Z. Wang, X. Zhou, C. Shi, H. Guo and C. Feng, *Bioresource Technology*, 2015, **181**, 360–362.
316 Y. Zhang, Y. Wang and I. Angelidaki, *Journal of Power Sources*, 2015, **291**, 108–116.
317 S. Xu, Y. Qin, C. Xu, Y. Wei, R. Yang and Z. L. Wang, *Nat Nanotechnol*, 2010, **5**, 366–373.
318 X. Wang, J. Song, J. Liu and Z. L. Wang, *Science*, 2007, **316**, 102–105.
319 R. G. Horn, D. T. Smith and A. Grabbe, *Nature*, 1993, **366**, 442–443.

320 J. Henniker, *Nature*, 1962, **196**, 474.
321 F.R. Fan, Z.Q. Tian and Z. Lin Wang, *Nano Energy*, 2012, **1**, 328–334.
322 J. Chen, J. Yang, Z. Li, X. Fan, Y. Zi, Q. Jing, H. Guo, Z. Wen, K. C. Pradel, S. Niu and Z. L. Wang, *ACS Nano*, 2015, **9**, 3324–3331.
323 G. Zhu, Y. S. Zhou, P. Bai, X. S. Meng, Q. Jing, J. Chen and Z. L. Wang, *Advanced Materials*, 2014, **26**, 3788–3796.
324 Y. Zhu, B. Yang, J. Liu, X. Wang, L. Wang, X. Chen and C. Yang, *Scientific Reports*, 2016, **6**, 22233.
325 R. D. I. G. Dharmasena, K. D. G. I. Jayawardena, C. A. Mills, J. H. B. Deane, J. V. Anguita, R. A. Dorey and S. R. P. Silva, *Energy Environ. Sci.*, 2017, **10**, 1801–1811.
326 S. Wang, L. Lin and Z. L. Wang, *Nano Energy*, 2015, **11**, 436–462.
327 Y. Zheng, L. Cheng, M. Yuan, Z. Wang, L. Zhang, Y. Qin and T. Jing, *Nanoscale*, 2014, **6**, 7842–7846.
328 B. Meng, W. Tang, Z. Too, X. Zhang, M. Han, W. Liu and H. Zhang, *Energy Environ. Sci.*, 2013, **6**, 3235–3240.
329 Y. Mao, N. Zhang, Y. Tang, M. Wang, M. Chao and E. Liang, *Nanoscale*, 2017, **9**, 14499–14505.
330 X. Li, J. Tao, W. Guo, X. Zhang, J. Luo, M. Chen, J. Zhu and C. Pan, *J. Mater. Chem. A*, 2015, **3**, 22663–22668.
331 Y. Feng, Y. Zheng, Z. U. Rahman, D. Wang, F. Zhou and W. Liu, *J. Mater. Chem. A*, 2016, **4**, 18022–18030.
332 Y. Yang, H. Zhang, Y. Liu, Z.-H. Lin, S. Lee, Z. Lin, C. P. Wong and Z. L. Wang, *ACS Nano*, 2013, **7**, 2808–2813.
333 Y. Yang, H. Zhang, S. Lee, D. Kim, W. Hwang and Z. L. Wang, *Nano Lett.*, 2013, **13**, 803–808.
334 Z. Li, J. Chen, J. Yang, Y. Su, X. Fan, Y. Wu, C. Yu and Z. L. Wang, *Energy Environ. Sci.*, 2015, **8**, 887–896.
335 S. Chen, N. Wang, L. Ma, T. Li, M. Willander, Y. Jie, X. Cao and Z. L. Wang, *Advanced Energy Materials*, 2016, **6**, 1501778.
336 M.-H. Yeh, H. Guo, L. Lin, Z. Wen, Z. Li, C. Hu and Z. L. Wang, *Advanced Functional Materials*, 2016, **26**, 1054–1062.

337 S. Gao, Y. Chen, J. Su, M. Wang, X. Wei, T. Jiang and Z. L. Wang, *ACS Nano*, 2017, **11**, 3965–3972.

338 Z. Li, J. Chen, J. Zhou, L. Zheng, K. C. Pradel, X. Fan, H. Guo, Z. Wen, M.-H. Yeh, C. Yu and Z. L. Wang, *Nano Energy*, 2016, **22**, 548–557.

339 Q. Jiang, Y. Jie, Y. Han, C. Gao, H. Zhu, M. Willander, X. Zhang and X. Cao, *Nano Energy*, 2015, **18**, 81–88.

340 Y. Chen, M. Wang, M. Tian, Y. Zhu, X. Wei, T. Jiang and S. Gao, *Nano Energy*, 2017, **42**, 314–321.

341 S. Gao, M. Wang, Y. Chen, M. Tian, Y. Zhu, X. Wei and T. Jiang, *Nano Energy*, 2018, **45**, 21–27.

342 S.B. Jeon, S. Kim, S.J. Park, M.L. Seol, D. Kim, Y. K. Chang and Y.K. Choi, *Nano Energy*, 2016, **28**, 288–295.

343 J. Yang, W. Liao, Y. Liu, M. Murugananthan and Y. Zhang, *Electrochimica Acta*, 2014, **144**, 7–15.

344 Y. Liu, J. Li, B. Zhou, S. Lv, X. Li, H. Chen, Q. Chen and W. Cai, *Applied Catalysis B: Environmental*, 2012, **111**–**112**, 485–491.

345 Y. Liu, J. Li, B. Zhou, X. Li, H. Chen, Q. Chen, Z. Wang, L. Li, J. Wang and W. Cai, *Water Res.*, 2011, **45**, 3991–3998.

346 K. Li, H. Zhang, T. Tang, Y. Xu, D. Ying, Y. Wang and J. Jia, *Water Research*, 2014, **62**, 1–10.

347 J. Bai, R. Wang, Y. Li, Y. Tang, Q. Zeng, L. Xia, X. Li, J. Li, C. Li and B. Zhou, *Journal of Hazardous Materials*, 2016, **311**, 51–62.

348 M. Kaneko, J. Nemoto, H. Ueno, N. Gokan, K. Ohnuki, M. Horikawa, R. Saito and T. Shibata, *Electrochemistry Communications*, 2006, **8**, 336–340.

349 M. Sui, Y. Dong and H. You, *RSC Adv.*, 2015, **5**, 94184–94190.

350 Y. Liu, L. Liu and F. Yang, *RSC Adv.*, 2016, **6**, 12068–12075.

351 L. Li, S. Xue, R. Chen, Q. Liao, X. Zhu, Z. Wang, X. He, H. Feng and X. Cheng, *Electrochimica Acta*, 2015, **182**, 280–288.

352 J. Li, J. Li, Q. Chen, J. Bai and B. Zhou, *Journal of Hazardous Materials*, 2013, **262**, 304–310.

353 K. Zhao, Q. Zeng, J. Bai, J. Li, L. Xia, S. Chen and B. Zhou, *Water Research*, 2017, **108**, 293–300.

354 H. Akbari, M. C. Browne, A. Ortega, M. J. Huang, N. J. Hewitt, B. Norton and S. J. McCormack, *Solar Energy*, *In Press*.

355 Q. Li, Y. Liu, S. Guo and H. Zhou, *Nano Today*, 2017, **16**, 46–60.

356 T. M. Gür, *Energy Environ. Sci.*, 2018, **11**, 2696–2767.

357 J. Zhang, G. Jiang, P. Xu, A. G. Kashkooli, M. Mousavi, A. Yu and Z. Chen, *Energy Environ. Sci.*, 2018, **11**, 2010–2015.

358 K. J. Kim, M.-S. Park, Y.J. Kim, J. H. Kim, S. X. Dou and M. Skyllas-Kazacos, *J. Mater. Chem. A*, 2015, **3**, 16913–16933.

359 X. Li, H. Zhang, Z. Mai, H. Zhang and I. Vankelecom, *Energy Environ. Sci.*, 2011, **4**, 1147–1160.

360 P. Leung, X. Li, C. P. de León, L. Berlouis, C. T. J. Low and F. C. Walsh, *RSC Adv.*, 2012, **2**, 10125–10156.

361 S. Park and H. Kim, *J. Mater. Chem. A*, 2015, **3**, 12276–12283.

362 P. Vanýsek and V. Novák, *Journal of Energy Storage*, 2017, **13**, 435–441.

363 D.J. Park, K.S. Jeon, C.H. Ryu and G.J. Hwang, *Journal of Industrial and Engineering Chemistry*, 2017, **45**, 387–390.

364 M. Skyllas-Kazacos and J. F. McCann, in *Advances in Batteries for Medium and Large-Scale Energy Storage*, Woodhead Publishing, 2015, pp. 329–386.

365 M. Skyllas-Kazacos, M. H. Chakrabarti, S. A. Hajimolana, F. S. Mjalli and M. Saleem, *J. Electrochem. Soc.*, 2011, **158**, R55–R79.

366 R. López-Vizcaíno, E. Mena, M. Millán, M. A. Rodrigo and J. Lobato, *Renewable Energy*, 2017, **114**, 1123–1133.

367 M. Millán, M. A. Rodrigo, C. M. Fernández-Marchante, S. Díaz-Abad, M. C. Peláez, P. Cañizares and J. Lobato, *Electrochimica Acta*, 2018, **270**, 14–21.

368 *Membrane Technology*, 2014, **2014**, 9–10.

369 N. C. Wright, *San Diego*, 9.

370 M. Lucas, F. J. Aguilar, J. Ruiz, C. G. Cutillas, A. S. Kaiser and P. G. Vicente, *Renewable Energy*, 2017, **111**, 26–37.

371 S. Nižetić, D. Čoko, A. Yadav and F. Grubišić-Čabo, *Energy Conversion and Management*, 2016, **108**, 287–296.
372 A. M. Urtiaga, G. Pérez, R. Ibáñez and I. Ortiz, *Desalination*, 2013, **331**, 26–34.
373 A. Dominguez-Ramos and A. Irabien, *Ind. Eng. Chem. Res.*, 2013, **52**, 7534–7540.
374 O. García, E. Isarain-Chávez, S. Garcia-Segura, E. Brillas and J. M. Peralta-Hernández, *Electrocatalysis*, 2013, **4**, 224–234.
375 F. E. Durán, D. M. de Araújo, C. do Nascimento Brito, E. V. Santos, S. O. Ganiyu and C. A. Martínez-Huitle, *Journal of Electroanalytical Chemistry*, 2018, **818**, 216–222.
376 J. Lobato, P. Cañizares, M. A. Rodrigo, C. Sáez and J. J. Linares, *International Journal of Hydrogen Energy*, 2006, **31**, 1780–1790.
377 J. Jiang, M. Chang and P. Pan, *Environ. Sci. Technol.*, 2008, **42**, 3059–3063.
378 K. Cho, D. Kwon and M. R. Hoffmann, *RSC Adv.*, 2013, **4**, 4596–4608.
379 C. Risco, R. López-Vizcaíno, C. Sáez, A. Yustres, P. Cañizares, V. Navarro, M.A. Rodrigo, *Chemical Engineering Journal*, 2016, **285**, 128–138.
380 C. Risco, S. Rodrigo, R. López-Vizcaíno, C. Sáez, P. Cañizares, V. Navarro, M.A. Rodrigo, *Science Total Environ.*, 2016, 545–546, 256–265.
381 R. López-Vizcaíno, V. Navarro, M. J. León, C. Risco, M.A. Rodrigo, C. Sáez, P. Cañizares, *Journal Hazardous Materials*, 2016, **315**, 135–143
382 L. He, P. Du, Y. Chen, H. Lu, X. Cheng, B. Chang and Z. Wang, *Renewable and Sustainable Energy Reviews*, 2017, **71**, 388–403.